UNIVERSITY OF CALIFORNIA

Santa Barbara

Methodological Developments in Consequential Life Cycle Assessment

A dissertation submitted in partial satisfaction of the

requirements for the degree Doctor of Philosophy

in Environmental Science & Management

by

Joseph William Palazzo

Committee in charge:

Professor Roland Geyer, Co-Chair

Professor Douglas G. Steigerwald, Co-Chair

Professor Richard Startz

Professor Sangwon Suh

June 2019

The dissertation of Joseph William Palazzo is approved.

_____
Richard Startz

_____
Sangwon Suh

_____
Douglas G. Steigerwald, Committee Co-Chair

_____
Roland Geyer, Committee Co-Chair

June 2019

Methodological Developments in Consequential Life Cycle Assessment

ACKNOWLEDGEMENTS

It has been a long and winding road leading to this dissertation. This work would not have been possible without the gracious support of my PhD committee; however I must thank folks from long before this stage in my professional life. First, I dedicate the scientific contribution of this piece to the late James O'Herron, who inspired me to become a scientist with his physics class in Middletown High School in New York. The chemistry and mathematics teachers Shirley Thompson and Elvira Scotto-Padavono from Middletown also provided endless inspiration and support for the beginning of my path in the sciences. I am eternally grateful to the four academic professionals connected to my time in Rensselaer Polytechnic Institute who recommended me for a PhD at the Bren School: Gwo-Ching Wang, James Napolitano, Eddie Ade Knowles, and Mark Changizi. In particular, Dr. Wang's guidance during my Master's degree in physics was instrumental, helping me to produce two impactful co-authorships and come away with numerous pieces of wisdom about navigating academia. Thank you for supporting my decisions to pivot my career from academia to the semiconductor industry and back again once I found my topic of passion.

As far as my time here goes, it wouldn't have happened at all without the acceptance and support of Roland Geyer. We both took a tremendous gamble in creating this partnership, and it has paid off in spades. Roland's open-minded approach to mentoring resulted in the most enjoyable five years of my life in both a personal and professional sense. From Roland, I learned that trusting your gut and defying many of the norms of your field can be cornerstones of a recipe for success. In fact, in interdisciplinary settings, I have come to believe that those qualities are a competitive advantage.

I must also acknowledge my other three committee members. First, I thank Douglas G. Steigerwald, who watched a presentation on my research ideas in his econometrics class, and from there initiated a research mentorship that changed the course of my PhD. Without our frequent, honest, and genuinely transparent meetings, the third and fourth chapters of this dissertation would be years behind where they need to be. Further, I would not have nearly the required level of expertise and confidence to continue pursing applied econometrics as a professional. My econometrics training has come almost completely from firsthand experience rather than classes. To that end, Dick Startz has also been a great contributor. He pushed me to refine my ideas and crystallize the fundamentals using simulations. This workflow helped me take multiple papers over the finish line. Last but not least, I thank Sangwon Suh for challenging my narratives about how life cycle assessment has been and should be done. His written and oral questions throughout my PhD produced the primary thrust for Chapter 1. They also helped me to navigate a field that I had zero experience in five years ago. For all of that, I am eternally grateful.

Of course, navigating a task as daunting and intense a PhD is not possible without a tremendous network of family and friends. The list is too long for me to name. However, I must mention my mother Eileen McManus, my father Anthony Palazzo, and my sisters Gina and Julie Palazzo. All four of you keep me afloat in various ways and this achievement is something shared between all of us. I am also blessed to have pursued

music in parallel with a scientific career since a very young age, and have managed to record and perform in professional settings during my time in Santa Barbara and long before. To the hundreds of people I have shared the stage with, thank you for giving me an outlet to be in the moment and ease the frustrations of academia. Finally, to my life partner, Keila Cristina Cunha e Silva, thank you for everything. You are an absolute rock star in academia, and remind me every day that I can continue to dream big and take risks. You are the perfect partner for a person like me, and I strive every day to make you proud and become a better person.

VITA OF JOSEPH WILLIAM PALAZZO
June 2019

EDUCATION

Bachelor of Science, Physics, Rensselaer Polytechnic Institute, December 2009, *summa cum laude*
Master of Science, Physics, Rensselaer Polytechnic Institute, May 2011
Doctor of Philosophy in Environmental Science and Management, University of California, Santa Barbara, June 2019 (expected)

PROFESSIONAL EMPLOYMENT

2014-2019: Graduate Student Researcher, Bren School of Environmental Science and Management, University of California, Santa Barbara
2016-2019: Teaching Assistant, Bren School of Environmental Science and Management, University of California, Santa Barbara
2017: Environmental Technologies Intern, Apple, Inc. Cupertino, California
2012-2014: Process Engineer, GLOBALFOUNDRIES, Inc. Malta, New York
2011-2012: Process Development Engineer, Cree, Inc. Durham, North Carolina
2010-2011: Graduate Student Researcher, Rensselaer Polytechnic Institute, Troy, New York

PUBLICATIONS

Palazzo, J., Geyer, R. (2019). Consequential Life Cycle Assessment of Automotive Material Substitution: Replacing Steel with Aluminum in Production of North American Vehicles. *Environmental Impact Assessment Review*. 75, 47-58.
Palazzo, J., Geyer, R., Startz, R., Steigerwald, D.G. (2019). Causal Inference for Quantifying Displaced Primary Production from Recycling. *Journal of Cleaner Production. 2*10, 1076-1084.
Magalhães, R.F., Danilevicz, A.M.F., **Palazzo, J.** (2019). Managing trade-offs in complex scenarios: a decision-making tool for sustainability projects. *Journal of Cleaner Production.* 212, 447-460.
Couture, J., Geyer, R., Øvrum, J., Kuczenski, B., Øverland, M., **Palazzo, J.**, Sahlmann, C., Lenihan, H. (2019). Environmental benefits of novel non-human food inputs to salmon feeds. *Environmental Science & Technology.* 53(4), 1967-1975.
Palazzo, J., Liu, O.R., Stillinger, T., Song, R., Wang, Y., Hiroyasu, E.H., Zenteno, J., Anderson, S., Tague, C. (2017). Urban Responses to Restrictive Conservation Policy during Drought. *Water Resources Research.* 53, 4459-4475.
Krawicz, A., **Palazzo, J.**, Wang, G.-C., Dinolfo, P. (2012). Layer-by-layer Assembly of Zn (II) and Ni (II) 5,10,15,20-tetra(4-ethynylphenyl)porphyrin Multilayers on Au Using Copper Catalyzed Azide-alkyne Cycloaddition. *Royal Society of Chemistry Advances.* 2(19), 7513-7522.

Gaire, C., **Palazzo, J.**, Bhat, I., Goyal, A., Wang, G.-C., Lu, T.-M. (2012). Low Temperature Epitaxial Growth of Ge on CaF_2 Buffered Cube-textured Ni. *Journal of Crystal Growth.* 343(1), 33-37.

Changizi, M., Weber, R., Kotecha, R., **Palazzo, J.** (2011). Are Wet-Induced Wrinkled Fingers Primate Rain Treads? *Brain, Behavior, and Evolution.* 77(4), 286-290.

AWARDS
2014-2016, 2018-2019: Deckers Outdoor Corporation Fellowship, Bren School of Environmental Science and Management, University of California, Santa Barbara
2014-2015: Holbrook Fellowship, Institute for Energy Efficiency, University of California, Santa Barbara
2010-2011: National Science Foundation Integrated Graduate Education & Research Traineeship (IGERT) Fellow, Rensselaer Polytechnic Institute
2008: Ruck Scholar, Sigma Phi Epsilon

FIELDS OF STUDY
Major field: Industrial Ecology
Studies in Life Cycle Assessment with professors Roland Geyer and Sangwon Suh
Studies in Econometrics and Research Methods with professors Richard Startz and Douglas G. Steigerwald

ABSTRACT

Methodological Developments in Consequential Life Cycle Assessment

by

Joseph William Palazzo

Life Cycle Assessment (LCA) seeks to quantify the environmental impacts of product systems and services from “cradle-to-grave”, or from raw material extraction through the end-of-life. The ideal outcome of this exercise is the identification of actions that can be taken by firms and policymakers to reduce global environmental damage. LCA is quite young relative to the classical academic disciplines, and faces significant challenges in establishing its relevance for decision-making. Mainstream LCA practice seeks to account for environmental damage using a class of frameworks termed Attributional LCA (ALCA). This typically involves the use of normative, technology-focused rules to allocate inputs, outputs and emissions over product systems that interact with each other. The application of such rules can sever cause-effect relationships that strongly influence the environmental consequences of changes to industrial systems. This thesis develops and demonstrates new methodologies pertaining to Consequential LCA (CLCA), which has not been standardized and fully adopted in mainstream practice. In CLCA, I seek to assess the net environmental outcomes of decisions, rather than attribute environmental

impacts using a set of normative rules. This leads to an inevitable focus on social dynamics and causal inference, which are scarcely addressed in the LCA field.

The first chapter is an extensive literature review on the history and current state of methods for characterizing the environmental consequences of actions in LCA. I first discuss the major existing differences between ALCA and CLCA in the literature. Then, I provide a detailed review of methods that have been proposed to evolve the structure of CLCA models towards a robust representation of cause-effect relationships. I recommend the use of an iterative framework between structural CLCA models and causal inference analysis, a class of methods largely absent from the LCA literature. The remainder of my dissertation applies this iterative framework and focuses on the integration of LCA with the modelling and quantification of social mechanisms. In Chapter 2, I build a CLCA model of automotive material substitution including parameterized market forces that drive the environmental impacts of changes in scrap generation and recycling activity. I show that market forces contribute significantly to uncertainty in modelling the greenhouse gas consequences of automotive material substitution using local and global sensitivity analysis. I also find that in 16% of trials of a Monte Carlo simulation, substituting aluminum for steel in a fleet of vehicles does not constitute a net decrease in greenhouse gas emissions. This finding contrasts with previous studies on the topic, and is influenced by the incorporation of market forces into the model. Chapter 3 explores the environmental consequences of recycling as an example of these market forces in greater depth. I generalize this concept as a question of the cause-effect relationship between recycling and production of materials from primary resources. For the first time in the industrial ecology literature, I propose the use of difference-in-differences (DID), a quasi-

experimental statistical method that classifies observational data into treatment and control groups, to test hypotheses about this key relationship. I simulate the application of the DID estimator to the question of whether or not increases in the use of recycled aluminum in the automotive industry would lead to an equivalent reduction in the use of primary aluminum. Finally, in Chapter 4, I exploit the fact that water is used, recycled, and reused in localized units to create treatment and control groups of recycled water users. I design an empirical DID study that explores the question of whether or not increases in wastewater recycling lead to equivalent reductions in potable water usage. I find that in a large urban water district in California, the wastewater recycling program has displaced over 25 million cubic feet of potable water production with a displacement rate of 93.4%. Chapter 4 is the first empirical application of quasi-experimental methods to quantifying the relationship between recycling and primary production, and the first attempt to test hypotheses regarding the potable water savings achieved from wastewater recycling.

TABLE OF CONTENTS

LIST OF FIGURES

LIST OF TABLES

1. A review of methods for characterizing the environmental consequences of actions in life cycle assessment

1.1 Abstract

Understanding the environmental consequences of actions is becoming increasingly important in the field of industrial ecology in general, and in life cycle assessment (LCA) more specifically. However, a consensus on how to operationalize this idea has not been reached. A variety of methods have been proposed and applied to case studies that cover various aspects of consequential life cycle assessment (CLCA). Previous reviews of the topic have focused on the broad agenda of CLCA and how different modelling frameworks fit into its goals. However, explicit examination of the spectrum of methods and their application to the different facets of CLCA is lacking. Here I provide a detailed review of methods that have been used to construct models of the environmental consequences of actions in CLCA. First, I cover the following structural modelling approaches: (1) economic equilibrium models, (2) system dynamics models, (3) technology choice models, and (4) agent-based models. I provide a detailed review of particular applications of each model in the CLCA domain. The advantages and disadvantages of each are discussed, and their relationships with CLCA are clarified. From this, I am able to map all of these models onto the established aspects of CLCA. I learn that structural models alone are not sufficient to quantify the uncertainty distributions of underlying parameters in CLCA, which are essential components of a robust analysis of consequences. To address this, I provide a brief introduction to the causal inference approach to parameter identification and uncertainty analysis that is emerging in the CLCA literature. I recommend that a research path forward

for the future of CLCA is the establishment of feedback loops between empirical estimates and structural models.

1.2 Introduction

The inquiry over the robustness of quantitative methods used in the industrial ecology community for decision-making has persisted throughout its history (Tillman 2000; Weidema 1993; Ekvall et al. 2016; Weidema 2003; Earles and Halog 2011; Zamagni et al. 2012; Plevin et al. 2014; Dale and Kim 2014; Brandão et al. 2014). Fundamentally, this can be understood as the industrial ecology asking itself the following question: do the results of our analysis adequately represent the environmental consequences of actions? The labelling of a fraction of life cycle assessment (LCA) studies as "consequential" naturally implies that a particular subset of LCA studies do the job of representing the consequences of actions (Curran et al. 2002). However, there is a lack of consensus on what exactly constitutes a consequential LCA (CLCA, Rajagopal 2016; Earles and Halog 2011; Yang 2016; Suh and Yang 2014; Zamagni et al. 2012; Ekvall et al. 2016). For example, authors have suggested CLCA is the merging of traditional attributional LCA (ALCA) with supply-demand equilibrium models (Earles and Halog 2011), that CLCA should be computed using general equilibrium techniques (Rajagopal 2016), that CLCA is the combination of ALCA and scenario analysis (Yang 2016), and that CLCA is rather an aspiration than an operational model and that actual practice lies in the continuum "from ALCA to the ideal CLCA" (Suh and Yang 2014).

Despite the ongoing debate over what constitutes CLCA, there are specific features of CLCA that are accepted in the literature. For example, CLCA requires that data collection be guided by the goal to analyze the consequences of a change to a product system. Thus,

the inventory data should be reflective of the precise sources used to fulfill the increases (or decreases) in products and services affected by the change, which are referred to as "marginal" in the case of small changes and "incremental" in the case of large ones (Ekvall et al. 2016). Other themes of CLCA that appear in literature are the use of system expansion to address issues where flows are shared between product systems (Ekvall and Weidema 2004; Ekvall et al. 2016; Weidema 2003; Majeau-bettez et al. 2014; Weidema 2001), the addition of a time dimension to LCA (Stasinopoulos et al. 2012), and the inclusion of social and economic mechanisms (Zamagni et al. 2012; Earles and Halog 2011). A number of approaches have been used to mechanistically characterize change-oriented data, expand system boundaries, include a time dimension, and parametrize social and economic processes. This diversity of approaches is supported by the notion that there are "different models for different purposes" (Anex and Lifset 2014).

Some authors have associated the use of a specific modelling approach with CLCA. This includes the use of economic equilibrium models (Rajagopal 2014; Earles and Halog 2011; Ekvall and Andrae 2006), system dynamics models (Stasinopoulos et al. 2012), agent-based models (Querini and Benetto 2015), and the technology-choice model (Kätelhön et al. 2016). In one way or another, these models specify a set of input parameters and a corresponding set of equations that govern hypothesized cause-effect relationships in the system. Herein, I refer to this as a structural model for CLCA.

Much of the existing CLCA review literature is focused on comparing and contrasting traditional linear process-based and economic input-output LCA models with LCA models which utilize economic equilibrium approaches (Earles and Halog 2011; Zamagni et al. 2012; Yang and Heijungs 2017; Marvuglia et al. 2013). Authors have also conducted in-

depth reviews regarding the inclusion of other market mechanisms, such as the concepts of constrained and unconstrained suppliers, in CLCA (Ekvall and Weidema 2004; Ekvall et al. 2016). The gaps in existing reviews are the following: 1) approaches other than economic equilibrium modelling are mostly absent; 2) the relative merits of each approach for informing the individual accepted facets of CLCA are unclear; 3) the role that hypothesis testing and statistical inference play in CLCA is not specified.

The objectives of this chapter are thus three-fold: first, to provide a comprehensive review of the key assumptions, applications, advantages and disadvantages of the full array of models proposed as structures for CLCA. Secondly, I aim to map these models onto the individual aspects of CLCA that I described above. Third, I seek to tie these models together with causal inference in order to promote the integration of cause-effect and uncertainty analyses into the research agenda of CLCA.

The following chapter first focuses on four structural models for consequential life cycle inventories: (1) economic equilibrium models, (2) systems dynamics models, (3) technology choice models, and (4) agent-based models. For each model, I provide an overview of the key concepts and assumptions. Next, I provide descriptions of specific applications of each model in the industrial ecology literature, and specify where these fit into the CLCA puzzle. The advantages and disadvantages of each are discussed both in absolute terms and relative to each other. Then, I introduce observational methods that can be used to test hypotheses generated by structural CLCA models, and in turn inform the input parameters and their underlying uncertainties. I conclude by discussing how existing CLCA models highlight critical hypotheses that underpin the environmental consequences of decisions, which are testable via observational methods. Then, the results from these hypothesis tests can be used

to refine the structural model used in a given CLCA. In this way, structural models and observational methods can be integrated in a feedback loop in an effort to advance CLCA as a cause-effect analysis framework.

1.3 Review of structural models for CLCA

1.3.1 Economic Equilibrium Models

The terminology of "general" and "partial" equilibrium has been a source of great confusion in scholarly literature. Therefore, I begin our discussion by providing some historical context and specifying a clear definition of what is meant by an "economic equilibrium model" for the purposes of this review.

The contribution of general equilibrium theory to the economic literature is credited to Arrow and Debreu (1954). Its theoretical grounding traces to the work of Léon Walrus, who is credited with introducing the classical market-clearing equilibrium condition; that supply equals demand for all goods in a perfectly competitive market (Walrus 1900). Arrow-Debreu equilibrium specifies the existence of a vector of prices for all goods in the economy for which all markets clear, or reach equilibrium, under a set of assumptions (Mitra-kahn 2008). One can approximate a solution for the vector using a computational algorithm such as Scarf's algorithm (Scarf 1967).

In mainstream practice, computable general equilibrium (CGE) models, such as the global trade analysis project (GTAP), are not a complete manifestation of Arrow-Debreu general equilibrium theory (see Mitra-kahn 2008). They are market models constructed using simultaneous equations of supply and demand for goods as a function of price and a series of exogenous variables. Therefore, I refer to "general equilibrium" approaches as the exercise in determining price and quantity jointly in all sectors and regions in the world

economy using a solvable system of equations, which aligns with its mainstream definition today. This exercise requires price responses and substitution responses between sectors as an essential input. I note that in practice, these price responses are calculated as ratios of percentages and referred to as “elasticities”.

Some applications of economic equilibrium modelling in CLCA are referred to “partial equilibrium” models (PEMs). This terminology is used for models that use simultaneous equations of supply and demand, along with the equilibrium condition, to represent the market for a particular good (or small set of goods) in isolation from the rest of the economy. Given the enormous challenges associated with building a general equilibrium model of the world economy, the majority of cases applicable to CLCA have used a partial equilibrium approach. This also requires the calculation of price elasticities and substitution elasticities, but with significantly fewer inputs in comparison with GEMs. Together, PEMs and GEMs as described above are what I refer to as “economic equilibrium models” during this review.

1.3.1.1 Assumptions

The most elementary of assumptions in economic equilibrium models is that there are two sets of agents that interact on a market or set of markets. These two sets are referred to as the “supply side” and “demand side” (Cardenete 2012). On the supply side, there are agents which are assumed to produce goods and services in a profit-maximizing manner. In other words, they choose the production recipe that minimizes the difference between their costs and the selling price of their product. The demand side is made up of consumers, which are seeking to maximize their utility function. Another key assumption in economic equilibrium models is that the market in question is competitive. In short, this means that no

single agent of supply or demand prescribes the operating parameters of the market (for more detailed definitions see Stigler, 1957). It is also assumed that following a shock to supply or demand, an equilibrium condition where supply equals demand will be reached in subsequent time periods. While not necessary, most of the underlying relationships between prices and quantities are defined using linear functions, meaning that they assume the effect of price is linear and homogenous.

The parameters underlying simultaneous equations of supply and demand that comprise economic equilibrium models are sometimes estimated using two-stage least squares regressions with instrumental variables, and may have *ceteris paribus* causal interpretations (Stock 2001; Wooldridge 2012). For example, in the background of economic equilibrium models, the *ceteris paribus* causal effect of a unit change in price on the quantity of a good supplied is sometimes estimated, and called the "own-price" response of supply. The own-price response of demand may also be estimated in an economic equilibrium model based on simultaneous equations. When two goods A and B are included in the economic equilibrium model, the effect of a unit change in the price of A on the quantity demanded of B (and vice versa) may also be estimated econometrically, or otherwise calculated. These are referred to as "cross-price" or "substitution" responses. In cases where regressions are used to estimate the underlying parameters, non-price variables are included as exogenous shifters of supply and demand and used as the instrumental variables in the regressions that generate the price response estimates (Wooldridge 2012). The ideal aspiration of an economic equilibrium model is then to establish causal relationships between supply and demand for a commodity and its own price, the price of its inputs, the price of competing products and other economy-wide controls such as real GDP (Blomberg and Hellmer 2000; Zink et al. 2017).

However, it is important to note that PEM and CGE models as a whole are not causal inference models even if the underlying parameters are estimated econometrically. By applying PEM and CGE models, we are not testing the hypothesis that their structure is reflective of the underlying causal mechanisms in the economy.

1.3.1.2 Applications

Perhaps the most influential case of the use of PEMs in industrial ecology is a study of the consequences of indirect land use change in the environmental impact assessment of shifts towards biofuels (Searchinger et al. 2008). The authors conclude that the conversion of land for food and feed crops in response to increased bio-ethanol demand was unaccounted for in previous LCA studies of biofuels. The consideration of this indirect effect in the LCA resulted in findings that contrasted with earlier studies, which concluded that using ethanol may reduce greenhouse gas (GHG) emissions (Macedo et al. 2004; Wang et al. 1999; Farrell et al. 2006). A PEM created by the Center for Agriculture and Rural Development (CARD) at Iowa State University models the relationship between changes to demand in corn-derived ethanol and changes in the amount of land used for food and feed production. The idea that increased corn ethanol can lead to increased land conversion for crop production is a major driver of their result. In subsequent research, economic equilibrium models were proposed in general as a means to expand the system boundary in a CLCA of biofuels (Marvuglia et al. 2013).

Another example of the use of PEM in industrial ecology originates from the following research question: What is the relationship between increases in recycling activity and production of primary materials from raw resources (Zink et al. 2017, 2015)? One approach to the question is to construct a simultaneous equations model of supply and demand for

primary and secondary alternatives of the same material. The markets are linked through substitution elasticity, or a coefficient on the price difference between the two. Both markets reach equilibrium following the shock in secondary supply or demand. The response of primary supply to increases in secondary supply is termed "displacement". For example, if an increase in secondary supply of one unit results in a one-unit decrease in primary production, the displacement rate is 100%. Estimating displacement using PEMs is an example of avoiding the need to allocate recycling benefits between scrap users and generators by expanding the system boundary to include the scrap and material markets (Ekvall 2000; Zink et al. 2017).

PEMs are also applied in an early CLCA study of the transition to lead-free solders in the electronics industry (Ekvall and Andrae 2006). In this paper, a partial equilibrium structure for the lead and scrap lead markets is suggested. However, the price elasticities of supply and demand for both lead and scrap lead are assumed rather than estimated. The authors conclude that long-run elasticities are more relevant than short-term elasticities, as "[…] environmental systems analyses are primarily conducted due to concern about the long-term future environment."

Rajagopal (2016) discusses how a multi-market PEM can be built up into a GEM for the purposes of conducting CLCA. The supply and demand functions as well as equilibrium conditions are outlined for a hypothetical economy that produces food and fuel from land and energy inputs. A theoretical example of a policy shock stimulating fuel production from the land endowment (i.e. biofuel) is provided. However, in reality such a policy will have effects on other sectors of the economy besides agriculture and energy. This is the argument for building a GEM that links this system with the remaining sectors in the economy. By

linking supply and demand functions for all sectors, one could simulate the response of all sectors to a policy-driven shock to biofuel production. This is suggested as a potential overall framework for CLCA due to the intuitive appeal of including the interactions between sectors that are unaccounted for in PEMs.

1.3.1.3 Advantages & Disadvantages

There are several particular strengths regarding the use of PEMs for modelling the consequences of actions. The functions driving PEMs are usually estimated using causal inference techniques such as instrumental variables and two-stage least squares. This means that the price elasticity estimates have a *ceteris paribus* cause-and-effect interpretation conditional on past observations, even though the use of PEMs on the whole is not necessarily a direct measure of causality as discussed in section 2.1.1. The use of exogenous instruments for prices in the supply and demand functions are intended to produce the causal interpretation of the underlying parameters (Stock 2001). This statement should be interpreted with caution, however, as the instrument validity assumption implies that the instrumental variable is uncorrelated with the unobserved portion of the model, which can never be proven conclusively. Thus, the causal interpretation of instrumental variables relies on logical arguments, and should not be interpreted as reflecting a true random assignment experiment. Nonetheless, prices are a significant predictor of consumer behavior in competitive, developed economies and price responses are useful for thinking about the consequences of changes in the economy.

Another strength of PEMs is that the structural equations are quite detailed and specific, in comparison with GEMs which tend to aggregate commodities into sectors, have opaque structures and require massive amounts of effort and data to produce (Gohin and Moschini

2006). An intuitive analogy can be drawn between the PEM to GEM relationship and the process to input-output LCA relationship. In a general sense, process-based LCA lends itself to a more detailed analysis, whereas the input-output method relies on heavily aggregated data (Suh and Huppes 2005). This analogy is strengthened by the fact that partial equilibrium has been used in process-based CLCA (Ekvall and Andrae 2006) and economic input-output theory is considered a part of the foundation for general equilibrium models (Rose 1995).

Although they are a powerful tool, PEMs also contain several further limitations. The first one is that PEMs model the interactions of one or two sectors in isolation from the rest of the economy. Consider the secondary production and primary production example mentioned above. A shock in the supply of secondary aluminum, for example, may displace primary aluminum. The growth in secondary aluminum production and the reduction in primary aluminum production have a net effect on the market for electricity, as the electricity consumption of the aluminum industry would decrease if there was truly a net increase in primary production. On a global scale, this reduction may be significant, and would not be accounted for in a single-sector PEM.

As discussed previously, GEMs are an exercise in adapting the principles of economic equilibrium to an entire economy, made of many sectors, as opposed to just a select few. They are also equipped to handle inter-regional and inter-national dependencies, in contrast to standard input-output models, which are based on the accounts of a single nation (Rose 1995). Relative to PEMs, using GEMs for modelling the consequences of actions presents the advantage that they are able to handle international trade. For example, GTAP constructed a database containing 140 regions and 57 sectors that contains information about

the input-output structure of the sectors and heterogeneous household consumption preferences across countries (Hertel and Tsigas 1997). One could then evaluate the consequences of a carbon tax imposed on electricity-intensive imports from a country that has a grid mix with high carbon intensity. Consider the example of importing aluminum from China, which has an electricity mix grid with a higher than average carbon footprint (Hao et al. 2015). Reducing imports of Chinese aluminum and increasing imports from a nation that uses mostly hydroelectric power appears to reduce carbon emissions to first order. However, there may be unintended consequences, for example if the alternative source of aluminum requires greater inputs from the transportation sector. Under the assumptions of perfect competition and market clearing equilibrium, GEMs will provide insights regarding the cascading consequences of this change in global trade.

GEMs operate with the disadvantage that the sectors are highly aggregated, even more so than in the single nation input-output models commonly used in IO-LCA. Linking the input-output tables between multiple nations naturally requires some additional aggregation. The inability to account for competing technologies within a nation is another limitation of GEMs. Given that GEMs rely on the input-output account of nations, GEM tables are compiled on an intermittent basis and are frequently rooted in data from the fairly distant past, roughly 5-10 years (Hertel and Tsigas 1997). Data gaps in substitution elasticities are sometimes filled using data that are even older, exacerbating the data age issue. They are also based off the calculation of Armington elasticities, which present an issue in modelling the upstart production of a good in a region which did not produce it before (Springer and Duchin 2014). These issues are problematic when modelling the consequences of a decision made today, and the potential need to shift production of critical goods to new economies.

The theoretical construct of marginal input-output tables that could feed into marginal GEMs exists (Miller and Blair 2009), but in practice is based on calculating the change in the input-output structure between two consecutive editions of input-output tables. The tables used to calculate the marginal coefficients are still in the form of aggregated sectors and remain based on information produced in large time intervals, which remains problematic in terms of forecasting consequences increasing the demand for particular technological processes into the future. Lastly, GEMs are not very useful in exploring the consequences of decisions that have impact on developing economies, as these areas frequently have unstable trade conditions and governments, lack transparency in their economic policy and perform much of their trade on the black market.

In general, one must also bear in mind that a static equilibrium condition is the counterfactual for the responses quantified in these analyses. This is unlikely to be a sustainable assumption in the long term, and the uncertainty associated with the estimated effects in an economic equilibrium model increase with the time frame under which the studied transformation occurs. Lastly, economic equilibrium models are based on classical economic assumptions such as perfect information and rationality. These are not realistic in many situations, for example in relatively monopolistic or otherwise distorted markets; therefore it is likely that what we actually observe after a supply or demand shock will differ from what a PEM tells us.

1.3.2 **System Dynamics Models**

System dynamics modelling originated from a “pencil and paper simulation” of the feedback loops between industrial inventories, production volumes, and employment which was inspired by an optimization problem posed by General Electric in the 1950s (Forrester

1989). The complexity of the calculation of optimal employment practices led to the development of the original computing frameworks for system dynamics, namely SIMPLE and eventually DYNAMO. This development corresponds with the original academic version of system dynamics (Forrester 1958). Throughout the 1960s, interest in the use of Forrester's modelling framework for problems outside of industry intensified. A 1970 report by the Club of Rome used the *World3* model, derived from Forrester's original framework, to predict a collapse of modern society by 2100 due to the depletion of Earth's natural resources if trends in industrial activity were left unchanged. This is widely considered the first application of system dynamics to a sustainability problem. Over the subsequent decades, system dynamics became a key modelling and simulation technique in supply chain management research (Angerhofer and Angelides 2000), which makes its eventual overlap with industrial ecology and LCA unsurprising.

The system dynamics framework starts with a network with nodes that are linked by a series of causal pathways, most often illustrated using a causal loop diagram (Ahmad et al. 2016). The method is rooted in stock and flow calculations. Goods, capital, information, and other flows accumulate in the nodes of the causal pathways. There are time delays to the release of the various stocks, and they flow to the nodes that they are connected to, which in turn interact with the next nodes, and so forth. Given the node-level heterogeneity in dynamic effects, the existence of numerous feedback loops, and the randomness introduced by uncertainty in the inputs, nonlinear emergent properties of the model over time are observed. Increases in computing power have enabled the use of system dynamics for a broader range of problems of increasing complexity.

1.3.2.1 Applications

System dynamics has been used to add a time dimension to life cycle inventories, which aids in the modelling of a marginal background system. This gives the technique a different purpose in LCA compared with economic equilibrium models, which are most frequently used as an avenue for system expansion. In one case, system dynamics was used to analyze the energy benefits of changes in automotive body materials and was termed a "consequential energy LCI" (Stasinopoulos et al. 2012). Using systems dynamics, the authors introduce a time delay in capturing the marginal environmental benefits of recycling aluminum when it is substituted for steel. The study also highlights the difference between dynamic effects in a single product LCA versus that of an entire fleet of products.

In another example, system dynamics is applied to the analysis of environmental impacts of various end-of-life management scenarios for mobile phones in China (Yao et al. 2018). The authors examine the sensitivity of the system dynamics model to changes in landfill and incineration rates of the main components of mobile phones (casing, PCBs, LCDs, and batteries). The results suggest that increasing recycling rates of mobile phones increases human health and resource consumption, but has a positive influence on ecosystems in the long term. However, the positive influence on ecosystem health over time is negatively correlated with incineration rates. The system dynamics component of this study captures the time delay from mobile phone purchase to the environmental impacts of end-of-life management. An earlier study of end-of-life management of mobile phones used a dynamic stock-and-flow analysis to suggest that high recycling rates are critical for achieving real energy savings from mobile phone recycling, especially in the face of rapidly increasing demand (Mclaren et al. 1999).

Modelling short and long-term dynamics of supply and demand in the electricity sector is another application of system dynamics that is of interest to the industrial ecology community, and specifically aids the identification of marginal electricity supply. A 2016 review identifies "[…] models developed for policy assessment, generation capacity expansion, financial instruments, demand side management, mixing methods, and finally micro-worlds" (Ahmad et al. 2016). Of particular interest to the industrial ecology community are models of capacity expansion and demand, both of which effect the production and use phases of the LCIs of most household products. Ford (2001), for example, uses system dynamics to demonstrate the "boom-bust" pattern in electricity generation capacity expansion in California. This implies that utilities and investors respond to large increases in electricity demand in a sub-optimal manner. The LCI of marginal electricity generation in California is certainly affected by the dynamics of its supporting infrastructure.

1.3.2.2 Advantages & Disadvantages

One advantage of system dynamics in CLCA is the characterization of the timing of inventory data, emissions and associated environmental impacts. This is quite advantageous for identifying marginal inventory data, which are expected to evolve over time. From a policy standpoint, time horizons are frequently associated with sustainability goals. For example, the University of California zero waste plan, United Nations Sustainable Development Goals, and Hawai'i Sustainability Plan have time horizons of 2020, 2030, and 2050, respectively (State of Hawai'i 2008; University of California 2017; United Nations 2015). Thus, building models that evaluate the environmental consequences of such policies will inevitably involve a time component, which can be aided by the use of system dynamics

simulation. The system dynamics framework is also highly parameterized; giving it increased flexibility relative to economic equilibrium models.

System dynamics requires a set of pre-programmed parameters that set the initial conditions for stock and flow relationships. Thus, the directions of causal loops are also pre-determined from primary research, previous literature, and intuition. This pre-determination presents a disadvantage from a cause-and-effect standpoint, as the parameter sets are often too large to be completely determined using empirical methods. Economic equilibrium models, on the other hand, are parameterized with price elasticities that are determined using statistical methods. System dynamics models are sometimes considered less transparent than economic equilibrium models, since they are not likely to rely on public information or government accounts. Due to the complexities of the simulation, system dynamics also have a truncated system boundary compared with typical LCA models. Thus, system dynamics may be better suited for examinations of effects in smaller-scale systems, as in the case of local electricity generation capacity examined earlier.

1.3.3 **Technology Choice Models**

A technology choice model is one that optimizes the mix of multiple technologies used to produce sufficient quantities of goods to satisfy total demand from the various sectors of the economy. The optimization is subject to specified objectives and constraints. These may be related to costs, resource constraints, or other environmental outcomes, for example (Katelhon et al. 2015; Duchin and Levine 2012). In this section, I describe the Rectangular Choice of Technology (RCOT) model and an evolved version of RCOT referred to as the Technology Choice Model (TCM), which has been proposed as a component of CLCA (Kätelhön et al. 2016).

In a traditional input-output analysis, the technology matrix is square and the rows and columns are matching sectors. The RCOT model is an extension of the traditional input-output analysis framework where sectors can have multiple choices of technologies. Each technology is assumed to derive its input from the aggregated sectors, so the rows remain unchanged, but the technology matrix becomes rectangular instead of square. The objective of the RCOT model is to solve several types of linear optimization problems (Duchin and Levine 2011, 2012).

A key assumption of the RCOT model is that final demand for all sectors is met via a linear combination of activity levels of the technology options and that the outputs scale linearly with activity levels. It is also assumed that the outputs of the sectors in the RCOT model are all non-zero. RCOT further relies on the idea of "factors of production" which include resources that are not captured by the inputs from other sectors such as land and water. Factors need to have costs associated with them, which can be zero, and it is assumed that the objective of the economy is to minimize its factor costs subject to a series of constraints. The RCOT model can be further extended to include multiple regions that may trade the outputs of sectors with one another, with an objective of minimizing the total factor costs across all regions. The factors of production themselves, however, are not traded. Thus, different regions can have different factor use and cost structures.

As stated earlier, there are several types of optimization problems that may be solved with the RCOT model. The most basic one minimizes the factor costs for a region while meeting final demand. The objective function problem looks like this: $minZ = \pi' F^* x^*$ s.t. $(I^* - A^*)x^* \geq y$, where π is the vector of factor prices, F^* is the rectangular matrix of factors, x^* are the activity levels, I^* is the rectangular identity matrix, A^* is the rectangular input-

output coefficient matrix, and *y* is the vector of final demand. In this most basic case, given no constraints on quantities of factors or technologies, the optimization problem will dictate that the lowest cost technology is used to meet all demand in each sector. Other conditions may be added to the objective function problem, such as factor endowments or maximum capacities for different technologies. This increases the complexity of the optimization problem and increases the likelihood that there will be no solution. On its own, RCOT is not a complete framework for LCA, as it does not characterize the environmental impacts of the elements of the input-output matrix, nor does it specify a functional unit. However, given that input-output matrices are used to compute life cycle inventories (Heijungs and Suh 2002; Suh and Kagawa 2005), the RCOT model can be readily integrated into an LCA computational structure.

This leads to the TCM, which is the integration of RCOT into the matrix formulation of LCA (Kätelhön et al. 2016). Integration is achieved by introducing a scaling vector for the activity levels of the sectors in the economy needed to achieve the functional unit of the LCA. The rectangular environmental matrix *B* is introduced, which contains the direct flows to and from the environment from each process option in all sectors. One can proceed by using a characterization model to produce environmental impact indicators as would be done in any LCA. The difference is that the *A* matrix is rectangular and the ratios of the activity levels for multiple technologies available in a given sector has been optimized using the RCOT model. By using Monte Carlo simulation to perturb the input parameters to TCM, the authors propose what they call “stochastic TCM” as a model for CLCA that addresses both technology choice optimization and uncertainty analysis. In the context of CLCA, TCM is a

pathway for the identification of marginal technologies, which aligns with the strengths of system dynamics.

1.3.3.1 Applications

Springer and Duchin (2014) apply the RCOT model along with the World Trade Model (Duchin 2005) to tackle the question of how to feed a population of nine billion under various scenarios. The required increase in agricultural production in 2050 compared with baseline levels in 2000 for three regions (Africa, Latin America, and Rest of World) is estimated. The authors find that feeding nine billion is possible, even when accounting for increases in daily caloric intake in developing countries, when all usable land and water on earth are made available and agricultural technologies remain constant everywhere. However, once the available land is constrained to exclude clearing additional forests and available water is reduced to 20% of "renewable supply", the model has no solution with all other variables held constant. In subsequent scenario analyses, the paper concludes that lowering caloric intake in developed countries and improving agricultural technologies to reduce land requirements provides a solution even when land and water use are restricted. All scenarios with a solution require increasing agricultural production in Africa by at least 400%.

Kätelhön et al. (2016) use the stochastic TCM to explore a hypothetical case of rice production, in particular the source of thermal energy, and how the climate change impacts vary with different factor constraints. The authors also analyze the uncertainty introduced when there are deviations from the optimized technology mix generated using RCOT. The analysis shows that the climate change impact per kilogram of rice production rises from 0.9 to 1.3 kg CO_2e/kg when the lowest-cost fuel (local rice husk) for thermal energy becomes

constrained. Alternative fuel sources must be imported from long distances, and when demand is high enough natural gas and wood pellets become part of the mix. Using TCM, the authors also show that the average climate change impact per functional unit of rice production is substantially lower than the marginal climate change impact.

1.3.3.2 Advantages & Disadvantages

The constraint modelling is a key advantage in using the RCOT model to examine the environmental consequences of actions. It helps us to determine what combinations of technologies are needed to meet our combination of economic and environmental objectives, given the assumption that the input and factor cost structures are realistic. In theory, this would allow us to examine seemingly infinite scenarios where different types of pollution are capped at different levels, for example, in an effort to determine whether or not such caps are actually reasonable given a certain level of final demand. Then, one could add another constraint stating that a certain low pollution technology is constrained in its production capacity and see whether or not a solution still exists. From there, insights may be gained regarding the need to add additional capacity of certain technologies or modify the endowments of certain factors in order to meet our objectives. This has great appeal in terms of informing policy decisions.

While the RCOT model is quite powerful, it still has limitations in the context of CLCA. The RCOT model does not account for potential technology learning curves, or the idea that the inputs and factors of a given technology may not scale linearly with activity levels. According to Springer and Duchin (2014), the data to produce factor endowments, a key component of the RCOT model, are scarce. Therefore, their values may be highly uncertain. Inputs for the base sectors in Springer and Duchin (2014) are pulled from the year 2000,

introducing a significant time lag in the baseline input structures and factors of production. One other limitation is the use of static factor prices. In the agricultural example, this means that a factor price was assigned today to arable land and renewable water in 2050. Given that water is a commodity with a distorted market, one could imagine that the factor price may change quite a bit between today and 2050. The use of static factor prices also reduces confidence in a cause-and-effect interpretation of the results.

1.3.4 **Agent-Based Models**

Agent-based computational economics (ACE) is an emerging approach to modelling emergent properties of complex systems that are influenced by human interaction. Agents are discrete units that behave according to a set of pre-programmed rules. Agents' behavior may also be influenced by learning outcomes via artificial intelligence, over a series of iterations. The goals of agent-based studies range from determining the optimal strategy of a basic economic game to learning-based adoption of new technologies (Chen 2011; Ringler et al. 2016).

The assumptions that go into ACE modelling vary along an extremely broad spectrum. Chen (2011) provides a detailed review of the types of agents that exist and what assumptions go into each. The most basic type of agents is zero-intelligence, or randomly behaving agents. These agents make random decisions, with some probability of following the decisions of neighbors, but lack the ability to learn. They may interact with agents that have minimal intelligence and follow along, with emergent properties emulating the behavior of swarms of insects.

On the next level of complexity, there are agents that have the ability to learn and make non-random decisions. The second broad category agents described in Chen (2011) are

human programmed agents. The origins of this type of agents are economic tournaments such as Iterated Prisoner's Dilemma tournaments, where participants submitted individually programmed agents with unique algorithms to compete against one another in the game. Thus, human programmed agents are just that – assigned a set of rules by a human programmer for how they interact with each other, the simulated environment, and the decisions at hand in a particular game or analysis. They are unable to learn autonomously, i.e. beyond the learning rules generated from their initial programming. The third broad category of agents is autonomous agents, which are initialized by humans but able to learn thereafter without human intervention.

1.3.4.1 Applications

Querini and Benetto (2015, 2014) use ACE to compute LCIs for mobility systems under a number of simulated responses to policy and call it a form of CLCA. The policy interventions pertain to the adoption of hybrid and electric vehicles. There are an unknown number of parameters used to calibrate the agents, but their sensitivity analysis involves varying at least 23 different parameters. These range from agents' initial attitudes towards HEVs and BEVs, driving habits, prices of electricity and charging infrastructure ability, among others. LCAs are performed for every vehicle purchased, used and discarded by the agents in the period 2013-2020 in Luxembourg and Lorraine, in order to contrast two locations with different electricity grid mixes. The results suggest that large scale adoption of Battery Electric Vehicles (BEVs) may decrease global warming impacts and depletion of fossil resources, but increase impacts in other categories such as metal depletion and ionizing radiation because of battery production. In the ACE model, the rate at which BEVs

are adopted depends on simulated preferences and attitudes toward the environment, and not purely price-quantity relationships.

Zhao et al. (2011) hybridize ACE and system dynamics to assess the adoption of solar PV systems. This implementation of ACE includes the effects of advertising and sharing of information between agents and their electricity consumption behavior. The specific policy interventions examined in the study are Investment Tax Credits and Feed-In Tariffs in both New York City and Tuscon, Arizona. Real demographic data from the two localities are used to program some parameters for the ACE simulation. Feedback loops between PV systems and the electricity grid are modelled using system dyanmics based on the timing and intensity of electricity usage inferred via the patterns determined by the ACE simulation. The results suggest that residents in New York City are less responsive to PV adoption incentives than those in Tucson. This is partially attributed to the lower average daily solar power generation capacity in New York, but could also be because agents in such a large city are programmed to be less interactive.

Davis et al. (2009) suggest an integrated feedback loop between an LCA model and ACE, pointing out that they are both "tools that employ systems approaches." Furthermore, LCA (when the system is represented as a technology matrix) and ACE are both interconnected networks that behave according to a set of programmed relationships. However, the technology matrix in a traditional LCA framework is static, whereas the relationships simulated in ACE are dynamic. The authors suggest that ACE can be used to simulate the formation of supply chains, and that at each step of the simulation one can perform an LCA by inverting the *A* matrix of each agent in the simulated supply chain. In turn, the environmental impacts can be fed back to the agents as inputs for the next step of

the simulation. The functionality of the model is demonstrated in a hypothetical case study of increasing electricity demand that is met with bio-based electricity feedstocks. A CO_2 tax is simulated along with various bio-based electricity feedstocks that have different price-quantity curves. As electricity demand increases, new electricity producers enter the market using feedstocks that are determined by their decision making process in the ACE model. The simulation shows that agents programmed with a profit-maximizing decision-making process behave differently than those that aim to minimze GWP. All of these applications explicitly address the inclusion of social processes into CLCA.

1.3.4.2 Advantages & Disadvantages

A benefit offered by ACE to CLCA is the ability to include effects that emerge from communication between a network of agents, such as technology adoption, into LCA models. A traditional LCA contains very limited insight into the effects of behavior. Properties beyond price signals, such as those associated with consumer preferences and community demographics, can be incorporated into the LCA domain. In this sense, ACE results may both include the signals captured by economic equilibrium models, but also account for additional non-price factors influenceing market behavior.

One potential disadvantage of the use of ACE is the level of complexity, and resulting lack of transparency in the model behavior. The number of parameters used to initialize an ACE model can be in the hundreds, or even the thousands. This makes it challenging for the outside audience to understand how well the simulation reflects reality. This contrasts with other models explored here, such as PEMs and the RCOT model, which have a simpler set of governing equations. This does not mean PEMs and RCOT are a better reflection of reality; it simply implies that the path to assessing this is sometimes clearer. Thus, it seems

ACE is most appropriate for approaching localized questions, where large sets of parameters are reasonable to research. For instance, studying EV adoption in a locale such as Luxembourg may be feasible, but in the United States the driving habits and attitudes vary so widely that one would have great difficulty defining the baseline set of parameters, especially regarding habits and attitudes. Zhao et al. (2011) is also an example of how ACE can be a powerful tool to help us understand the environmental consequences of policies. However, it also shows that one may need to combine ACE with other approaches to obtain meaningful results for a CLCA.

1.4 Causal Inference

The reviewed models from Section 2 provide structures and parameter sets for evaluating the environmental consequences of changes to product systems. However, these structures do not explicitly address the empirical proof of causal relationships. To some extent, economic equilibrium models can be considered an exception to this. The price response coefficients used in economic equilibrium models are derived using instrumental variables regression analysis, which fits under the umbrella of causal inference from observational data. However, performing this analysis is generally not a part of the application of economic equilibrium in CLCA, with the exception of Zink et al. (2017). In all other cases, previously determined price responses are input into the economic equilibrium structure. However, the world of causal inference is much broader than instrumental variables regression, and much of its potential is untapped as of today in CLCA. In general, observational settings are scarcely addressed in this domain; thus I introduce an observational component to my review herein.

Causal inference is the exercise of testing hypotheses regarding cause-effect relationships using observations of the past. This can be achieved, for example, by finding "natural experiments" in observational data. A natural experiment is analyzed through the lens of Rubin's causal model. Rubin's framework relies on the construction of counterfactuals which represent an outcome of interest in a treatment group in if it were in an untreated state (Rubin 1974). Since a single unit cannot be in a treatment state and control state simultaneously, counterfactuals are unobserved. Natural experiments utilize relationships between treatment and control groups to provide estimates of these counterfactuals. Treatment effects in this framework are a function of the difference between treated observations and the estimates of their unobserved counterfactuals. As has been noted before, this presents a challenge in the case of sustainability science because we only have one planet in which to test policy (Cucurachi and Suh 2017, 2015). Given the absence of parallel worlds, I am unable to form treatment and control groups at the planetary level in order to establish global treatment effects due to policies. However, causal inference can be used to inform environmental policy by examining heterogeneity in responses to sustainability interventions across space and time in subsets of the planetary population. The research requires defensible arguments that some segments of the population are suitable counterfactuals for others under a particular policy regime.

There are a number of statistical strategies that can be used to perform causal inference in an observational setting. The choice of method depends on the data structures, the problem at hand, and the type of treatment effect to be analyzed (i.e. average treatment effect in the population vs. average treatment effect on the treated). Natural experiments may be analyzed using statistical techniques including, but not limited to, difference-in-

differences, propensity score methods, instrumental variables, matrix completion methods, and regression discontinuity (Angrist and Pischke 2009; Caliendo and Kopeinig 2005; Imbens and Lemieux 2007; Angrist et al. 1996; Stock 2001; Athey and Imbens 2016).

In chapter 3 of this dissertation, I suggest that avoided primary production caused by recycling could be estimated by analyzing a natural experiment where a subset of firms in a given sector is exposed to a recycling policy. If those firms are well matched with others in the sector, a difference-in-differences approach could be used to estimate how much primary material is avoided by each kilogram of additional recycled supply (Palazzo et al. 2019). In general, LCA results can be quite sensitive to the amount of primary material avoided from recycling (Mcmillan et al. 2012; Weidema 2003; Geyer et al. 2015; Geyer 2008; Ekvall 2000). This quantity has also been identified as a key issue in the development of CLCA methodology (Koffler and Finkbeiner 2018; Yang 2016; Zink et al. 2015).

The main advantage of using causal inference in CLCA is that it provides a pathway to estimating the treatment effects of policies using empirical data. This is a more direct measure of causality in a system compared with simulation-based models such as system dynamics and ACE. On the other hand, defensible treatment and control groups are hard to come by in observational settings. The treatment effects are also based on our past observations, which introduce challenges for projecting the significance of findings for future policy decisions.

1.5 Discussion

1.5.1 Strengths and weaknesses of structural CLCA models

Given the aspiration of CLCA to support decision-making by quantifying the environmental consequences of actions, it is important not to restrict the analysis space to

any one particular method. I have shown that there are a plethora of methods available to characterize consequences, which have unique sets of advantages and disadvantages. One aspect of the path forward for CLCA is then to identify the pieces of life cycle inventories that are most sensitive to the social and economic phenomena that are not included in a traditional ALCA or required by the ISO standards. Once those aspects of the LCI are identified, a model is designed using the most appropriate method for the problems at hand and the data available. This piecewise approach is evident in many of the papers reviewed here, whereas others endorse a certain technique as a comprehensive framework for CLCA. The use of one methodology exclusively limits the potential of CLCA due to the diversity in social and economic mechanisms that potentially affect LCA outcomes. Thus, before designing the cause-effect research for a CLCA, one must accumulate detailed knowledge of the dynamics of the particular policy intervention and product system(s) affected. This allows for an investigation of the optimal methods for quantifying the key consequential effects, for which this review serves as one potential guide. Table 1.1 solidifies this by providing a summary of the aspects of CLCA addressed to date in the literature using the reviewed models, as well as the referenced studies that use each one.

Model	Applications Reviewed	Aspects of CLCA addressed	Aspects of CLCA not addressed
Economic Equilibrium	Ekvall 2000 Ekvall and Andrae 2006 Searchinger et al. 2008 Marvuglia et al.	• System expansion • Effects of macro-scale price and quantity changes	• Non-price social mechanisms • Time dimension • Innovation and technology change • Identification of marginal technologies

	2013 Rajagopal 2016 Zink et al. 2017		
System Dynamics	Mclaren et al. 1999 Ford 2001 Stasinopoulos et al. 2012 Yao et al. 2018	• Identification of marginal technologies • Time dimension • Innovation and technology change	• System expansion • Social Mechanisms (price or non-price)
Technology Choice	Springer and Duchin 2014 Kätelhön et al. 2016	• Identification of marginal technologies • Effects of micro-scale price and quantity changes • Innovation and technology change	• System expansion • Time dimension • Non-price social mechanisms
Agent-Based	Davis et al. 2009 Zhao et al. 2011 Querini and Benetto 2014, 2015	• Identification of marginal technologies • Both price and non-price social mechanisms	• System expansion • Innovation and technology change

Table 1.1: A summary of the applications of structural models reviewed in this paper. I highlight the aspects of CLCA that are addressed and not addressed to date using these methods.

From this, I can infer several additional insights. For example, economic equilibrium models are desirable when it comes to the kind of questions that involve macro-scale changes that significantly affect the price and quantity such as fiscal reform and tariffs. These models also explicitly address the issue of co-production in LCA using a cause-effect lens, which is not as clear in the other models reviewed. However, GEMs or PEMs are limited to economic systems and do not address population increase, innovation &

technology change, where system dynamics and the TCM showed strengths. Agent-based models are particularly effective when the non-price social mechanisms such as communication among agents are of concern. This is not handled adequately by any other models reviewed. Finally, the TCM's strength lies in the situation where detailed technological specification and costs are known, and when the level of detail goes beyond what GEM or PEM generally deal with.

1.5.2 **Combining structural models and causal inference**

What all of the reviewed structural models have in common is that they start with a set of input parameters, which are then subject to a set of transformations to generate components of a life cycle inventory. However, it is scarcely pointed out that regardless of the complexity of the structural model, its output can be viewed as a point of departure for an uncertainty analysis of the environmental consequences of changes to product systems. Thus, a critical component of combining structural models and causal inference is the quantification of contributions to uncertainty from the inputs to structural models. This can be achieved via local (i.e. one-at-a-time) and/or global (i.e. Monte Carlo) uncertainty analysis.

Figure 1.1 presents three conceptual frameworks of how researchers can combine structural CLCA models with causal inference analysis in order to produce conclusions and future research directions. In framework (a), LCA models are developed in parallel with empirical work regarding the environmental consequences of actions, but in some cases the insights and conclusions complement one another. This resembles how literature on the environmental benefits of energy-efficient technologies has developed. One example is the environmental assessment of efficient vehicle powertrain technologies. There are many

existing LCA studies that examine this based on technical input-output relationships (Granovskii et al. 2006; Hawkins et al. 2013; Samaras and Meisterling 2008). In parallel, a substantial effort has been made to empirically estimate the degree to which consumers may respond to reduced fuel expenditures per mile by driving more, a market-mediated mechanism known as direct rebound (Sorrell et al. 2009). However, market-mediated mechanisms are not included in the initial LCAs. Insights into the environmental consequences of efficient powertrains are taken in parallel from the two lines of literature.

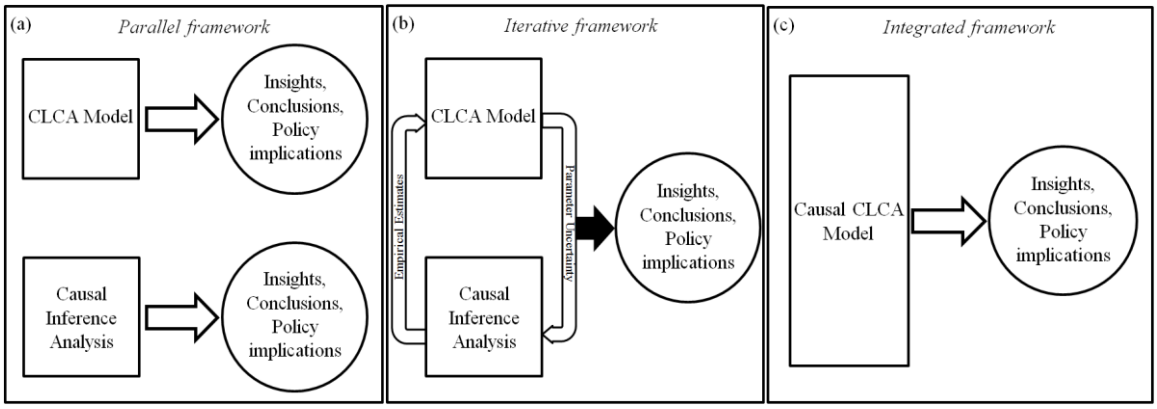

Figure 1.1: Three conceptual frameworks of how one could combine structural CLCA models with causal inference. Panel (a), the parallel framework, is most reflective of historical practice. Panel (b), the iterative framework, is the path forward recommended from this review. Panel (c), the integrated framework, is a hypothetical case where an entire LCA model is built using a causal inference approach.

To illustrate framework (b), the iterative framework, I return to the example of quantifying displaced primary material impacts caused by recycling. In chapter 2 of this dissertation, I demonstrate the application of framework (b) in a CLCA model of vehicle light-weighting via material substitution. Displacement is integrated into my model using a market-mediated mechanism. The parameter values associated with the market-mediated flows are substantial contributors to the high variance in model outcomes. One of the

reasons for this is that the underlying uncertainties in this causal effect are poorly understood. A suggested item for future research in automotive material substitution is then to conduct statistical inference to inform the underlying distribution of displacement, for example by using the methods described in chapters 3 and 4. Theoretically, updated distributions can be cycled back into the model and possibly have an effect on its interpretation. Building additional market forces related to material production and the use phase into the model using robust parameterization is another suggestion for moving forward in this research along the direction posed by framework (b).

Framework (c) is an idealistic aspiration that uses causal inference to identify all of the parameters in an LCA model. In essence, this amounts to constructing statistical counterfactuals for entire life cycle inventories that have been subject to an exogenous change. Given the number of parameters that are generally included in LCA modelling, this is an unrealistic approach for providing policy-relevant guidance in a timely manner. Such a causal LCA model has not been produced as of today.

1.5.3 **Conclusions**

My suggestions for future directions in CLCA emphasize a development path focused on cause-and-effect analysis. There are myriad proposals for how to structure a CLCA model, and what the input parameters should be. However, research into the causal mechanisms and uncertainties that inform these parameters is just beginning. This direction includes work in the observational setting using natural experiments and causal inference methods in order to characterize the net environmental impacts of past decisions and increase the predictive power of life cycle inventories. However, it also includes the notion that decisions or policies aiming to reduce environmental impacts are sometimes rolled out heterogeneously

through time and space. In this sense, I envision a future where, when possible, policies are intentionally rolled out in a way that creates the opportunity to analyze treatment effects across environmental impact indicators. When this is not possible, I encourage practitioners of CLCA to seek out natural experiments in response to the sources of uncertainty in their structural models, and design research to estimate treatment effects. These treatment effects provide critical information about the values and uncertainties in parameters that underpin CLCA models. This approach captures the essence of idealized CLCA; that we accumulate maximum knowledge of cause-and-effect relationships between changes to industrial systems and the natural environment over time. The subsequent chapters of this dissertation illustrate my attempt to evolve CLCA practice in the spirit of this review and its conclusions.

1.6 References

Ahmad, S., Mat, R., Muhammad-sukki, F., Bakar, A., 2016. Application of system dynamics approach in electricity sector modelling : A review. Renew. Sustain. Energy Rev. 56, 29–37. doi:10.1016/j.rser.2015.11.034

Anex, R., Lifset, R., 2014. Life Cycle Assessment: Different Models for Different Purposes. J. Ind. Ecol. 18, 321–323. doi:10.2166/wst.2011.258

Angerhofer, B.J., Angelides, M.C., 2000. System dynamics modelling in supply chain management: research review, in: Winter Simulation Conference. pp. 342–351. doi:10.1109/WSC.2000.899737

Angrist, J., Pischke, J.-S., 2009. Parallel worlds: Fixed effects, differences-in-differences and panel data, in: Mostly Harmless Econometrics: An Empiricist's Companion.

Angrist, J.D., Imbens, G.W., Rubin, D.B., 1996. Identification of Causal Effects Using

Instrumental Variables Identification of Causal Effects Using Instrumental Variables. J. Am. Stat. Assoc. 91, 444–455. doi:10.1080/01621459.1996.10476902

Arrow, K.J., Debreu, G., 1954. Existence of an Equilibrium for a Competitve Economy. Econometrica 22, 265–290.

Athey, S., Imbens, G., 2016. The State of Applied Econometrics - Causality and Policy Evaluation. J. Econ. Perspect. 31, 3–32. doi:10.1257/jep.31.2.3

Blomberg, J., Hellmer, S., 2000. Short-run demand and supply elasticities in the West European market for secondary aluminium. Resour. Policy 26, 39–50.

Brandão, M., Clift, R., Cowie, A., Greenhalgh, S., 2014. The Use of Life Cycle Assessment in the Support of Robust (Climate) Policy Making: Comment on "Using Attributional Life Cycle Assessment to Estimate Climate-Change Mitigation..." J. Ind. Ecol. 18, 461–463. doi:10.1111/jiec.12152

Caliendo, M., Kopeinig, S., 2005. Some practical guidance for the implementation of propensity score matching. Inst. Study Labor 1–29.

Cardenete, M.A., 2012. An Overview of General Equilibrium Theory, in: Applied General Equilibrium. Springer-Verlag, Berlin.

Chen, S., 2011. Varieties of agents in agent-based computational economics : A historical and an interdisciplinary perspective. J. Econ. Dyn. Control 1–25. doi:10.1016/j.jedc.2011.09.003

Cucurachi, S., Suh, S., 2017. Cause-effect analysis for sustainable development policy. Environ. Rev. 379, er-2016-0109. doi:10.1139/er-2016-0109

Cucurachi, S., Suh, S., 2015. A Moonshot for Sustainability Assessment. Environ. Sci. Technol. 49, 9497–9498. doi:10.1021/acs.est.5b02960

Curran, M.A., Mann, M., Norris, G., 2002. Report on the International Workshop on Electricity Data for Life Cycle Inventories. National Renewable Energy Laboratory, Cincinatti, Ohio.

Dale, B.E., Kim, S., 2014. Can the Predictions of Consequential Life Cycle Assessment Be Tested in the Real World? Comment on "Using Attributional Life Cycle Assessment to Estimate Climate-Change Mitigation..." J. Ind. Ecol. 18, 466–467. doi:10.1111/jiec.12151

Davis, C., Nikolíc, I., Dijkema, G.P.J., 2009. Integration of life cycle assessment into agent-based modeling toward informed decisions on evolving infrastructure systems. J. Ind. Ecol. 13, 306–325. doi:10.1111/j.1530-9290.2009.00122.x

Duchin, F., 2005. A world trade model based on comparative advantage with m regions, n goods, and k factors. Econ. Syst. Res. 17, 141–162. doi:10.1080/09535310500114903

Duchin, F., Levine, S.H., 2012. The rectangular sector-by-technology model : not every economy produces every product and some products may rely on several technologies simultaneously. J. Econ. Struct. 1, 1–11. doi:10.1186/2193-2409-1-3

Duchin, F., Levine, S.H., 2011. Sectors may use multiple technologies simultaneously: The Rectangular Choice of Technology model with binding factor constraints (revised). Rensselaer Work. Pap. Econ. 1–25.

Earles, J.M., Halog, A., 2011. Consequential life cycle assessment: a review. Int. J. Life Cycle Assess. 16, 445–453. doi:10.1007/s11367-011-0275-9

Ekvall, T., 2000. A market-based approach to allocation at open-loop recycling. Resour. Conserv. Recycl. 29, 91–109.

Ekvall, T., Andrae, A., 2006. Attributional and Consequential Environmental Assessment of

the Shift to Lead-Free Solders. Int. J. Life Cycle Assess. 11, 344–353.

Ekvall, T., Azapagic, A., Finnveden, G., Rydberg, T., Weidema, B.P., Zamagni, A., 2016. Attributional and consequential LCA in the ILCD handbook. Int. J. Life Cycle Assess. 21, 293–296. doi:10.1007/s11367-015-1026-0

Ekvall, T., Weidema, B.P., 2004. System boundaries and input data in consequential life cycle inventory analysis. Int. J. Life Cycle Assess. 9, 161–171. doi:DOI 10.1065/lca2004.03.148

Farrell, A.E., Plevin, R.J., Turner, B.T., Jones, A.D., O'Hare, M., Kammen, D.M., 2006. Ethanol can contribute to energy and environmental goals. Science (80-.). 311, 506–508. doi:10.1126/science.1121416

Ford, A., 2001. Waiting for the boom: a simulation study of power plant construction in California. Energy Policy 29, 847–869. doi:10.1016/S0301-4215(01)00035-0

Forrester, J.W., 1989. The Beginning of System Dynamics.

Forrester, J.W., 1958. Industrial Dynamics: A Major Breakthrough for Decision Makers. Harv. Bus. Rev. 36, 37–66.

Geyer, R., 2008. Parametric Assessment of Climate Change Impacts of Automotive Material Substitution. Environ. Sci. Technol. 42, 6973–6979.

Geyer, R., Kuczenski, B., Zink, T., Henderson, A., 2015. Common Misconceptions about Recycling. J. Ind. Ecol. 0, 1–8. doi:10.1111/jiec.12355

Gohin, A., Moschini, G., 2006. Evaluating the market and welfare impacts of agricultural policies in developed countries: Comparison of partial and general equilibrium measures. Rev. Agric. Econ. 28, 195–211. doi:10.1111/j.1467-9353.2006.00281.x

Granovskii, M., Dincer, I., Rosen, M.A., 2006. Life cycle assessment of hydrogen fuel cell

and gasoline vehicles. Int. J. Hydrogen Energy 31, 337–352. doi:10.1016/j.ijhydene.2005.10.004

Hao, H., Geng, Y., Hang, W., 2015. GHG emissions from primary aluminum production in China : Regional disparity and policy implications. Appl. Energy. doi:10.1016/j.apenergy.2015.05.056

Hawkins, T.R., Singh, B., Majeau-Bettez, G., Strømman, A.H., 2013. Comparative Environmental Life Cycle Assessment of Conventional and Electric Vehicles. J. Ind. Ecol. 17, 53–64. doi:10.1111/j.1530-9290.2012.00532.x

Heijungs, R., Suh, S., 2002. The Computational Structure of Life Cycle Assessment. Kluwer Academic, Dordrecht, Netherlands.

Hertel, T.W., Tsigas, M.E., 1997. Structure of GTAP, Global Trade Analysis: Modeling and Applications. doi:10.1126/science.1146886

Imbens, G., Lemieux, T., 2007. Regression Discontinuity Designs: A Guide to Practice, NBER Working Series.

Katelhon, A., Assen, N. Von Der, Suh, S., Jung, J., Bardow, A., 2015. Industry-Cost-Curve Approach for Modeling the Environmental Impact of Introducing New Technologies in Life Cycle Assessment. Environ. Sci. Technol. 49, 7543–7551. doi:10.1021/es5056512

Kätelhön, A., Bardow, A., Suh, S., 2016. Stochastic Technology Choice Model for Consequential Life Cycle Assessment. Environ. Sci. Technol. 50, 12575–12583. doi:10.1021/acs.est.6b04270

Koffler, C., Finkbeiner, M., 2018. Are we still keeping it “real”? Proposing a revised paradigm for recycling credits in attributional life cycle assessment. Int. J. Life Cycle Assess. 23, 181–190.

Macedo, I.D.C., Leal, M.R.L.V., Silva, J.E.A.R. Da, 2004. Assessment of greenhouse gas emissions in the production and use of fuel ethanol in Brazil.

Majeau-bettez, G., Wood, R., Strømman, A.H., 2014. Unified Theory of Allocations and Constructs in Life Cycle Assessment and Input-Output Analysis. J. Ind. Ecol. 18, 747–770. doi:10.1111/jiec.12142

Marvuglia, A., Benetto, E., Rege, S., Jury, C., 2013. Modelling approaches for consequential life-cycle assessment (C-LCA) of bioenergy: Critical review and proposed framework for biogas production. Renew. Sustain. Energy Rev. 25, 768–781. doi:10.1016/j.rser.2013.04.031

Mclaren, J., Wright, L., Parkinson, S., Jackson, T., 1999. A Dynamic Life-Cycle Energy Model of Mobile Phone Take-back and Recycling. J. Ind. Ecol. 3, 77–91.

Mcmillan, C.A., Skerlos, S.J., Keoleian, G.A., 2012. Evaluation of the Metals Industry's Position on Recycling and its Implications for Environmental Emissions. J. Ind. Ecol. 16, 324–333. doi:10.1111/j.1530-9290.2012.00483.x

Miller, R., Blair, P.D., 2009. Input-Output Analysis: Foundation & Extensions. Cambridge University Press, New York, New York.

Mitra-kahn, B.H., 2008. Debunking the Myths of Computable General Equilibrium Models (No. 1), Schwartz Center for Economic Policy Analysis and Department of Economics, The New School for Social Research, Working Paper Series, 2008. New York, New York.

Palazzo, J., Geyer, R., 2019. Consequential Life Cycle Assessment of Automotive Material Substitution: Replacing Steel with Aluminum in Production of North American Vehicles. Environ. Impact Assess. Rev. 75, 47–58.

Palazzo, J., Geyer, R., Startz, R., Steigerwald, D.G., 2019. Causal Inference for Quantifying Displaced Primary Production from Recycling. J. Clean. Prod. 210, 1076–1084. doi:10.1016/j.jclepro.2018.11.006

Plevin, R.J., Delucchi, M. a., Creutzig, F., 2014. Using Attributional Life Cycle Assessment to Estimate Climate-Change Mitigation Benefits Misleads Policy Makers. J. Ind. Ecol. 18, 73–83. doi:10.1111/jiec.12074

Querini, F., Benetto, E., 2014. Agent-based modelling for assessing hybrid and electric cars deployment policies in Luxembourg and Lorraine. Transp. Res. Part A 70, 149–161. doi:10.1016/j.tra.2014.10.017

Querini, F., Benetto, E., 2015. Combining Agent-Based Modeling and Life Cycle Assessment for the Evaluation of Mobility Policies. Environ. Sci. Technol. 49, 1744–1751. doi:10.1021/es5060868

Rajagopal, D., 2016. A Step Towards a General Framework for Consequential Life Cycle Assessment. J. Ind. Ecol. 0. doi:10.1111/jiec.12433

Rajagopal, D., 2014. Consequential life cycle assessment of policy vulnerability to price effects. J. Ind. Ecol. 18, 164–175. doi:10.1111/jiec.12058

Ringler, P., Keles, D., Fichtner, W., 2016. Agent-based modelling and simulation of smart electricity grids and markets - A literature review. Renew. Sustain. Energy Rev. 57, 205–215. doi:10.1016/j.rser.2015.12.169

Rose, A., 1995. Input-output economics and computable general equilibrium models. Struct. Chang. Econ. Dyn. 6, 295–304. doi:10.1016/0954-349X(95)00018-I

Rubin, D.B., 1974. Estimating Causal Effects of Treatments in Randomized and Nonrandomized Studies. J. Educ. Psychol. 66, 688–701.

Samaras, C., Meisterling, K., 2008. Life Cycle Assessment of Greenhouse Gas Emissions from Plug-in Hybrid Vehicles: Implications for Policy. Environ. Sci. Technol. 42, 3170–3176. doi:10.1021/es702178s

Scarf, H., 1967. On the Computation of Equilibrium Prices (No. 232), Cowles Foundation Discussion Paper No. 232.

Searchinger, T., Heimlich, R., Houghton, R.A., Dong, F., Elobeid, A., Fabiosa, J., Tokgoz, S., Hayes, D., Yu, T., 2008. Use of U.S. Croplands for Biofuels Increases Greenhouse Gases Through Emissions from Land-Use Change. Science (80-.). 423, 1238–1241.

Sorrell, S., Dimitropoulos, J., Sommerville, M., 2009. Empirical estimates of the direct rebound effect: A review. Energy Policy 37, 1356–1371. doi:10.1016/j.enpol.2008.11.026

Springer, N.P., Duchin, F., 2014. Feeding Nine Billion People Sustainably : Conserving Land and Water through Shifting Diets and Changes in Technologies. Environ. Sci. Technol. 48, 4444–4451.

Stasinopoulos, P., Compston, P., Newell, B., Jones, H.M., 2012. A system dynamics approach in LCA to account for temporal effects-a consequential energy LCI of car body-in-whites. Int. J. Life Cycle Assess. 17, 199–207. doi:10.1007/s11367-011-0344-0

State of Hawai'i, 2008. Hawai'i 2050 Sustainability Plan [WWW Document]. URL http://www.oahumpo.org/wp-content/uploads/2013/02/Hawaii2050_Plan_FINAL.pdf (accessed 3.5.18).

Stigler, G., 1957. Perfect Competition, Historically Contemplated. J. Polit. Econ. 65, 1–17.

Stock, J.H., 2001. Instrumental Variables in Statistics and Econometrics, 2nd Editio. ed,

International Encyclopedia of the Social & Behavioral Sciences. Elsevier. doi:10.1016/B978-0-08-097086-8.42037-4

Suh, S., Huppes, G., 2005. Methods for Life Cycle Inventory of a product. J. Clean. Prod. 13, 687–697. doi:10.1016/j.jclepro.2003.04.001

Suh, S., Kagawa, S., 2005. Industrial ecology and input-output economics : an introduction. Econ. Syst. Res. 17, 349–364. doi:10.1080/09535310500283476

Suh, S., Yang, Y., 2014. On the uncanny capabilities of consequential LCA. Int. J. Life Cycle Assess. doi:10.1007/s11367-014-0739-9

Tillman, A.M., 2000. Significance of decision-making for LCA methodology. Environ. Impact Assess. Rev. 20, 113–123. doi:10.1016/S0195-9255(99)00035-9

United Nations, 2015. Transforming our world: the 2030 agenda for sustainable development [WWW Document]. URL https://sustainabledevelopment.un.org/post2015/transformingourworld (accessed 3.5.18).

University of California, 2017. Zero Waste 2020 [WWW Document]. URL https://zerowaste2020.universityofcalifornia.edu/ (accessed 3.5.18).

Walrus, L., 1900. Éléments d'économie politique pure, 4th editio. ed. Paris, France.

Wang, M., Saricks, C., Santini, D., 1999. Effects of Fuel Ethanol Use on Fuel-Cycle Energy and Greenhouse Gas Emissions. Argonne, Illinois. doi:10.2172/4742

Weidema, B., 2001. Avoiding Co-Product Allocation in Life-Cycle Assessment. J. Ind. Ecol. 4, 11–33.

Weidema, B.P., 2003. Market information in life cycle assessment, Danish Ministry of the Environment. Copenhagen, Denmark.

Weidema, B.P., 1993. Market aspects in product life cycle inventory methodology. J. Clean. Prod. 1, 161–166.

Wooldridge, J.M., 2012. Simultanenous Equation Models, in: Introductary Econometrics, A Modern Approach. pp. 554–582.

Yang, Y., 2016. Two sides of the same coin: consequential life cycle assessment based on the attributional framework. J. Clean. Prod. 127, 274–281. doi:10.1016/j.jclepro.2016.03.089

Yang, Y., Heijungs, R., 2017. On the use of different models for consequential life cycle assessment. Int. J. Life Cycle Assess. 751–758. doi:10.1007/s11367-017-1337-4

Yao, L., Liu, T., Chen, X., Mahdi, M., Ni, J., 2018. An Integrated Method of Life-cycle Assessment and System Dynamics for Waste Mobile Phone Management and Recycling in China. J. Clean. Prod. 187, 852–862. doi:10.1016/j.jclepro.2018.03.195

Zamagni, A., Guinée, J., Heijungs, R., Masoni, P., Raggi, A., 2012. Lights and shadows in consequential LCA. Int. J. Life Cycle Assess. 17, 904–918. doi:10.1007/s11367-012-0423-x

Zhao, J., Mazhari, E., Celik, N., Son, Y.-J., 2011. Hybrid agent-based simulation for policy evaluation of solar power generation systems. Simul. Model. Pract. Theory 19, 2189–2205. doi:10.1016/j.simpat.2011.07.005

Zink, T., Geyer, R., Startz, R., 2017. Toward Estimating Displaced Primary Production from Recycling: A Case Study of U.S. Aluminum. J. Ind. Ecol. 0, 1–13. doi:10.1111/jiec.12557

Zink, T., Geyer, R., Startz, R., 2015. A Market-Based Framework for Quantifying Displaced Production from Recycling or Reuse. J. Ind. Ecol. 0, 1–11. doi:10.1111/jiec.12317

2. Consequential life cycle assessment of automotive material substitution: replacing steel with aluminum in production of North American vehicles

Reprinted (adapted) with permission from:

Consequential life cycle assessment of automotive material substitution: replacing steel with aluminum in production of North American vehicles

Joseph Palazzo and Roland Geyer.

Environmental Impact Assessment Review. **2019,** 75, 47-58

DOI: 10.1016/j.eiar.2018.12.001

2.1 Abstract

The substitution of aluminum for steel in vehicle body and closure components is a common strategy for reducing fuel consumption. In order to assess the greenhouse gas (GHG) consequences of this decision, the system must be examined using a life cycle approach. Furthermore, attributional life cycle assessment (ALCA) does not suffice for a number of reasons, including the fact that ALCA does not model the incremental system and that allocating the benefits of recycling inhibits the modelling of system-wide consequences caused by the decision studied. This chapter thus uses a consequential life cycle assessment (CLCA) framework. I examine the physical and economic processes that guide the North American light-duty vehicle fleet from its initial state in 2012 to a state in 2050. Industry projections are used to model the production and use phases. The system is expanded to

include the scrap and material markets. This generates new insights regarding the environmental consequences of changes in scrap generation and recycling in automotive material substitution. The method is applied to the fleet in order to forecast if and when aluminum intensification constitutes net GHG reduction under various conditions. Using baseline parameter values compiled from public and industry data; I calculate a GHG payback period of 25 years, i.e. before a net reduction in emissions relative to a no change counterfactual is achieved. A local sensitivity analysis is performed, showing that the net GHG reduction may be achieved in a period as short as 12 years, or never be achieved at all. A global sensitivity analysis is performed using Monte Carlo simulation, where 16% of trials never reach a net reduction in GHG emissions. I also estimate which parameters contribute the most to variance in the model outcomes. The material replacement coefficient, or the amount of aluminum it takes to functionally replace one kilogram of steel, is the top contributor to the variance (29.8%). Overall, the results are most sensitive to parameters governing the amount of mass that can be replaced by each kilogram of additional aluminum, the GHG intensity of additional aluminum production, and the response of the aluminum scrap and material markets to additional aluminum scrap generation. I conclude that given the current lack of understanding of key parameters and their underlying uncertainties, it is not possible to definitively state that substituting aluminum for steel results in a net reduction in GHG emissions from a fleet of vehicles.

2.2 Introduction

2.2.1 Vehicle Emission Standards

In 2012, the United States Department of Transportation released a set of decreasing tailpipe greenhouse gas (GHG) emission targets to be met between 2017 and 2025 (EPA,

2012). While the executive summary mentions that "[…] standards should ultimately reflect a life cycle analysis", there is minimal elaboration on what this means in practice, and the targets are set for the use phase explicitly. A recent European Union vehicle emissions policy update also points out that "Greenhouse gas emissions related to energy supply and vehicle manufacturing and disposal […] are likely to significantly increase in importance in the future" and a proposed amendment to the policy would require manufacturers to report life cycle GHG emissions as of 2025 (Dalli, 2018; European Parliament, 2014). One pervasive strategy for industry compliance with such emission policies is to decrease vehicle mass, and therefore use-phase energy consumption, by replacing steel with a lighter material. There are a number of material options considered by auto manufacturers including aluminum, advanced high-strength steel, magnesium, and polymers with and without carbon reinforcement. Recent market research has projected that the automotive industry will increase its aluminum consumption dramatically and provided detailed forecasts of this trend (Ducker Worldwide, 2015, 2014). The use of aluminum creates the kind of trade-off the quotes above allude to, as the GHG emissions of primary aluminum production range from 6.7-21.7 kg CO_2/kg, which is up to eleven times higher than those of primary steel (European Aluminum, 2018; Hao et al., 2015; Thinkstep, 2015). Reductions in fuel consumption during the use phase help "pay back" the GHG investment, or cause the system to produce net negative GHG emissions relative to a no change counterfactual, but the size of the effect depends on vehicle design decisions and the composition of the fleet. The potential emission savings due to recycling aluminum scrap are a critical component of any environmental assessment of such automotive material substitution, as secondary aluminum ingot production creates just 7-14% of the emissions of its primary equivalent (Hao et al.,

2015; International Aluminum Institute, 2014; The Aluminum Association, 2013; Thinkstep, 2015). Thus, the need for a life cycle perspective is abundantly clear.

2.2.2 Attributional vs. Consequential Life Cycle Assessment of Automotive Materials

Two principal approaches for this type of analysis are identified in the literature: attributional and consequential life cycle assessment (ALCA and CLCA, Curran et al. 2002; Ekvall et al. 2016). In ALCA, a static inventory of inputs and outputs is taken for all processes in the life cycle of a product or service and scaled linearly to a functional unit (Koffler et al., 2014). ALCA inventories typically reflect global or national averages of the involved unit processes (Ekvall and Andrae, 2006). They also solve co-product allocation problems using the ISO hierarchy, frequently severing cause-effect relationships (Ekvall and Finnveden, 2001; ISO, 2006). The static, average, allocated nature of ALCA can inhibit its ability to inform environmental policy (Plevin et al., 2014).

The treatment of recycling as a co-product allocation problem in ALCA studies of automotive material substitution is particularly problematic. Typically, assumed recycling benefits are entirely allocated to either the user or producer of scrap, using the "recycled content" or "avoided burden" methods, respectively (Frischknecht, 2010). When the baseline input data of this study is used in a comprehensive, peer-reviewed model for comparative GHG ALCAs of steel and aluminum body structures, recycled content and avoided burden methods yield opposite conclusions in terms of net GHG emissions (Geyer, 2017). When the results are linearly scaled to North American light duty vehicle production in 2015, i.e. 17.5 million vehicles, the recycled content method results in a net GHG

increase of 22 Mt CO_2eq, while the avoided burden method results in a net GHG decrease of 33 Mt CO_2eq.

Alternatively, CLCA is an emerging technique that assesses the consequences of a change to the life cycle using marginal (or incremental) data and maintaining cause-effect relationships by avoiding allocation (Earles and Halog, 2011; Ekvall and Andrae, 2006; Stasinopoulos et al., 2012; Weidema et al., 2009). The term "marginal" is used for very small changes, and "incremental" for large changes such as the one analyzed here (Ekvall et al., 2016; Weidema et al., 2009). As of today, there are a number of arguments about how exactly CLCA should be done. These included the integration of LCA and market equilibrium models (Earles and Halog, 2011; Ekvall and Weidema, 2004; Rajagopal, 2016), the combination of ALCA and scenario analysis (Yang, 2016), and the merging of LCA with more advanced modelling tools such as system dynamics and agent-based modelling (Florent and Enrico, 2015; Stasinopoulos et al., 2012). In this analysis, I apply CLCA as an examination of the physical and economic processes that are affected by a well-defined change to the studied product system, causing it to evolve over time from its initial state. I identify key consequential parameters and model the sensitivity of the results to their variation, but do not limit the quantification of these parameters to any one particular method. The computational structure is generalizable to any set of materials and any impact category, with the GHG consequences of substituting aluminum for steel in vehicles used as a demonstrative case study.

2.2.3 **Previous LCA Studies of Automotive Material Substitution**

A recent meta-analysis of LCA studies of vehicle light-weighting via material substitution analyzed 33 peer-reviewed articles (Kim and Wallington, 2013). The

harmonization of the results is achieved by applying consistent assumptions to the life cycle inventories. The fact that harmonization parameters include allocation keys shows that the 33 studies and the meta-analysis are rooted in ALCA.

A small number of consequential studies of automotive material substitution are also in the literature. Several authors have modelled time-dependent, non-linear effects across the fleet (Das, 2000; Field et al., 2001; Stasinopoulos et al., 2012). One dynamic fleet-based LCA with detailed stock-and-flow simulations and various aluminum intensification scenarios emphasizes the benefits of moving towards closed-loop aluminum recycling (Modaresi et al., 2014). Other forward looking projections of the energy benefits of light weighting are focused on modelling the production and use phases (Das et al., 2016; Serrenho et al., 2017). Agent-based modelling has also been used to simulate the adoption of electric vehicles in Luxembourg and Lorraine under various policy schemes (Querini and Benetto, 2015). I build upon these studies by examining additional consequential aspects.

In contrast to existing studies, I deploy system expansion to explore the market effects of changes in scrap generation and use. This is a critical point, as prior research has shown that potential GHG savings from aluminum recycling are of the same order of magnitude as the use phase savings due to light-weighting, and that these potential savings are unlikely to be fully realized (Geyer, 2008; Zink et al., 2017). The insights from sensitivity analysis of scrap market parameters introduced in this research are different from those obtained from mechanistic comparisons of open vs. closed-loop recycling. This further supports the view that the distinction between closed- and open-loop recycling is of limited use for LCA in general, as neither one has "intrinsically higher environmental benefits" as pointed out by Geyer et al. (2015). In addition, I model growth in the imported share of incremental North

American primary aluminum due to capacity constraints (Accenture LLC, 2015; IAI, 2018). Finally, industry and government projections of the powertrain composition of the vehicle fleet, which effects the fuel savings per mass savings, are utilized (Ducker Worldwide, 2015, 2014; IEA, 2010; Wohlecker et al., 2007).

The goals of this chapter are four fold: (1) To produce a computational structure for CLCA of automotive material substitution that is generalizable to any set of materials and any impact category; (2) To identify the parameters that contribute most significantly to variation in model outcomes using one-at-a-time sensitivity analysis (OAT-SA) and Monte Carlo simulation; (3) To draw conclusions regarding the environmental consequences of large-scale substitution of aluminum for steel in body and closure components of newly produced vehicles in North America between 2012 and 2050 and; (4) To contribute to the methodological development of CLCA by incorporating economic processes into the model and presenting uncertainty as a decision-relevant finding.

2.3 Methods and data

2.3.1 Functional Unit and Reference Flow

The functional unit of the study consists of the transportation services provided between 2012 and 2050 by all light vehicles produced annually in North America between 2012 and 2050. This implies that not all cars conclude their use phase, since vehicle use and end-of-life (EOL) management after 2050 are excluded. The studied change in this product system is a progressive annual replacement of steel with aluminum in the body and closure parts. Additional aluminum content and production volumes are held constant from 2028 to 2050. This assumption creates a steady state annual emission profile by the end of the modelling period and eases the interpretation of the results. As I show in Appendix A, Figure A.4,

continuing the growth in aluminum production through the entire modelling period does not affect the conclusions of the study, nor does the continuation of modelling beyond 2050. A set of input data compiled from current public and industry sources are used to compute a change in reference flows for the system, from which a net change in greenhouse gas emissions is calculated each year and cumulatively. Herein, I refer to the analysis using these data, which are described in detail with references in Section 2.3.4, as the "baseline" case. The baseline serves as the point of departure for the uncertainty analyses in Section 2.4 and Appendix A. While the model currently uses global warming potentials as the sole impact indicator, it could be readily extended to include additional impact categories; hence I use the generic notation $\boldsymbol{I}^n$ for each major change in impact modelled (e.g. $kg\ CO_2eq$) and I_y^x for impact intensities (e.g. $kg\ CO_2eq/kg\ or\ MJ$).

2.3.2 **System Boundary**

The changes in flows calculated within the system boundary of this model are shown in Figure 2.1. The seven quantities given by $\boldsymbol{I}^n$ capture the main environmental consequences caused by the studied change. Seven distinct system-wide consequences are modelled: Changes in 1) production of the steel and 2) aluminum used in the modeled body and closure parts and the secondary mass savings; 3) the fuel economy of the mass-reduced vehicles; the generation and use of 4) steel and 5) aluminum scrap from material forming processes (termed "prompt" scrap); and the same from 6) steel and 7) aluminum vehicle EOL scrap. All of these consequences occur in response to one studied change, namely the increasing aluminum content of body and closure components in North American light duty vehicles. These consequences are combined into one model in order to gain insights into how this singular change propagates through the components of the system. However, the

computational structure handles the seven changes in impact individually, and in Section 2.4 I explore the uncertainties pertaining to the GHG consequences of changes to individual components of the system. Changes in emissions which are expected to be small, relative to the main consequences that are modelled, are excluded to avoid modelling an indeterminately large number of consequences. The baseline data are an estimate of the incremental process inventory based on the comprehensive set of references described in Section 2.3.4 and detailed explicitly for every input in Section A.3 of Appendix A. I address the uncertainties surrounding the incremental inventory using local and global sensitivity analysis in Section 2.4. System expansion is used to model the economic consequences of changes in the scrap flows into and out of the physical product system as detailed in Figure 2.2. The recycling of prompt and/or EOL scrap can also be modeled in a closed loop, i.e. the scrap is used directly for the production of vehicles in North America.

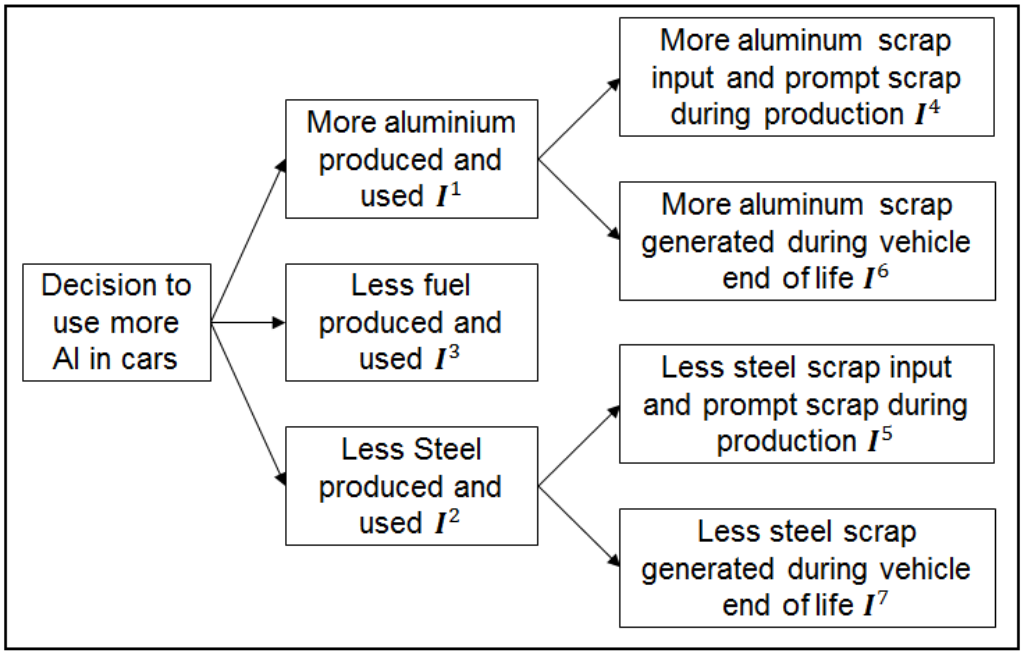

Figure 2.1: The changes in environmental impact calculated in the system boundary of this CLCA model. $\boldsymbol{I}^1$, $\boldsymbol{I}^2$, *and* $\boldsymbol{I}^3$ *correspond to the changes in impact caused by the first order*

changes in material flows that arise due to the studied increase in aluminum usage in vehicles. The second order consequences are then captured by the changes in impact $\boldsymbol{I^4}$-$\boldsymbol{I^7}$ *that arise due to subsequent changes in scrap generation.*

2.3.3 **Computational Structure**

Here, I provide a series of equations that facilitate the calculation of changes in environmental impacts corresponding to changes in the major flows in this product system as described in Section 2.3.2. Since I calculate changes in GHG emissions, the resulting quantities are all calculated relative to a counterfactual of no change in body and closure material composition. In other words, this creates the possibility of negative values, such as in steel and fuel production. This does not imply that the system produces negative quantities of steel or fuel. For example, prior to the start of the analysis the body and closure composition of vehicles is 99% steel and 1% aluminum per Ducker Worldwide (2014). By 2025, this shifts to 74% steel and 26% aluminum. Thus, relative to a no change counterfactual, the amount of steel production decreases, and the change in environmental impact calculated in (2) takes a negative value. Detailed derivations of all equations are given in Section A.1 of Appendix A.

2.3.3.1 Material Production and Forming

Given the time series of total aluminum additions of type l, $TAA_l(t)$, the total environmental impact of additional aluminium production in year t is calculated as

$$\boldsymbol{I}^1(t) = \sum_l \frac{TAA_l(t)}{\gamma_l^a} I_l^a(t) > 0 \qquad (2.1)$$

with γ_l^a being the forming yield of aluminium type l and $I_l^a(t)$ the impact of producing one additional kg of aluminum type l (sheet, extrusions, or castings). The amount of aluminum

required to achieve the functional equivalence of the removed steel is characterized by the material replacement coefficient, *k*, in kg aluminum/kg steel. Reducing the mass of vehicle body and closures enables mass reduction of additional components such as the suspension and transmission (Alonso et al., 2012). This is accounted for using the secondary mass savings parameter s, in kg secondary/kg primary mass savings). The environmental impact of reduced production of steel type *l* in year *t* relative to a no change scenario as a function of aluminum additions is calculated as

$$\boldsymbol{I}^2(t) = \sum_l \frac{1}{\gamma_l^s}\left[-\sum_m TAA_m\,(t)\left(\frac{pf_l+(1-k)\cdot s\cdot sf_l}{k}\right)\right] I_l^s(t) < 0 \qquad (2.2)$$

with γ_l^s being the forming yield of steel type *l* (flat, long, or castings), pf_l the fraction of steel type *l* in primary savings, sf_l the fraction of steel type *l* in secondary savings, $I_l^s(t)$ the impact of producing one less kg of steel type *l* (flat, long, or castings), and *m* the type of aluminum (sheet, extrusions, or castings). Both aluminum and steel have primary and secondary production routes, which are reflected in the material production equations as follows:

$$I_l^x(t) = sc_l^x(t)\cdot I_{ingot}^{sx}(t) + \left(1 - sc_l^x(t)\right)\cdot I_{ingot}^{px}(t) + I_l^{fx},\ x = a, s \qquad (2.3)$$

with $sc_l^x(t)$ being the secondary content of material *x* of type *l*, I_{ingot}^{sx} the cradle-to-ingot secondary production impact of material *x* of type *l*, I_{ingot}^{px} the cradle-to-ingot primary production impact of material *x* of type *l*, and I_l^{fx} the gate-to-gate impact of forming material *x* into type *l* (all in impact/kg).

2.3.3.2 Vehicle Use

For each year of the analysis period the impact reductions during vehicle use are calculated as

$$\boldsymbol{I}^3(t) = \sum_{T,i} \left[IR_i^u \cdot (1+s)^{\frac{k-1}{k}} AAA_i(T) \frac{VM}{VL} N_i(T) FIU(t-T) \right] < 0 \quad (2.4)$$

with $AAA_i(T)$ being the average amount of aluminum added to vehicle type *i* in production year *T*, VM the lifetime vehicle driving distance (in km), VL the vehicle lifetime (in years), $N_i(T)$ the total number of type *i* vehicles produced in year *T*, and $FIU(t-T)$ the fraction of vehicles produced in year T still in use after $t-T$ years.

IR_i^u denotes the environmental impact reduction per kg mass savings and km driven and is calculated as

$$IR_i^u = es_i \cdot \Delta E_i \cdot I^e(T) + (1-es_i)\Delta F_i \cdot I^f(T) \quad (2.5)$$

with ΔF_i and ΔE_i being the relative fuel and electricity savings (in MJ/kg saved and km driven), $I^f(T)$ and $I^e(T)$ the average well-to-wheels impacts of electricity and fuel production and use for vehicles produced in year *T* (per MJ), and es_i the share of driving energy from electricity. The relationship between mass reduction and use phase energy savings is a function of the power train type *i*. It also depends on the extent to which the power train is resized after mass reduction, since a mass-reduced vehicle can achieve equal performance with a smaller engine or motor (Lewis et al., 2014). Fuel and electricity savings per mass savings are higher when the powertrain is resized (see Table S18 in SI). The model considers five powertrain types *i*: gasoline, diesel, standard hybrid, plug-in hybrid and electric. $FIU(t-T)$ is derived from a log-normal lifetime distribution, enabling accurate modelling of the timing of fuel savings and exit of vehicles from the fleet. Other distributions have been proposed for vehicle lifetimes (Field et al., 2001; Sakai et al., 2014; Yano et al., 2014). It is important to note that this feature does not imply that the model, as a whole, is stochastic in nature. I discuss the choice of lifetime distribution in Section A.4.2 of Appendix A.

2.3.3.3 Scrap generation and use

If recycling takes place in an open loop, scrap flows cross the initial system boundaries at the beginning and the end of each vehicle's physical life cycle (see Figure 2.2). Panel (a) shows the system expansion used to calculate the consequences of scrap generation and use during the production of vehicles, while (b) shows the analogous version at EOL. I model two tiers of system expansion: The first models the external scrap market and the second the external material market (Geyer, 2008). During material production and forming, scrap input (SIn) comes from the external scrap market in cases when it is readily available, for example in the case of cast aluminum (Modaresi and Müller, 2012). At the same time, prompt scrap ($ProS$) generated by the system goes to the external scrap market. The parameter $\alpha \in [0; 1]$ quantifies the effect of those two flows on external scrap collection. For example, a net increase in automotive scrap supply by one unit decreases external scrap collection by $(1 - \alpha)$ units. The value of α depends on how the scrap market responds to scrap generation from the physical vehicle product system. Consider the case where total scrap demand does not increase proportionally to an increase in vehicle scrap collection. This would yield a value of $\alpha < 1$, meaning some of the additional scrap simply displaces collection from other sectors instead of contributing to an increase in external secondary production (recycling). In order for reductions in primary production to be realized, scrap generation must first lead to additional recycling activity, which is the effect captured by α.

Assuming that scrap stocks are constant in the long run, the external scrap flow balance can be calculated as:

$$ProS + (\alpha - 1)(ProS - SIn) + s_p\beta Y(ProS - SIn) = SIn + s_r Y(ProS - SIn)$$

$$\Rightarrow Y = \frac{\alpha}{s_r - s_p\beta} \quad (2.6)$$

with s_r and s_p being the scrap inputs into recycled and primary production (in kg/kg). There is no scrap input into primary aluminum production, i.e. $s_p^a = 0$, which simplifies the scrap flow balance. Primary steel production, however, has a significant amount of scrap input. The parameter $\beta \in [0; 1]$ quantifies the effect that a change in external secondary production has on external primary production. For example, an increase in external secondary production by one unit causes a decrease in external primary production by β units. The value of β is termed the "displacement rate" (Zink et al., 2015), and the implications of $\beta < 1$ are a key issue in evaluating the environmental consequences of recycling (Koffler and Finkbeiner, 2017; Mcmillan et al., 2012; Vadenbo et al., 2017; Weidema, 2003; Yang, 2016). Thus, I use α and β together to quantify the change in primary material production and consequent environmental benefits caused by additional scrap generation as shown in Figure 2.2.

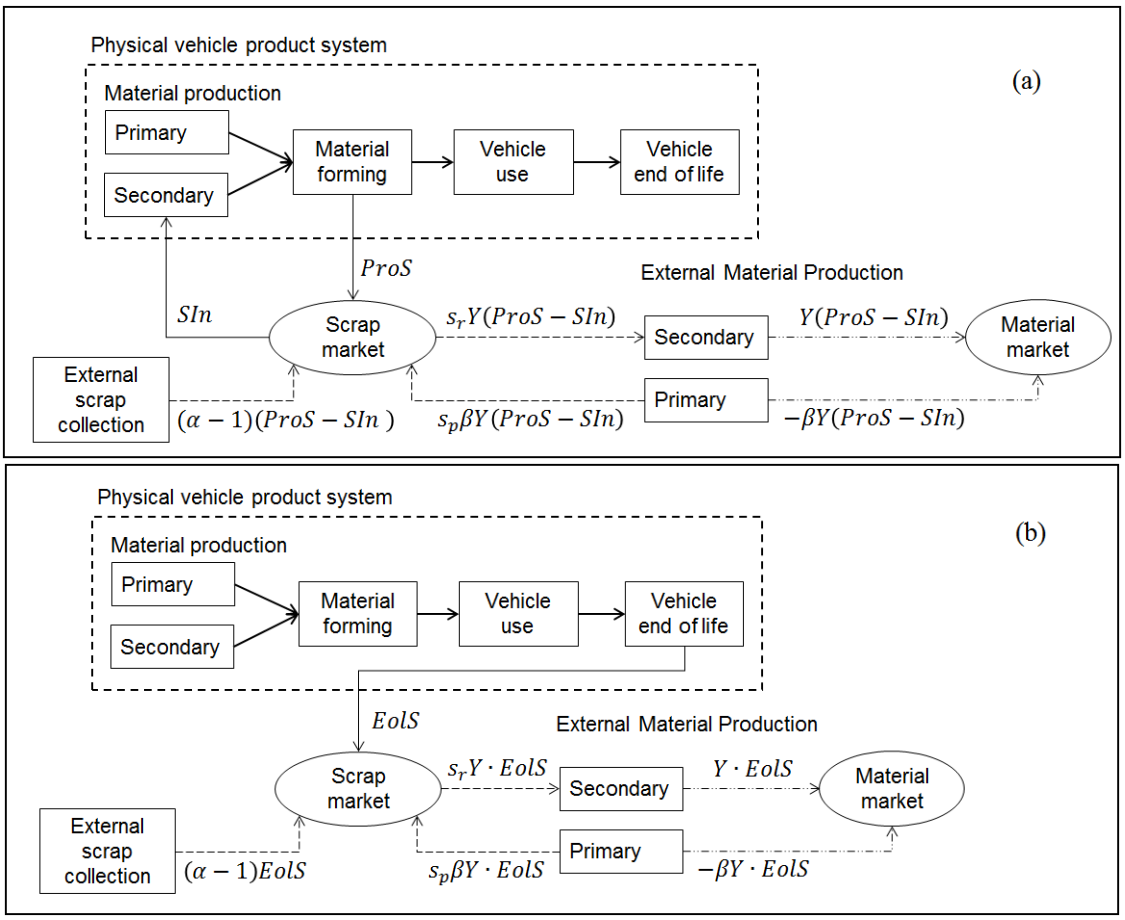

Figure 2.2: The system expansion model used to calculate impacts due to changes in scrap generation. Panel (a) shows the scrap balance during the production of vehicles, (b) at vehicle end of life. The rectangles are unit processes, ovals are markets, and arrows are flows. Here, SIn is the scrap input to the physical vehicle product system, $ProS$ is scrap from vehicle production processes, s_r and s_p are scrap inputs into external recycled and primary production, $EolS$ is the scrap generated at the end-of-life, α quantifies the effect of a change in scrap generation on external scrap collection, β quantifies the displacement of primary production due to increases in secondary production, and $Y = \frac{\alpha}{s_r - s_p\beta}$.

The change in environmental impact due to changes in scrap flows during production and forming of automotive material *x* during year *t* is now calculated as

$$\boldsymbol{I}^{4,5}(t) = \alpha^x \cdot \frac{(\sum_l ProS_l^x(t) - SIn_l^x(t))}{s_r^x - \beta^x \cdot s_p^x} \left(I_{ingot}^{sx}(t) - \beta^x \cdot I_{ingot}^{px}(t) \right), x = a, s \quad (2.7)$$

with $\sum_l SIn_l^x(t)$ being the total change in the amount of scrap used during production of material *x* during year *t*, and $\sum_l ProS_l^x(t)$ the change in total prompt scrap generation from material *x* during year *t*.

It follows that I can calculate the change in impact due to EOL scrap generation using the flows shown in Figure 2.2 (b). Again, I assume scrap stocks are constant in the long run, and calculate the external scrap balance for EOL as I did for prompt scrap in (2.6):

$$EolS + (\alpha - 1)EolS + s_p \beta Y EolS = s_r Y EolS$$

$$\Rightarrow Y = \frac{\alpha}{s_r - s_p \beta} \quad (2.8)$$

The change in environmental impact due to changes in automotive EOL scrap generation is then calculated as

$$\boldsymbol{I}^{6,7}(t) = \alpha^x \cdot \frac{EolS^x(t)}{s_r^x - \beta^x \cdot s_p^x} \left(I_{ingot}^{sx} - \beta^x \cdot I_{ingot}^{px}(t) \right), x = a, s \quad (2.9)$$

with $EolS^x(t)$ being the change in total generation of automotive EOL scrap from material *x* during year *t*.

2.3.4 **Data**

In this section, critical inputs from each life cycle stage contributing to the baseline cumulative GHG result are described. Comprehensive treatment and referencing of the spreadsheet formulas and baseline data are included in Appendix A.

2.3.4.1 Material Production and Forming

Industry data from Ducker Worldwide are used to set up the projection of total aluminum additions $TAA(t)$ and production units $N(t)$ on an annual basis (Ducker

Worldwide, 2015, 2014). Table 2.1 provides a sample of the time series. The complete series is available in section A.3 of Appendix A. The baseline material replacement coefficient, $k = 0.668$, is derived using the aforementioned harmonization study and vehicle-specific data suggesting a 50% split of mild and high-strength steel available to be replaced on average in body and closure components (Chapp and Shah, 2007; Kim and Wallington, 2013; Morgans, 2012; Pafumi, 2006). The distribution of vehicle classes amongst hybrid and electric vehicles is compiled from the monthly sales distribution reported by Argonne National Laboratory (ANL, 2015). The aluminum content, material replacement coefficient, powertrain distribution and vehicle class distribution data set the stage for producing the life cycle inventory on an annual basis.

Year	Additional sheet aluminum produced (million kg)	Additional extruded aluminum produced (million kg)	Additional cast aluminum produced (million kg)	Vehicles Produced in North America
2012	81.9	0	0	16,181,282
2017	681.6	38.2	27.3	17,609,612
2022	1303.0	81.9	65.5	19,000,000
2027	1778.0	115.0	93.0	20,000,000
2028-2050	1,790.0	115.0	95.0	20,000,000

Table 2.1: A sample of the time series inputs of additional aluminum content and total vehicles produced in North America

Recent literature suggests baseline secondary content values $sc_i^a(t)$ for wrought (both sheet and extrusions) and cast aluminum are 0% and 85%, respectively (Geyer, 2013; Løvik

et al., 2014; Modaresi and Müller, 2012). As shown in Table 2.1, most of the additional aluminum demanded by the system is sheet aluminum. Thus, the majority of this demand is met using primary material. The baseline secondary content of flat, long and cast steel $sc_l^s(t)$ are 5%, 85% and 100% (World Steel Association, 2010). However, I note that the model allows for changes in secondary content, including closed-loop recycling of all scrap. Baseline forming yields γ_l^a for sheet, extrusions and cast aluminum are 62%, 80% and 80% (Geyer, 2014, 2013; Milford et al., 2011). Baseline forming yield γ_l^s for flat, long and cast steel are 60%, 80% and 80% (Geyer, 2014, 2013; Milford et al., 2011). Baseline secondary mass savings are $s = 50\%$ (Kim and Wallington, 2013). Recent research indicates that the incremental supplier of primary steel is likely to be China (Beylot, 2016). Therefore, I use an initial value of 2.02 kg CO2eq/kg for the GHG intensity of primary steel production, I_{ingot}^{ps}, for the baseline case (calculated from Hasanbeigi et al., 2016). The baseline initial GHG intensity of secondary steel production, I_{ingot}^{ss}, is 0.399 kg CO_2eq/kg (World Steel Association, 2010). The uncertainties associated with these values and the potential decarbonization of their electricity inputs are addressed in the sensitivity analysis.

Industry analysis suggests that 36% of primary aluminum demand in North America was met using imports in 2015 (The Aluminum Association, 2015). Another report shows that North American smelters are near capacity, and estimates that the share of imported aluminum used to meet the increase in demand from the automotive industry will climb by 3.6% per year, reaching 72% in 2025 (Accenture LLC, 2015). Thus, the base case uses China as the supplier of imported primary aluminum (IAI, 2018).The initial GHG intensities used in this model are 16.5 kgCO_2eq/kg for imports from China (Hao et al., 2015) and 8.937 kg CO_2eq/kg for North America (International Aluminum Institute, 2014; The Aluminum

Association, 2013). The emissions inventory of primary aluminum, $I_{ingot}^{pa}(t)$, is a weighted average of the two values in each year, which serves as a proxy for the incremental supplier. A reduction in electricity input for primary aluminum ingot production in China is modelled following the trend detailed by Hao et al. (2015); therefore the annual emission inventory for imported primary aluminum follows a downward trajectory. Finally, I use an initial baseline secondary aluminum GHG intensity value of $I_{ingot}^{sa} = 0.508$ kg CO_2eq/kg (Thinkstep, 2015).

Importantly, I note that there is a high degree of uncertainty surrounding the GHG intensity of incremental suppliers of steel and aluminum in the both the short and long term. In the case of cradle-to-gate primary aluminum ingot production, I identified values as low as 6.7 kgCO_2eq/kg from Europe (European Aluminum, 2018) and as high as 21.7 kg CO_2eq/kg from parts of China (Hao et al., 2015). These are reflective of the electricity grid mixes in those regions, as primary aluminum production is an electricity-intensive process. For steel, I identify cradle-to-gate primary production GHG intensities as low as 1.27 kg CO_2eq/kg when applying a possible 32% decrease in the energy intensity of primary steel production to the global average (Energy Information Adminstration, 2018), and as high as 2.8 kg CO_2eq/kg from coal-dominated electricity grids (Columbia Climate Center, 2012). The uncertainties regarding the GHG intensity of all primary and secondary production processes is addressed in the sensitivity analyses conducted in Section 2.4 and section A.4 of Appendix A. In addition, I include a year-over-year decarbonization factor of 0.5% for primary and secondary material production processes in the model. This aims to reflect decarbonization of electricity grids globally, which is expected to happen gradually (Morvaj et al., 2017).

2.3.4.2 Vehicle Use

The annual sales projections for the five powertrain types are input from a Ducker analysis (Ducker Worldwide, 2015). The baseline model assumes that 50% of all mass-reduced vehicles also have their power trains resized, and that the plug-in hybrids receive 50% of their driving energy from external electricity. The used fuel and electricity savings per mass savings, ΔF_i and ΔE_i, by powertrain type, with and without resizing are from extensive powertrain simulations and available in Appendix A (Geyer and Malen, 2018; Malen and Geyer, 2018). Vehicle lifetimes are assumed log-normally distributed and used to determine the fraction-in-use from production year T in year t of use, $FIU(t-T)$. The baseline mean lifetime is $VL = 13$ years with a standard deviation of 3 years (National Highway Traffic Safety Administration, 2006). Lifetime vehicle distance travelled VM is 245,000 km (National Highway Traffic Safety Administration, 2006). Well-to-wheels GHG intensities of gasoline, diesel, and electricity production and use/combustion are 87.5, 82.7, and 150 gCO_2eq/MJ (Argonne National Laboratory, 2015; Thinkstep, 2015). The potential decarbonization of electricity production for battery electric vehicles (BEVs) is addressed in the sensitivity analysis, as I consider up to a 50% reduction in its initial GHG intensity (Figure A.5 of Appendix A), along with year-over-year decarbonization. In addition, I note that the GHG intensity of gasoline and diesel production may increase as less conventional sources are exploited (Brandt and Farrell, 2007). Thus, I also consider up to a 50% increase in GHG emissions from gasoline and diesel production in the sensitivity analysis (Figure A.5 of Appendix A).

2.3.4.3 Prompt and end-of-life scrap

Very little is known about the values of α and β for any given material, since it is difficult to generate robust estimates for these values. Recently, a micro-econometric framework was proposed to quantify the displacement rate β (Zink et al., 2015). The first estimation of this parameter was conducted for aluminum in the United States and yielded an initial median value of about 0.12, but values from -0.5 to 1 are included between the 5^{th} and 95^{th} percentiles (Zink et al., 2017). The case study calculates β from own-price and cross-price elasticities of supply and demand for primary and secondary aluminum, which are determined using partial equilibrium modeling and econometric time-series analysis (Zink et al., 2017, 2015). In the relevant literature, α also has an economic interpretation. For example, if the price elasticities of supply and demand for scrap are equal in magnitude, $\alpha = 0.5$ (Ekvall, 2000). The baseline case uses an open-loop with values of $\alpha = 1$ and $\beta = 1$ for both steel and aluminum. Although the mechanics are different, these specific values of α and β yield the equivalent outcome to closed-loop recycling.

2.4 Results

Here, I present the results from local one-at-a-time sensitivity analysis (OAT-SA) and global sensitivity analysis using Monte Carlo simulation. I start by presenting the contributions of each calculated change in GHG emissions to the baseline results, which serves as a point of departure for the uncertainty analysis. Then, OAT-SA is used to show how the shape of the cumulative GHG curve varies when perturbing individual parameters, holding all others constant at the values given in Section 2.3.4. OAT-SA alone is not sufficient for robust estimates of which parameters in the model contribute most to the overall variance in the results, especially when there are nonlinear interactions between

parameters (Saltelli and Annoni, 2010). One way in which this has been addressed in LCA is to use Monte Carlo simulation (Lloyd and Ries, 2007). Thus, I also conduct a global sensitivity analysis using Monte Carlo simulation in Section 2.4.5.

2.4.1 **Baseline GHG contributions and Local Sensitivity Analysis**

The baseline GHG curve shown in each component of Figure 2.4 is the cumulative sum of contributions from the seven system-wide changes as shown in Figure 2.3. These contributions are calculated using formulas from $\boldsymbol{I}^1(t)$ through $\boldsymbol{I}^7(t)$ as described in the Methods section. The standard for comparison is the x-axis, or the case in which there are no changes in aluminum content over time. The relative increase in annual GHGs due to prompt and EOL steel scrap contributions can be understood as the opposite of the avoided burden effect created by additional aluminum scrap. Since the baseline case uses an open-loop and assumes 1-to-1 displacement, the removal of steel scrap from the market will be compensated by additional primary steel production.

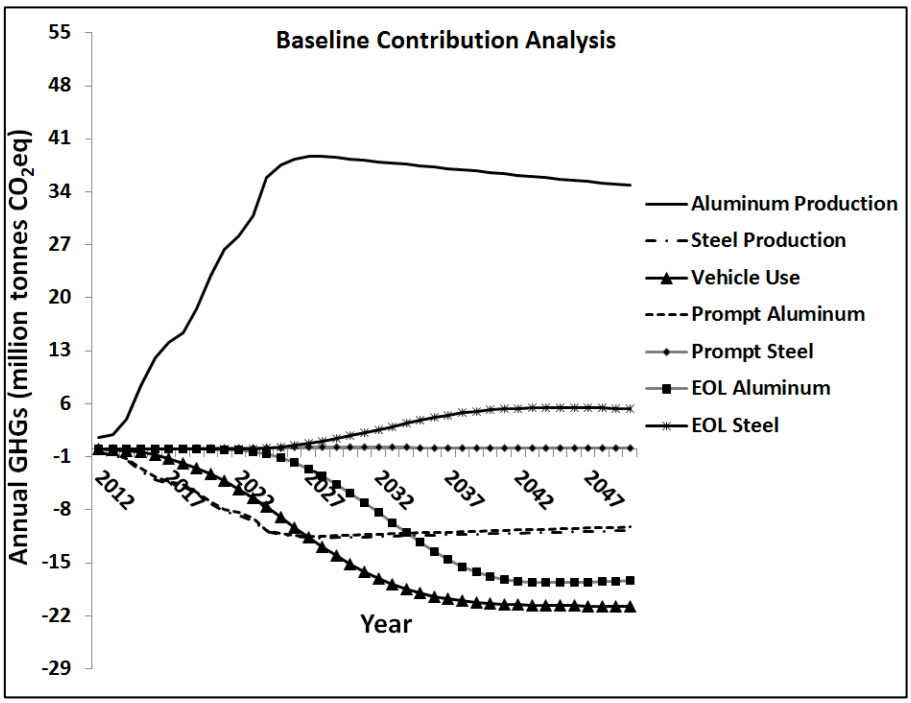

Figure 2.3: Contribution analysis for all seven distinct GHG consequences analyzed in the CLCA using data inputs described in Section 2.3.4, where "prompt" refers to emissions related to scrap generation from production processes, and "EOL" refers to emissions related to scrap generation from end-of-life. All of the lines represent changes in emissions from each change in flows relative to a counterfactual of no change in material composition. Initially, increases in emissions from aluminum production dominate the contribution analysis. Over time, emissions decreases accumulate due to reduced steel production, fuel production, and fuel combustion relative to the no change counterfactual. End-of-life recycling benefits in the form of displaced primary aluminum production accumulate even later.

Production and prompt scrap emission changes reach a steady state by the year 2028, while the steady state for use and EOL effects are delayed by vehicle lifetime effects. The year where the cumulative GHG curve crosses the x-axis is referred to as the "GHG payback year", and is calculated as 2037 at the baseline. Figures 2.4 (a), (b), (c), (d), (e), (f), (g), and (h) are the components of the local OAT-SA discussed in the following subsections. The interaction of various parameters is covered in Appendix A, as well as additional sensitivity analyses that apply to each component of the model individually. GHG payback must be interpreted with some caution, as warming occurs between the initial emissions and the arithmetic payback year that cannot be reversed and that I am unable to account for in this model.

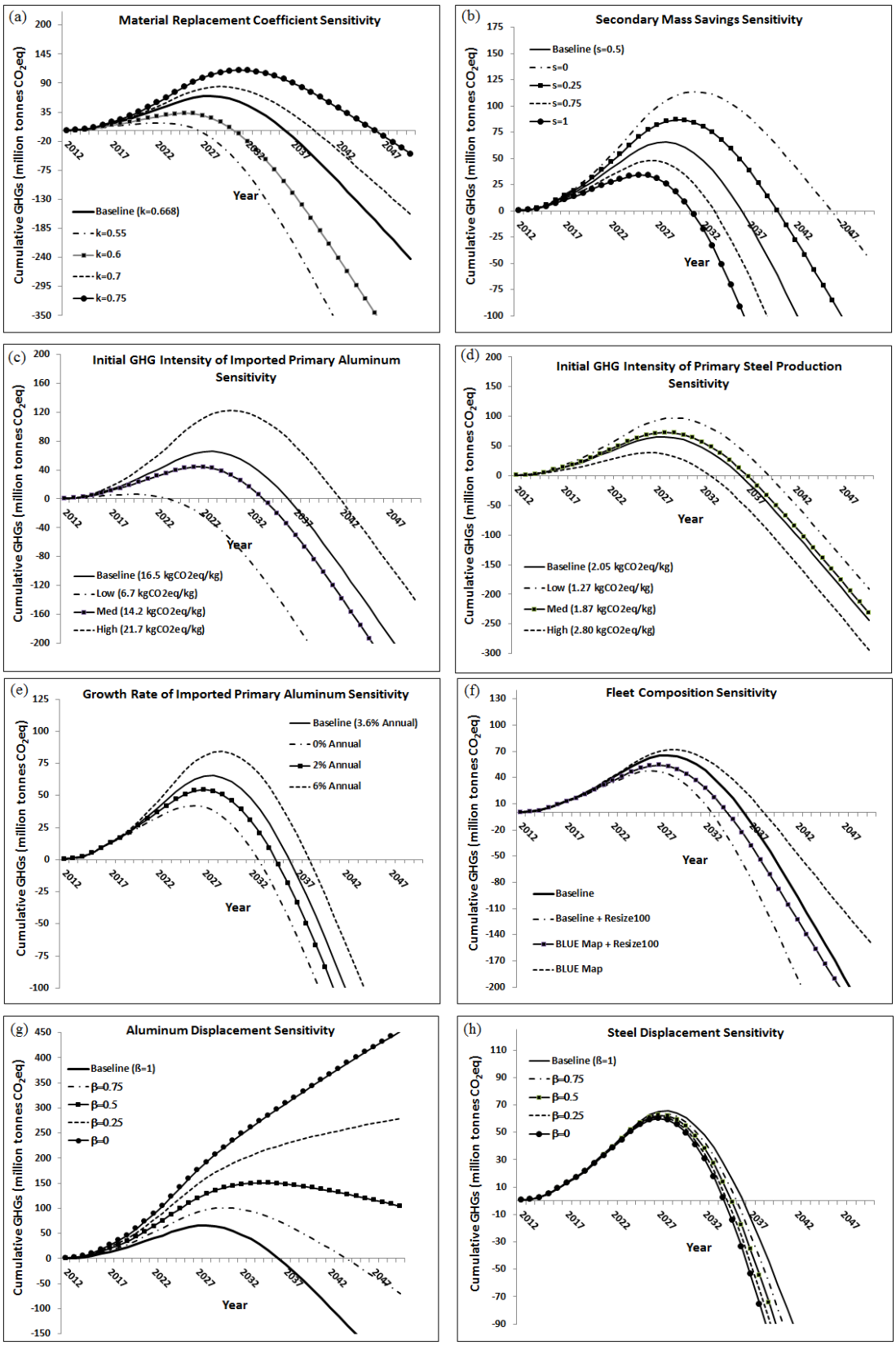
(a)
Material Replacement Coefficient Sensitivity
Cumulative GHGs (million tonnes CO2eq)
Year
Baseline (k=0.668)
k=0.55
k=0.6
k=0.7
k=0.75
(b)
Secondary Mass Savings Sensitivity
Baseline (s=0.5)
s=0
s=0.25
s=0.75
s=1
(c)
Initial GHG Intensity of Imported Primary Aluminum Sensitivity
Baseline (16.5 kgCO2eq/kg)
Low (6.7 kgCO2eq/kg)
Med (14.2 kgCO2eq/kg)
High (21.7 kgCO2eq/kg)
(d)
Initial GHG Intensity of Primary Steel Production Sensitivity
Baseline (2.05 kgCO2eq/kg)
Low (1.27 kgCO2eq/kg)
Med (1.87 kgCO2eq/kg)
High (2.80 kgCO2eq/kg)
(e)
Growth Rate of Imported Primary Aluminum Sensitivity
Baseline (3.6% Annual)
0% Annual
2% Annual
6% Annual
(f)
Fleet Composition Sensitivity
Baseline
Baseline + Resize100
BLUE Map + Resize100
BLUE Map
(g)
Aluminum Displacement Sensitivity
Baseline (ß=1)
β=0.75
β=0.5
β=0.25
β=0
(h)
Steel Displacement Sensitivity
Baseline (ß=1)
β=0.75
β=0.5
β=0.25
β=0

Figure 2.4: (a) Sensitivity of cumulative GHG curve to changes in the material replacement coefficient (k). (b) Sensitivity of cumulative GHG curve to secondary mass savings (s). (c) Sensitivity of cumulative GHG curve to the GHG intensity of additional imported primary aluminum, with the same for decreased primary steel in (d). (e) Sensitivity of cumulative GHG curve to changes in the growth rate of the imported share of primary aluminum. (f) Cumulative GHG curves for baseline and BLUE map fleet compositions with baseline powertrain resize rate (50%) and powertrain resize rate of 100% (Resize100). (g) Effect of partial displacement of aluminum recycling ($\beta<1$) on cumulative GHG curve, with the same shown for steel in (h).

2.4.2 **Sensitivity to material production parameters**

The output of the CLCA is very sensitive to the material replacement coefficient (*k*). At the baseline, I use a value of k=0.668. Alternative values of *k* are presented in Figure 2.4 (a) with a range corresponding to previous studies of automotive material substitution (Kim and Wallington, 2013). As expected, lowering the value of *k* improves the GHG payback time of the system. The realizable size of secondary mass savings (*s*) is quite uncertain and strongly affects the outcome. Holding other parameters fixed, varying *s* from 0 to 1 produces a GHG payback range of 15 years. Figures 2.4 (c) and 4 (d) show that the model results are more sensitive to the GHG intensity of primary aluminum production than they are to the GHG intensity of primary steel production. The shortest GHG payback period of all of the curves in Figure 2.4 is 12 years, when the initial GHG intensity of imported primary aluminum production takes its lowest identified value. In addition, the cumulative GHG curve is sensitive to the growth rate of imported primary aluminum production. Figure 2.4 (e) covers

the range from 0% growth to the theoretical maximum of 6%, which would drive the imported share of incremental production to 100% during the steady state.

2.4.3 **Sensitivity to use phase parameters**

The baseline time series of fleet composition is extracted from figures in two industry studies conducted by Ducker Worldwide (Ducker Worldwide, 2015, 2014). There is a steady decline in gasoline and diesel internal combustion vehicles (ICVs) and growth in vehicles with hybrid and electric powertrains. In 2010, the International Energy Agency (IEA) published an alternative evolution of powertrain technology shares as part of its BLUE map scenario (IEA, 2010; Modaresi et al., 2014). In this analysis, I examine the sensitivity of the model to the implementation of a BLUE map fleet where ICVs are diminished much more rapidly and replaced by hybrid and electric vehicles. For both fleet compositions, the response of GHG payback to an increase in resized powertrains to 100% from the baseline of 50% (Resize100) is modeled.

A counterintuitive result is shown in Figure 2.4 (f). In comparison to the baseline fleet, a shift toward more efficient powertrains results in a delay in GHG payback. This is because the mechanism of GHG reduction is the energy savings per mass savings achieved during the use phase. If the fleet follows a more efficient powertrain trajectory, the energy savings per mass savings are diminished (Geyer and Malen, 2018; Malen and Geyer, 2018; Wohlecker et al., 2007). Regardless of the fleet composition, increased powertrain resizing rates accelerate the GHG payback effect, since this increases the fuel economy effect of mass reduction.

2.4.4 **Sensitivity to scrap and material market responses**

Recycling is most likely in an open loop, i.e. market-mediated (Reck and Graedel, 2012; Shen et al., 2010). The effect of primary production displacement depends on the difference in GHG intensity between primary and secondary production. Therefore, it is imperative to examine conditions where the displacement rate for aluminum is less than one. The market-based interpretation of partial displacement is that recycled aluminum grows the material market without causing an equivalent decrease in primary production. This phenomenon may be governed, for example, by own and cross-price (substitution) elasticities of supply and demand for primary and secondary aluminum. In response to a supply shock, a low substitution elasticity of demand for primary aluminum would reduce displacement (Zink et al., 2015; Zink and Geyer, 2017). On the other hand, a high own-price elasticity of supply for primary aluminum would increase displacement.

Given that technological limitations currently prevent recycling all of the incremental aluminum scrap back into the wrought components (Løvik et al., 2014; Modaresi and Müller, 2012), partial displacement is quite likely. As the aluminum displacement rate (β_a) decreases, GHG payback is significantly delayed. As shown in Figure 2.4 (g), for values of $\beta_a < 0.35$, GHG payback is never achieved with other parameters fixed at baseline values. This insight would not be apparent if one were to simply allocate the benefits of recycling using the avoided burden method, which is equivalent to assuming $\alpha = \beta = 1$. Finally, as shown in Figure 2.4 (h), GHG payback shows strikingly limited sensitivity to β_s, highlighting the fact that the difference between the GHG intensity of primary and secondary production is an order of magnitude greater for aluminum than it is for steel (Geyer, 2013, 2008; Hao et al., 2015; Thinkstep, 2015). Figures A.7 (c) and (d) of Appendix

A show that GHG payback is just as sensitive to α_a as it is to β_a, and as insensitive to α_s as it is to β_s.

2.4.5 **Monte Carlo simulation**

Monte Carlo simulation begins with the assignment of probability distributions to the uncertain parameters in the model. The parameters are assigned uniform distributions with ranges given in Table 2.2. The use of a uniform distribution means that all possible values in the range have an equal probability of being sampled, which can be thought of as an unbiased approach given the lack of knowledge of the underlying uncertainties. After defining the ranges for the variables, I simulate the cumulative GHG curve 100,000 times by randomly sampling all of the parameters in Table 2.2 simultaneously. Then, I record statistics on the value of cumulative GHG emissions in 2050, the final year of the model. The simulation is conducted using the Oracle Crystal Ball plug-in for Microsoft Excel (Oracle Company, 2018a).

Parameter	Unit	Minimum	Maximum
Material Replacement Coefficient	kg aluminum/kg steel	0.55	0.75
Initial GHG intensity of Imported Primary Aluminum Production	kg CO_2eq/kg	6.70	21.70
Secondary Mass Savings	kg secondary/kg primary mass savings	0	1
Fraction of Powertrains Resized	%	0	100
Aluminum Beta	unitless	0	1
Aluminum Alpha	unitless	0	1
Vehicle Lifetime Distance Driven	km	200,000	300,000

Aluminum Sheet Yield	%	52	72
Year-over-year decarbonization of material production processes and electricity production for BEVs	%/year	0	2
Initial GHG intensity of Primary Steel Production	kg CO_2eq/kg	1.27	2.80
Growth Rate of Imported Primary Aluminum Production	%/year	0.00	6.00
Flat Steel Yield	%	50	70
Initial GHG intensity of North American Primary Aluminum Production	kg CO_2eq/kg	6.70	8.94
Initial GHG intensity of Secondary Aluminum Production	kg CO_2eq/kg	0.254	1.016
Initial GHG intensity of Secondary Steel Production	kg CO_2eq/kg	0.199	0.798
Initial GHG intensity of Electricity Production for BEVs	kg CO_2eq/MJ	0.075	0.15
Initial GHG intensity of Gasoline Production	kg CO_2eq/MJ	15.50	23.25
Initial GHG intensity of Diesel Production	kg CO_2eq/MJ	7.74	11.61
Steel Alpha	unitless	0	1
Steel Beta	unitless	0	1
Year-over-year carbon intensification of gasoline and diesel production	%/year	0	2

Table 2.2: The parameters sampled for the Monte Carlo simulation with their units, minimum values, and maximum values. All parameters were assigned a uniform distribution.

The cumulative GHG emissions in 2050 are normally distributed with a mean of -135 million tonnes CO_2eq and a standard deviation of 359 million tonnes CO_2eq. In 35% of the iterations, cumulative GHGs remain positive in 2050. In 16% of the iterations, cumulative GHG emissions in 2050 are above 207 million tonnes CO2eq, which is an approximate

threshold value indicating that GHG payback will never be achieved (see note in Appendix A section A.3.4). Because the input distributions are not empirically determined and the model itself is a coarse approximation of real-world dynamics, I focus the discussion of the results on the contributions to variance from the input parameters, rather than the output distribution. Crystal Ball calculates the contributions to variance using the rank correlation coefficients of each input variable with the outcome variable (cumulative GHG emissions in 2050) over all 100,000 simulations. The rank correlation coefficients are squared and normalized to 100% (Oracle Company, 2018b). Figure 2.5 shows the top eleven contributions to variance from the inputs given in Table 2.2. The remaining parameters contribute less than 1%.

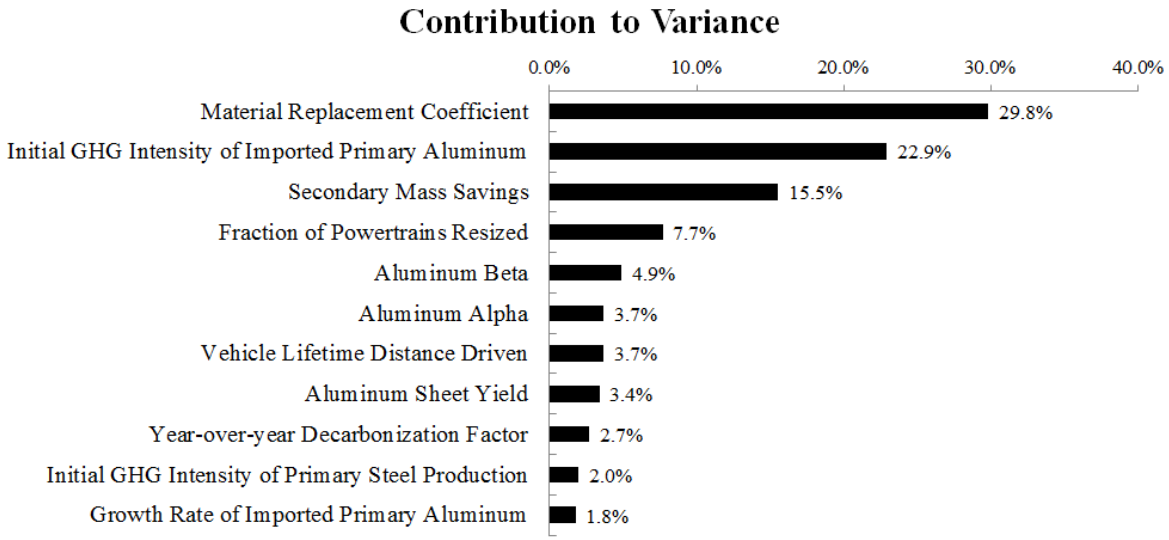

Figure 2.5: The contributions to variance in the model attributed to individual input parameters after Monte Carlo simulation with 100,000 iterations.

Parameters related to the calculation of changes in GHG emissions from changes in material production dominate the contributions to variance. The material replacement coefficient, GHG intensity of imported primary aluminum, and secondary mass savings are

all key factors in the determination of GHG emissions from changes in aluminum and steel production using equations (1) and (2). This finding is robust to an alternative scenario where I narrow the range of GHG intensities of imported primary aluminum production. All three of these parameters remain in the top five contributors to variance as shown in Figure A.10 of the Appendix A. The main contribution to variance from the use phase calculation is the fraction of powertrains resized in the fleet, which strongly affects the calculation of fuel savings per mass savings via equation (2.5). In the calculation of changes in GHG emissions due to changes in scrap generation using equations (2.7) and (2.9), the aluminum market response parameters alpha and beta make the largest contribution to the variance.

2.5 Discussion

The results of my analysis reiterate why CLCA is the correct choice of modelling approach for understanding the GHG consequences of large-scale shifts in automotive body and closure materials. The consideration of how the scrap and material markets respond to additional scrap generated from the system has a significant impact on the cumulative net GHG curve and makes a large contribution to the variance in model outcomes. Such market interactions are not part of the traditional ALCA framework, which relies on average inventory data and technical input-output relationships. Here, I have instead modelled the system-wide changes in GHG emissions caused by the decision to increase aluminum content in vehicles, which includes the interactions with the scrap and material markets.

One key feature of all of the cumulative GHG curves generated by this model is that they show large-scale shifts of closure and body part material from steel to aluminum in the production of North American light vehicles will initially increase GHG emissions. This means that the fact that less material is needed in the production of vehicles cannot make up

for the higher GHG intensity of primary aluminum production. As the GHG intensity of incremental aluminum production increases, this effect becomes more pronounced.

The results are highly sensitive to the material replacement and secondary mass savings coefficients. Varying these parameters within the range of previous literature corresponds with GHG payback ranges of 20 and 15 years. There is still controversy over the actual values of those two parameters, since they are not directly observable. The magnitude of the use phase savings significantly depends on the power train composition of the vehicle fleet and on the extent to which power trains, in particular internal combustion engines, are resized when vehicles are mass reduced. The use phase savings of light-weighting are diminished as the fleet shifts toward more efficient powertrains.

The GHG benefits of aluminum scrap recycling are potentially larger than the use phase savings, but occur even later. The model results are particularly sensitive to the assumptions behind the GHG consequences of aluminum scrap collection, recycling, and use. Relevant literature, including the first market-based estimates, suggests a high likelihood that recycling of aluminum displaces primary production by less than 100%, which would significantly delay or even eliminate GHG payback (Løvik et al., 2014; Modaresi and Müller, 2012; Zink et al., 2017, 2015).

That the parameters with the largest uncertainty, i.e. k, s, α_a, and β_a, are also the ones with the largest impact on the GHG payback is the most important insight from this CLCA. The lack of understanding of the underlying uncertainty distributions for these parameter values, as well as the inherent uncertainty in modelling human behavior decades into the future, renders the comparison of the environmental performance of aluminum and steel indeterminate. In contrast to previous studies, I conclude that it is thus not possible to draw a

definitive conclusion regarding the net GHG consequences resulting from the substitution of aluminum for steel due to the lack of robust estimates for the most sensitive parameters.

2.6 Conclusions

2.6.1 Limitations and Future Work

The behavior of the affected external scrap and material markets are key consequential effects. The first and second-order consequences of scrap generation in this CLCA are characterized by the four parameters: $\alpha_a, \beta_a, \alpha_s$ and β_s as explained in Section 2.3.3.3. For the moment, sensitivity analysis is the most evident way to provide useful insights, since there is currently no knowledge of their actual values. Rigorous estimations of α do not exist for any material. The argument has been made that in the absence of robust information, using $\alpha = 0.5$ "will minimize the maximum error in the estimation of indirect effects" (Ekvall, 2000) in the market- based framework. A partial equilibrium model was used to provide the first estimate of β_a , but no analogue exists for β_s (Zink et al., 2017).

Modelling additional market dynamics of substituting primary aluminum for primary steel should be considered in the future. One could envision the possibility that the steel industry aggressively targets sales of primary material to other sectors such as construction in response to softened demand from the automotive industry. The reduction in sales to the automotive industry could also trigger a small price reduction that stimulates demand from other sectors. These mechanisms, in turn, may diminish the reduction in steel production modelled here using equation (2.2). Thus, future work includes the development of a system expansion model that incorporates the effect of decreased demand from the automotive sector on the market for primary steel.

An important area for future research is thus in the development of additional methodologies to measure consequential parameters. The partial equilibrium models used to estimate β_a in the literature are exercises in eliciting causal effects, subject to various assumptions, from our actual observations of the world (Stock, 2001). This does not mean that partial equilibrium is the *only* path to conducting estimations of consequential effects.

Going forward, it is imperative that CLCA does not limit itself to being the intersection of LCA and classical economics, as some have suggested (Earles and Halog, 2011). CLCA stands to benefit from the full suite of methods for causal inference, of which partial equilibrium modelling is only one. For example, the direct rebound effect may apply to this CLCA, as one may expect consumers to respond to fuel savings by increasing the frequency and length of automobile travel (Sorrell et al., 2009). While partial equilibrium is one option to measure this effect, a well-designed field experiment or survey study would be an informative complement originating from outside of classical economics. Perhaps the rebound effect is an emergent property of interactions between consumers with heterogeneous preferences. In this case, simulation frameworks such as agent-based modelling may also be informative. Depending on the particular research question and available data, a wide array of methods originating from outside of classical economics could be applicable to a given CLCA. In this sense, I align with literature recommending that practitioners explore multi-method approaches and weigh the relative advantages and disadvantages of methods that could be used to answer the research questions identified during a CLCA analysis (Anex and Lifset, 2014; Sandén and Karström, 2007; Yang and Heijungs, 2017).

Chapter 3 of this dissertation introduces and applies new methodology for causal inference in the CLCA domain. In chapter 3, I simulate the use of the difference-in-differences, a quasi-experimental statistical method, to estimate firm-level displacement of primary aluminum usage due to increased aluminum recycling in the automotive sector. By collecting the type of dataset described in the simulation in Chapter 3, one could shed light on the underlying uncertainty distribution behind β_a and improve the resolution of this model. Such an exercise is a manifestation of the iterative framework for CLCA that I suggest in Chapter 1.

My analysis further reinforces the need for rigorous treatment of uncertainty in LCA studies. Here, I have shown that the range of possible outcomes in net GHG emissions from the substitution of aluminum for steel in vehicles is vast. As has been pointed out before in the CLCA discourse, these uncertainties reflect the "limits of scientific knowledge" that we have to date regarding these possible outcomes (Plevin et al., 2014). Focusing on the baseline curve, which is a point of departure for the sensitivity analysis, clearly leads to flawed conclusions. This has been identified as a fundamental problem in the formation of public policy based on science, with one facet of the solution being the orientation of science-based policy discussions on interval estimates and uncertainty (Manski, 2013). As a result, I encourage future research on the environmental impacts of automotive material substitution to focus on improving the characterization of uncertainty.

2.6.2 **Policy Implications**

The presented consequential analysis shows that vehicle light-weighting strategies based on replacing steel with aluminum will lead to significant initial increases in GHG emissions before the targeted use phase savings become effective. It highlights questions that need to

be answered to conclude when aluminum intensification in vehicles constitutes a net GHG benefit, if it does at all. The most concerning scenario occurs when aluminum scrap generation exhibits reduced levels of primary production displacement, as this directly leads to the possibility that a net reduction in GHGs is never achieved. The lack of understanding of the underlying uncertainties in most critical parameters is a further cause for re-evaluation of lightweight material substitution as a means to achieve policy-mandated reductions in GHG emissions from vehicles.

Nonetheless, there are several strategies to reduce the production/use-phase trade-off faced by GHG intensive lightweight materials. The most obvious one is to reduce the GHG intensity of their production. The potential for automotive aluminum to create the intended GHG benefits in the production of vehicles in North America is hindered by the fact that significant additional production is projected to come from imports, which often have higher GHG intensities than North American aluminum (Accenture LLC, 2015; Hao et al., 2015; Ou et al., 2011). The ongoing pursuits of low-carbon energy in countries that produce aluminum and process improvements reducing the electricity intensity of primary aluminum production help to mitigate this issue.

The most important strategy, however, is to increase the "impact reduction potential" (Geyer et al., 2015) of aluminum scrap generation, in other words to make sure that maximum levels of primary production displacement are achieved. One example would be to increase scrap quality, for example via advanced alloy identification technologies (Werheit et al., 2011). However, this paper demonstrates that understanding and influencing market behavior is more important than focusing on technical solutions. More research is urgently required in this domain.

An alternative to reducing trade-offs is to side-step them. Vehicle mass reduction without GHG trade-offs can be achieved by simply downsizing vehicles instead of using GHG intensive lightweight materials. Mass reduction is also possible by replacing mild with advanced high strength steel, which has a GHG intensity similar to mild steel.

Any policies that target a reduction in the GHG footprint of goods and services require careful examination of the implications on a system-wide basis. Moreover, unique insights into the environmental consequences of these policies are gained from utilizing a CLCA framework. The presented research shows how such a framework can be used for extensive sensitivity analysis and thus guides formulation, analysis, and implementation of environmental policy.

2.7 References

Accenture LLC, 2015. Executive Summary : North American Primary Aluminum Smelter Study.

Alonso, E., Lee, T.M., Bjelkengren, C., Roth, R., Kirchain, R.E., 2012. Evaluating the potential for secondary mass savings in vehicle lightweighting. Environ. Sci. Technol. 46, 2893–2901. doi:10.1021/es202938m

Anex, R., Lifset, R., 2014. Life Cycle Assessment: Different Models for Different Purposes. J. Ind. Ecol. 18, 321–323. doi:10.2166/wst.2011.258

ANL, 2015. Light Duty Electric Drive Vehicles Monthly Sales Updates [WWW Document]. Argonne Natl. Lab. URL http://www.anl.gov/energy-systems/project/light-duty-electric-drive-vehicles-monthly-sales-updates (accessed 10.8.15).

Argonne National Laboratory, 2015. GREET 2015.

Beylot, A., 2016. Example - Marginal supply of steel [WWW Document]. URL https://consequential-lca.org/clca/marginal-suppliers/increasing-or-slowly-decreasing-market/example-marginal-supply-steel/

Brandt, A.R., Farrell, A.E., 2007. Scraping the bottom of the barrel: Greenhouse gas emission consequences of a transition to low-quality and synthetic petroleum resources. Clim. Change 84, 241–263. doi:10.1007/s10584-007-9275-y

Chapp, J., Shah, V.C., 2007. Steel Use in Chrysler Sebring Sedan/ Convertible and Dodge Avenger [WWW Document]. URL http://www.autosteel.org/~/media/Files/Autosteel/Great Designs in Steel/GDIS 2007/05 - AHSS Technology in the 2007 Daimler Chrysler Sebring.pdf (accessed 7.11.17).

Columbia Climate Center, 2012. Mitigating Iron and Steel Emissions, The GNCS Factsheets.

Curran, M.A., Mann, M., Norris, G., 2002. Report on the International Workshop on Electricity Data for Life Cycle Inventories. National Renewable Energy Laboratory, Cincinatti, Ohio.

Dalli, M., 2018. Draft Report on the proposal of the European Parliament and of the Council setting emission performance standards for new passenger cars and for new light commercial as part of the Union’s integrated approach to reduce CO2 emissions from light-duty vehicl [WWW Document]. URL

http://www.europarl.europa.eu/sides/getDoc.do?pubRef=-%2F%2FEP%2F%2FNONSGML%2BCOMPARL%2BPE-619.135%2B01%2BDOC%2BPDF%2BV0%2F%2FEN

Das, S., 2000. The life-cycle impacts of aluminum body-in-white automotive material. J. Miner. Met. Mater. Soc. 52, 41–44. doi:10.1007/s11837-000-0173-2

Das, S., Graziano, D., Upadhyayula, V.K.K., Masanet, E., Riddle, M., Cresko, J., 2016. Vehicle lightweighting energy use impacts in U.S. light-duty vehicle fleet. Sustain. Mater. Technol. 8, 5–13. doi:10.1016/j.susmat.2016.04.001

Ducker Worldwide, 2015. AISI Materials Content Analysis: Final Report.

Ducker Worldwide, 2014. 2015 North American Light Vehicle Aluminum Content Study [WWW Document]. URL http://www.autonews.com/assets/PDF/CA95065611.PDF

Earles, J.M., Halog, A., 2011. Consequential life cycle assessment: a review. Int. J. Life Cycle Assess. 16, 445–453. doi:10.1007/s11367-011-0275-9

Ekvall, T., 2000. A market-based approach to allocation at open-loop recycling. Resour. Conserv. Recycl. 29, 91–109.

Ekvall, T., Andrae, A., 2006. Attributional and Consequential Environmental Assessment of the Shift to Lead-Free Solders. Int. J. Life Cycle Assess. 11, 344–353.

Ekvall, T., Azapagic, A., Finnveden, G., Rydberg, T., Weidema, B.P., Zamagni, A., 2016. Attributional and consequential LCA in the ILCD handbook. Int. J. Life Cycle Assess. 21, 293–296. doi:10.1007/s11367-015-1026-0

Ekvall, T., Finnveden, G., 2001. Allocation in ISO 14041—a critical review. J. Clean. Prod. 9, 197–208. doi:10.1016/S0959-6526(00)00052-4

Ekvall, T., Weidema, B.P., 2004. System boundaries and input data in consequential life cycle inventory analysis. Int. J. Life Cycle Assess. 9, 161–171. doi:DOI 10.1065/lca2004.03.148

Energy Information Adminstration, 2018. Changes in steel production reduce energy intensity [WWW Document]. URL https://www.eia.gov/todayinenergy/detail.php?id=27292 (accessed 7.8.18).

EPA, 2012. 2017 and Later Model Year Light-Duty Vehicle Greenhouse Gas Emissions and Corporate Average Fuel Economy Standards, Federal Register.

European Aluminum, 2018. Environmental Profile Report 2018. Brussels, Belgium.

European Parliament, 2014. Regulation (EU) No 253/2014 of the European Parliament and of the Council of 26 February 2014 amending Regulation (EU) No 510/2011 to define the modalities for reaching the 2020 target to reduce CO2 emissions from new light commercial vehicles. Off. J. Eur. Union 38–41.

Field, A.F., Kirchain, R., Clark, J., 2001. Life Cycle Analysis and Temporal Distributions of Emissions: Developing a Fleet-Based Analysis. J. Ind. Ecol. 4, 71–91.

Geyer, R., 2017. UCSB GHG Comparison Model Version 5.0. http://www.worldautosteel.org/life-cycle-thinking/ucsb-energy-ghg-model/.

Geyer, R., 2014. 14 April 2014 Data Update of Version 4 of the WorldAutoSteel Energy and

GHG Model. Santa Barbara, California.

Geyer, R., 2013. User Guide for Version 4 of the WorldAutoSteel Energy and GHG Model, on behalf of the World Steel Association. Brussels, Belgium.

Geyer, R., 2008. Parametric Assessment of Climate Change Impacts of Automotive Material Substitution. Environ. Sci. Technol. 42, 6973–6979.

Geyer, R., Kuczenski, B., Zink, T., Henderson, A., 2015. Common Misconceptions about Recycling. J. Ind. Ecol. 0, 1–8. doi:10.1111/jiec.12355

Geyer, R., Malen, D., 2018. Parsimonious powertrain modeling for environmental vehicle assessments: Part 2 - Electric and hybrid electric vehicles. In preparation.

Hao, H., Geng, Y., Hang, W., 2015. GHG emissions from primary aluminum production in China : Regional disparity and policy implications. Appl. Energy. doi:10.1016/j.apenergy.2015.05.056

Hasanbeigi, A., Arens, M., Cardenas, J.C.R., Price, L., Triolo, R., 2016. Comparison of carbon dioxide emissions intensity of steel production in China, Germany, Mexico, and the United States. Resour. Conserv. Recycl. 113, 127–139. doi:10.1016/j.resconrec.2016.06.008

IAI, 2018. Primary aluminum production statistics [WWW Document]. Int. Alum. Inst. URL http://www.world-aluminium.org/statistics/ (accessed 1.1.15).

IEA, 2010. Energy Technology Perspectives: Scenarios & Strategies to 2050. International Energy Agency.

International Aluminum Institute, 2014. 2014 Environmental Metrics Report - Year 2010 Data - Final. London, United Kingdom.

ISO, 2006. Environmental management - Life cycle assessment - Requirements and Guidelines. International Standards Organization, Geneva, Switzerland.

Kim, H.C., Wallington, T.J., 2013. Life-Cycle Energy and Greenhouse Gas Emission Benefits of Lightweighting in Automobiles : Review and Harmonization. Environ. Sci. Technol. 47, 6089–6097.

Koffler, C., Finkbeiner, M., 2017. Are we still keeping it "real"? Proposing a revised paradigm for recycling credits in attributional life cycle assessment. Int. J. Life Cycle Assess.

Koffler, C., Geyer, R., Volz, T., 2014. Life Cycle Inventory, in: Environmental Life Cycle Assessment: Measuring the Environemtnal Performance of Products. American Center for Life Cycle Assesmsnet, Vashon Island, Washington, pp. 46–57.

Lewis, A.M., Kelly, J.C., Keoleian, G.A., 2014. Vehicle lightweighting vs. electrification: Life cycle energy and GHG emissions results for diverse powertrain vehicles. Appl. Energy 126, 13–20. doi:10.1016/j.apenergy.2014.03.023

Lloyd, S.M., Ries, R., 2007. Characterizing, propagating, and analyzing uncertainty in life-cycle assessment: A survey of quantitative approaches. J. Ind. Ecol. 11, 161–179. doi:10.1162/jiec.2007.1136

Løvik, A.N., Modaresi, R., Mu, D.B., 2014. Long-Term Strategies for Increased Recycling

of Automotive Aluminum and Its Alloying Elements. Environ. Sci. Technol. 48, 4257–4265.

Malen, D., Geyer, R., 2018. Parsimonious powertrain modeling for environmental vehicle assessments: Part 1 - Internal combustion vehicles. In preparation.

Manski, C.F., 2013. Public policy in an uncertain world: analysis and decisions. Harvard University Press, Cambridge, Massachusetts.

Mcmillan, C.A., Skerlos, S.J., Keoleian, G.A., 2012. Evaluation of the Metals Industry's Position on Recycling and its Implications for Environmental Emissions. J. Ind. Ecol. 16, 324–333. doi:10.1111/j.1530-9290.2012.00483.x

Milford, R.L., Allwood, J.M., Cullen, J.M., 2011. Assessing the potential of yield improvements, through process scrap reduction, for energy and CO2 abatement in the steel and aluminium sectors. Resour. Conserv. Recycl. 55, 1185–1195. doi:10.1016/j.resconrec.2011.05.021

Modaresi, R., Müller, D.B., 2012. The role of automobiles for the future of aluminum recycling. Environ. Sci. Technol. 46, 8587–8594. doi:10.1021/es300648w

Modaresi, R., Pauliuk, S., Løvik, A.N., Mu, D.B., 2014. Global Carbon Benefits of Material Substitution in Passenger Cars until 2050 and the Impact on the Steel and Aluminum Industries. Environ. Sci. Technol. 48, 10776–10784.

Morgans, S., 2012. Advanced High- High - Strength Steel Technologies in the 2013 Ford Fusion [WWW Document]. URL

http://www.autosteel.org/~/media/Files/Autosteel/Great Designs in Steel/GDIS 2012/Advanced High-Strength Steel Technologies in the 2013 Ford Fusion.pdf (accessed 7.11.17).

Morvaj, B., Evins, R., Carmeliet, J., 2017. Decarbonizing the electricity grid: The impact on urban energy systems, distribution grids and district heating potential. Appl. Energy 191, 125–140. doi:10.1016/j.apenergy.2017.01.058

National Highway Traffic Safety Administration, 2006. Vehicle Survivability and Travel Mileage Schedules, Vehicle Survivability and Travel Mileage Schedules. doi:DOT HS 809 952

Oracle Company, 2018a. Oracle Crystal Ball [WWW Document]. URL http://www.oracle.com/technetwork/middleware/crystalball/overview/index.html (accessed 6.8.18).

Oracle Company, 2018b. How Crystal Ball Calculates Sensitivity [WWW Document]. URL https://docs.oracle.com/cd/E12825_01/epm.111/cb_user/frameset.htm?ch07s04s03.html

Ou, X., Xiaoyu, Y., Zhang, X., 2011. Life-cycle energy consumption and greenhouse gas emissions for electricity generation and supply in China. Appl. Energy 88, 289–297. doi:10.1016/j.apenergy.2010.05.010

Pafumi, M., 2006. Advanced High Strength Steel Technology in the 2006 Honda Civic [WWW Document]. URL http://www.autosteel.org/~/media/Files/Autosteel/Great Designs in Steel/GDIS 2007/07 - Advanced High Strength Steel Technology in the

2006 Honda Civic.pdf (accessed 7.11.17).

Plevin, R.J., Delucchi, M. a., Creutzig, F., 2014. Using Attributional Life Cycle Assessment to Estimate Climate-Change Mitigation Benefits Misleads Policy Makers. J. Ind. Ecol. 18, 73–83. doi:10.1111/jiec.12074

Querini, F., Benetto, E., 2015. Combining Agent-Based Modeling and Life Cycle Assessment for the Evaluation of Mobility Policies. Environ. Sci. Technol. 49, 1744–1751. doi:10.1021/es5060868

Rajagopal, D., 2016. A Step Towards a General Framework for Consequential Life Cycle Assessment. J. Ind. Ecol. 0. doi:10.1111/jiec.12433

Reck, B.K., Graedel, T.E., 2012. Challenges in metal recycling. Science (80-.). 337, 690–695. doi:10.1126/science.1217501

Sakai, S. ichi, Yoshida, H., Hiratsuka, J., Vandecasteele, C., Kohlmeyer, R., Rotter, V.S., Passarini, F., Santini, A., Peeler, M., Li, J., Oh, G.J., Chi, N.K., Bastian, L., Moore, S., Kajiwara, N., Takigami, H., Itai, T., Takahashi, S., Tanabe, S., Tomoda, K., Hirakawa, T., Hirai, Y., Asari, M., Yano, J., 2014. An international comparative study of end-of-life vehicle (ELV) recycling systems. J. Mater. Cycles Waste Manag. 16, 1–20. doi:10.1007/s10163-013-0173-2

Saltelli, A., Annoni, P., 2010. How to avoid a perfunctory sensitivity analysis. Environ. Model. Softw. 25, 1508–1517. doi:10.1016/j.envsoft.2010.04.012

Sandén, B.A., Karström, M., 2007. Positive and negative feedback in consequential life-

cycle assessment. J. Clean. Prod. 15, 1469–1481. doi:10.1016/j.jclepro.2006.03.005

Serrenho, A.C., Norman, J.B., Allwood, J.M., 2017. The impact of reducing car weight on global emissions: the future fleet in Great Britain. Philos. Trans. R. Soc. A Math. Phys. Eng. Sci. 375, 20160364. doi:10.1098/rsta.2016.0364

Shen, L., Worrell, E., Patel, M.K., 2010. Open-loop recycling: A LCA case study of PET bottle-to-fibre recycling. Resour. Conserv. Recycl. 55, 34–52. doi:10.1016/j.resconrec.2010.06.014

Sorrell, S., Dimitropoulos, J., Sommerville, M., 2009. Empirical estimates of the direct rebound effect: A review. Energy Policy 37, 1356–1371. doi:10.1016/j.enpol.2008.11.026

Stasinopoulos, P., Compston, P., Newell, B., Jones, H.M., 2012. A system dynamics approach in LCA to account for temporal effects-a consequential energy LCI of car body-in-whites. Int. J. Life Cycle Assess. 17, 199–207. doi:10.1007/s11367-011-0344-0

Stock, J.H., 2001. Instrumental Variables in Statistics and Econometrics, 2nd Editio. ed, International Encyclopedia of the Social & Behavioral Sciences. Elsevier. doi:10.1016/B978-0-08-097086-8.42037-4

The Aluminum Association, 2015. Industry Statistics - Facts at a Glance - 2015.

The Aluminum Association, 2013. The Environmental Footprint of Semi-Finished Aluminum Products in North America. Arlington, VA.

Thinkstep, 2015. GaBi Professional Database.

Vadenbo, C., Hellweg, S., Astrup, T.F., 2017. Let's Be Clear(er) about Substitution: A Reporting Framework to Account for Product Displacement in Life Cycle Assessment. J. Ind. Ecol. 21, 1078–1089. doi:10.1111/jiec.12519

Weidema, B.P., 2003. Market information in life cycle assessment, Danish Ministry of the Environment. Copenhagen, Denmark.

Weidema, B.P., Ekvall, T., Heijungs, R., 2009. Guidelines for application of deepened and broadened LCA, CALCAS.

Werheit, P., Fricke-Begemann, C., Gesing, M., Noll, R., 2011. Fast single piece identification with a 3D scanning LIBS for aluminium cast and wrought alloys recycling. J. Anal. At. Spectrom. 26, 2166–2174. doi:10.1039/c1ja10096c

Wohlecker, R., Johannaber, M., Espig, M., 2007. Determination of Weight Elasticity of Fuel Economy for ICE, Hybrid and Fuel Cell Vehicles. SAE Tech. Pap. 1. doi:10.4271/2007-01-0343

World Steel Association, 2010. Data Provided by World Steel Association (WSA).

Yang, Y., 2016. Two sides of the same coin: consequential life cycle assessment based on the attributional framework. J. Clean. Prod. 127, 274–281. doi:10.1016/j.jclepro.2016.03.089

Yang, Y., Heijungs, R., 2017. On the use of different models for consequential life cycle assessment. Int. J. Life Cycle Assess. 751–758. doi:10.1007/s11367-017-1337-4

Yano, J., Hirai, Y., Okamoto, K., Sakai, S. ichi, 2014. Dynamic flow analysis of current and future end-of-life vehicles generation and lead content in automobile shredder residue. J. Mater. Cycles Waste Manag. 16, 52–61. doi:10.1007/s10163-013-0166-1

Zink, T., Geyer, R., 2017. Circular Economy Rebound. J. Ind. Ecol. 21, 593–602. doi:10.1111/jiec.12545

Zink, T., Geyer, R., Startz, R., 2017. Toward Estimating Displaced Primary Production from Recycling: A Case Study of U.S. Aluminum. J. Ind. Ecol. 0, 1–13. doi:10.1111/jiec.12557

Zink, T., Geyer, R., Startz, R., 2015. A Market-Based Framework for Quantifying Displaced Production from Recycling or Reuse. J. Ind. Ecol. 0, 1–11. doi:10.1111/jiec.12317

3. Causal inference for quantifying displaced primary production from recycling

Reprinted (adapted) with permission from:

Causal inference for quantifying displaced primary production from recycling

Joseph Palazzo, Roland Geyer, Richard Startz, and Douglas G. Steigerwald.

Journal of Cleaner Production. **2019,** 210, 1076-1084

DOI: 10.1016/j.jclepro.2018.11.006

3.1 Abstract

Recycling only creates environmental benefits when it displaces other material production. Without displacement, it only delays rather than prevents ultimate disposal. It is therefore critically important that we improve our understanding of the causality between recycling and other material production. This research focuses on estimation of the causal link between an increase in recycling and a reduction in primary material. I first review how structural models of supply and demand, for both the primary material and the recycled material, can be used to identify a causal link. The supply and demand approach suffers from issues of endogeneity, which require the use of advanced regression techniques. These techniques, in turn, require detailed and large datasets, which are often hard to obtain. Here, I introduce the Difference-in-Differences estimator to the industrial ecology literature, as an alternative approach to quantifying the causal effect between additional recycling and

primary material production. The Difference-in-Differences estimator is based on a quasi-experimental approach, in that it classifies data into treatment and control groups. I introduce the method, analyze the data structures and assumptions needed for identification of causal effects, and discuss the advantages relative to the supply and demand framework. A hypothetical application of each method to aluminum recycling is provided, along with a simulated quantitative example of the Difference-in-Differences technique. My proposed method will help to better understand, measure, and promote the conditions under which recycling creates environmental benefits.

3.2 Introduction

Recycling is the process of converting what would otherwise be waste into secondary resources to be used again in the economy. In public environmental policy, recycling is seen as one way to keep solid waste out of landfill and reduce the environmental footprint of human activity. Recycling, or secondary material production, is also a topic that has received intense attention throughout the history of the field of industrial ecology. It turns out that the sole environmental benefit of secondary production is that it can displace, or avoid, other material production processes (Geyer et al., 2015; Yang, 2016; Zink et al., 2015). Recycling without displacement only delays rather than prevents ultimate disposal activities such as landfill, littering, or incineration (Zink and Geyer, 2018). Such displacement leads to all other perceived benefits of recycling such as landfill reduction, energy savings, and reductions in raw material usage (Geyer et al., 2015). Unfortunately, the actual mechanisms of displacement have not been studied until recently.

From early to recent times, displacement has simply been assumed to happen on a 100% basis, which means that each unit of recycled material displaces one unit of primary material. In environmental life cycle assessment (LCA), recycling causes a so-called allocation issue when it happens across two different product systems. Methods used to resolve this issue include recycled content, 50/50, avoided burden, value-corrected substitution, and multi-cycle approaches (Atherton, 2007; Frischknecht, 2010; Nicholson et al., 2009; Weidema, 2001). These methods typically account for yield losses, and some also consider limited technical substitutability. However, they uniformly ignore the fact that technical equivalence does not guarantee displacement. While authors have acknowledged that quantifying displacement precisely is important (Ekvall, 2000; Geyer, 2008; Geyer et al., 2015; Mcmillan et al., 2012; Vadenbo et al., 2017; Weidema, 2003), only one comprehensive statistical analysis of displacement exists in the industrial ecology literature (Zink et al., 2017).

The extent to which more scrap and waste collection leads to additional secondary production, and then to displacement, has predominantly been treated as a market equilibrium problem in the literature and approached by assuming or calculating price elasticities (Ekvall, 2000; Ekvall and Andrae, 2006; Weidema, 2003; Zink et al., 2017, 2015). Displacement has also been identified as a key issue in the methodological development of consequential life cycle assessment (CLCA), which strives to model the net environmental impacts of a change to an industrial system considering all physical and social processes affected (Brander et al., 2009; Ekvall et al., 2016; Koffler and Finkbeiner, 2017; Weidema, 2003; Zamagni et al., 2012). In general, much of the industrial ecology literature has equated social processes with markets and their equilibria (Earles and Halog,

2011; Rajagopal, 2016; Weidema, 2003; Weidema et al., 2009; Zamagni et al., 2012). CLCA has considerably advanced life cycle thinking, a pertinent example being the issue of direct and indirect land use change (LUC and ILUC, Marvuglia et al., 2013; Vázquez-Rowe et al., 2014). However, it has yet to be fully exploited to support decision-making for recycling or for circular economy activities more broadly. This may, in part, be due to its current focus on market equilibrium models, which turn out to be challenging and highly uncertain.

Structural market models of primary and secondary variants of one material in isolation from the rest of the economy have been the primary tool proposed and applied to calculating displacement (Ekvall, 2000; Ekvall and Andrae, 2006; Zink et al., 2017, 2015). It has been shown that this can be used to assess the displacement of primary aluminum due to aluminum recycling in North America (Zink et al., 2017). Supply and demand modelling has also been applied to other industrial ecology problems, such as direct energy efficiency rebound effects (Sorrell et al., 2009) and ILUC in biofuel production (Lapola et al., 2010; Plevin et al., 2010; Searchinger et al., 2008). However, supply and demand models are only one avenue to study cause-and-effect mechanisms using observational data. Authors have recently suggested that broader causal inference analysis will be necessary for industrial ecologists to support sustainable development (Cucurachi and Suh, 2017), but specific applications are still lacking in the literature.

In this paper, I generalize displacement as a question of the cause-and-effect relationship between secondary production and primary material and show that structural market equilibrium models are not the only possible approach. I identify and investigate the use of an alternative method for causal inference, Difference-in-differences (DID), for quantifying

the causal relationship between recycling and primary production. DID has a long history in applied microeconomics beginning with Ashenfelter and Card (1985). The novelty of this contribution lies in the application of DID to the industrial ecology literature. I thoroughly examine the statistical problems and assumptions, causal mechanisms, and operationalization of both structural supply and demand models and DID without loss of generality. Idealized case studies for the two methods are hypothesized using aluminum as a platform. A quantitative example of DID is provided using simulated data, illustrating key potential issues with its practice. Finally, I discuss applying these methods to other displacement problems and the significance of this research in environmental policy and the field of industrial ecology.

3.3 Generalized Displacement

Figure 3.1 shows a generalized displacement problem. The solid green line represents secondary aluminum production Q_{sec} over time for a regional aluminum market. Prior to the year 2000, secondary aluminum was not produced in this particular market. In the year 2000, an exogenous shock occurs, i.e. a shock that did not affect demand for aluminum directly, hence the dashed lines have the same slope before and after the year 2000. This shock leads to the production of 150 tons of secondary aluminum per year going forward. One example of such a shock would be a legislative act suddenly mandating aluminum producers to increase secondary production. I ask the following question: does additional secondary production cause a decrease in primary production? This question is critical because such an outcome reduces our reliance on raw natural resources and typically reduces the total impact of production. This impact reduction dynamic may affect the environmental assessment of policy-driven changes to product systems. One example is

material substitution in vehicles, where lack of displaced production through recycling would affect the environmental performance of light-weight materials (Geyer, 2008; Løvik et al., 2014; Modaresi et al., 2014; Modaresi and Müller, 2012). The dotted lines in Figure 3.1 (a) are the trends in primary aluminum production Q_{prim} over time, and in Figure 3.1 (b) they represent the trends in total aluminum production $Q_{tot} = Q_{sec} + Q_{prim}$.

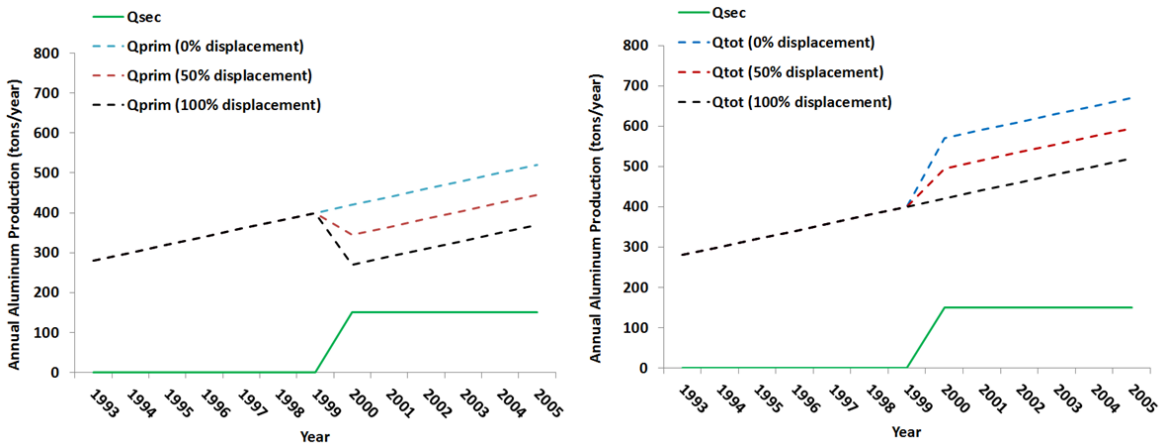

Figure 3.1: Total quantity of material produced as a function of time with an exogenous shock leading to additional secondary production in the year 2000. Displacement is a research question about what happens after this influx of secondary material. The question can be answered by observing what happens to the primary quantity produced after the shock. Panel (a) shows what happens to primary production for 0%, 50% and 100% displacement. Panel (b) shows the same for total production.

Consider the case where this influx of secondary material goes onto the regional market for automotive materials. In the scenario represented by the black line in Figure 3.1, all of the secondary aluminum is used to replace primary aluminum (i.e. 150 tons per year), which is 100% displacement. The red line represents the scenario where only 75 tons of the secondary aluminum is used to replace primary aluminum, which is 50% displacement. In a

third scenario represented by the blue line, none of the secondary aluminum is used to replace primary aluminum, which is 0% displacement. These examples illustrate the definition of displacement: $d = 1 - \frac{\Delta Q_{tot}}{\Delta Q_{sec}} = \frac{-\Delta Q_{prim}}{\Delta Q_{sec}}$.

In general, there are numerous forces affecting the regional demand for aluminum such as GDP, incomes, and the prices of substitute materials. These other forces will affect how much aluminum is used in automobile manufacturing. In consequence, one cannot estimate displacement simply by computing the observed change in primary and secondary production. To control for these other forces, one could specify a linear regression model with the functional form

$$Q_{prim} = \alpha + \beta_1 Q_{sec} + \beta_2 X_2 + \cdots + \beta_k X_k + \varepsilon \quad (3.1)$$

where $\sum_{i=2}^{k} \beta_i X_i$ capture the effect of these forces, and ε is the regression error term. Unfortunately, Ordinary Least Squares (OLS) estimates of the effect of Q_{sec} on Q_{prim} (β_1) are likely to be biased and inconsistent due to endogeneity. This presents itself when the explanatory variable of interest is correlated with the regression error term. It also threatens the identification of causal effects from the regression coefficients. Endogeneity arises for a number of reasons, but is frequently due to simultaneous causality between the dependent variable and the explanatory variable. While I expect secondary production to have an effect on primary production, I equally expect that changes in primary production affect secondary production; thus, simultaneous causality is a significant concern in the estimation of (3.1).

3.4 Previous approach to quantifying displacement: Supply and demand

3.4.1 Framework

A classical approach to address endogeneity is to estimate a structural model of supply and demand for primary and secondary aluminum using instrumental variable methods rather than OLS (also known as Partial Equilibrium Analysis). This approach has been used historically and frames displacement micro-econometrically, meaning that price responses of supply and demand are assumed to drive the causal relationship between secondary production and primary production (Ekvall, 2000; Ekvall and Andrae, 2006; Zink et al., 2017, 2015). One would estimate functional relationships between supply and demand of primary and secondary material and their explanatory variables, which include endogenous prices and exogenous shifters. Equation 3.2 shows a simplified set of simultaneous equations of supply and demand for primary and secondary material (QS_{prim}, QS_{sec}, QD_{prim} and QD_{sec}) along with equilibrium conditions.

$$QS_{prim} = \alpha_1 + \beta_1 P_{prim} + \pi_1 SHIFTS_{prim} + \varepsilon_1 \quad (3.2a)$$

$$QD_{prim} = \alpha_2 + \gamma_1 P_{prim} + \mu_1 (P_{sec} - P_{prim}) + \pi_2 SHIFTD_{prim} + \varepsilon_2 \quad (3.2b)$$

$$QS_{sec} = \alpha_3 + \beta_2 P_{sec} + \pi_3 SHIFTS_{sec} + \varepsilon_3 \quad (3.2c)$$

$$QD_{sec} = \alpha_4 + \gamma_2 P_{sec} + \mu_2 (P_{prim} - P_{sec}) + \pi_4 SHIFTD_{sec} + \varepsilon_4 \quad (3.2d)$$

$$QS_{prim} = QD_{prim} \quad (3.2e)$$

$$QS_{sec} = QD_{sec} \quad (3.2f)$$

In this system, α_n are intercepts, β_n are own-price responses of supply, $\gamma_n - \mu_n$ are own-price responses of demand, μ_n are cross-price responses of demand, $SHIFTX$ are the exogenous shifters, π_n represent the effect of changes in the exogenous shifters on supply

and demand, P_x are price variables and ε_n are unobserved error terms. Observations of quantities, prices, and shifters are gathered empirically and used to estimate a set of four regressions. After the coefficients on the equations are estimated, a shock is introduced to α_1, or to the supply of secondary material. Solving the system again after introducing a shock simulates how primary supply would respond to the change in the secondary supply. The algebra behind this is detailed in Zink et. al, 2015. I note that in practice, prices of substitutes and additional control variables are likely to come into play and complicate the algebra even further.

Before moving forward, it is critical to examine the meaning of all six components of (3.2) in depth. This system of equations represents a classical economic model of the behavior of supply-side agents and demand-side agents that interact simultaneously on a market for the primary and secondary variants of a material. In practice, multiple observations of all of the variables are collected over time. Here, (3.2a) states that a given observation of the quantity of primary material supplied to the market (QS_{prim}) is a function of a baseline intercept α_1, its market price at the time of the observation P_{prim}, the magnitude of one or more exogenous supply shifters at the time of the observation $SHIFTS_{prim}$, and an unobserved random variable ε_1. The researcher collects multiple observations of QS_{prim}, P_{prim}, and $SHIFTS_{prim}$ and uses them to estimate a regression in the form of (3.2a). This estimation yields values for α_1, β_1, and π_1. The coefficient β_1 is the change in the quantity of primary material supplied in response to a one unit change in its price (or the own-price response). The coefficient π_1 is the change in the quantity of primary material supplied in response to a one unit change in $SHIFTS_{prim}$, a variable other than price that affects primary supply. The correct choice of $SHIFTS_{prim}$ is dependent on the

particular market being analyzed. These regression coefficients are necessary in order to specify the dynamics between changes in the quantity of secondary material and changes in the quantity of primary material, which are linked through the components of (3.2).

The concept behind (3.2b) is nearly identical. However, the agents of demand are different than the agents of supply. Thus, QD_{prim} will respond differently to changes in price than QS_{prim}, and carries a different price response coefficient. In addition, the exogenous (non-price) shifter of demand is different than that of supply, hence the notation $SHIFTD_{prim}$. Finally, I introduce the consideration of the difference in prices between the primary and secondary variant of the material, which is salient to the agents of demand and may affect their decisions. The price difference also links the demand functions for primary and secondary material. After estimating a regression in the form of (3.2b), I have values for all of its coefficients. The interpretation is the same as that of (3.2a), except that I add μ_1, which is the change in the quantity of primary material demand in response to a one-unit change in the price difference between the primary and secondary variant. The interpretation of the variables and coefficients in (3.2c) and (3.2d) follow immediately from that of (3.2a) and (3.2b). The distinction is that data collection and estimation involve analogous variables related to secondary materials, as opposed to primary.

Finally, consider (3.2e) and (3.2f). These equilibrium conditions reflect the classical economic assumption that supply and demand are equivalent in the long term on a competitive market, or a market where no one agent or small group of agents determines how the market operates. Exogenous shocks to supply and demand, such as those analyzed in quantifying displacement, cause the market to settle into a new equilibrium condition that satisfies the entire system of equations shown in (3.2).

Estimating four simultaneous equations bypasses the particular statistical issue posed in the OLS estimation of (3.1). However, price is endogenous in the vast majority of markets, leaving us with a new statistical issue. Prices cause supply and demand to change, but changes in supply and demand also affect price, which clearly constitutes simultaneous causality (Wooldridge, 2012). The supply and demand framework approach restores the causal interpretation of price-response parameters by estimating four two-stage least squares (2SLS) equations with instrumental variables. The first stage of 2SLS consists of estimating a regression with the endogenous variable as the dependent variable, and the instrument(s) as well as all other exogenous covariates on the right-hand side. This generates an estimate for the value of the problem (endogenous) variable that corrects for endogeneity bias, which is substituted into the original regression equation. The second stage is estimating the original regression using the values of the endogenous variable estimated from the first stage. In practice, 2SLS software commands avoid the need for two separate regressions and ensure correct estimates of standard errors. However, it is still worthwhile to walk through the theoretical construct of the first-stage.

Consider the first two components of (3.2). In the case of primary supply, the price of primary material is the endogenous variable. For primary demand, both the price of primary material and the price difference between primary and secondary material are endogenous. Estimating 2SLS requires that there are at least as many instruments as endogenous variables for each equation. The instruments for the primary supply equation are exogenous shifters of primary demand, secondary supply, and secondary demand. The instruments for the primary demand equation are exogenous shifters of primary supply, secondary supply, and secondary demand. Thus, there are at least three instruments for each equation,

assuming that I am able to find unique and exogenous shifters for primary supply, primary demand, secondary supply, and secondary demand. Equation 3.3 provides an example of a first stage regression for the primary supply equation, which generates $\widehat{P_{prim}}$, the estimate for P_{prim} that corrects for endogeneity.

$$P_{prim} = \delta_1 + \tau_1 SHIFTD_{prim} + \tau_2 SHIFTS_{sec} + \tau_3 SHIFTD_{sec} + \tau_4 SHIFTS_{prim} + \omega_1 \quad (3.3a)$$

$$\widehat{P_{prim}} = \widehat{\delta_1} + \widehat{\tau_1} SHIFTD_{prim} + \widehat{\tau_2} SHIFTS_{sec} + \widehat{\tau_3} SHIFTD_{sec} + \widehat{\tau_4} SHIFTS_{prim} + \widehat{\omega_1} \quad (3.3b)$$

In specifying (3.3), I assume that the four exogenous shifters are "relevant" instruments for the price of primary material P_{prim}. This means that the shifters of the supply and demand curves are correlated with P_{prim}. By estimating (3a), I generate values of P_{prim} that are a function of only the variables that are exogenous to the supply and demand system specified in (3.2). In essence, this provides a correction for the simultaneous causality issue that leads to bias in an OLS estimate of the price response coefficients in the first four components of (3.2). After collecting a series of observations of P_{prim} and the four exogenous shifters, I estimate (3.3a). This results in an estimated vector of values for P_{prim}, which I notate as $\widehat{P_{prim}}$. The variables on the right-hand side of (3.3b) are the estimated functional form of $\widehat{P_{prim}}$. Its intercept is $\widehat{\delta_1}$, it changes by $\widehat{\tau_n}$ in response to a unit change in the exogenous shifters, and it has an estimated error term $\widehat{\omega_1}$. This exercise is repeated for all of the price variables, as I must replace all price variables in (3.2) with their corrected versions. It turns out that identifying the unique, exogenous shifters is not so straightforward. In practical applications, the exogeneity of shifters is frequently debatable, which threatens the identification of causal effects. The following discussion illustrates ideal, but hypothetical shifters for all four equations in the case of aluminum.

A truly unique and exogenous shifter of primary aluminum supply would be a measure of political unrest in countries that are primary bauxite suppliers, as bauxite is the key raw material input for aluminum production. One could create a variable indicating how many bauxite-producing countries experience unrest in a given year, for example. Of course, there must be variation in unrest over time. In the case of primary aluminum demand, consider increased costs of shipping for iron ore that increase the cost of steel, making steel sheet for automotive body parts prohibitively expensive. Primary aluminum is the best-known substitute, thus demand for primary aluminum is shifted exogenously by the variation in iron ore shipping costs.

Legislation aimed at increasing recycling rates, such as the "bottle bills" offering deposits for recycling aluminum cans throughout the United States (State of Hawai'i, 2002; State of Oregon, 1971), have been shown to be exogenous shifters of secondary aluminum supply (Container Recycling Institute, 2005). For use in the structural market model, it is required that such policies vary over time, for example by gradually increasing in geographic scope. Finally, an exogenous shifter of secondary aluminum demand would be the purity of recycled aluminum over time, which may increase due to technological improvements. This would exogenously increase the amount of applications where recycled aluminum is a viable substitute.

Figure 3.2 illustrates the causal pathways of the supply and demand framework via price-quantity relationships, showing how the supply and demand curves for primary aluminum are shifted by the instrumental variables. Shifting the primary demand curve traces out the primary supply curve, and vice versa. This is the key concept in restoring the causal relationship between quantity and price (Stock, 2001).

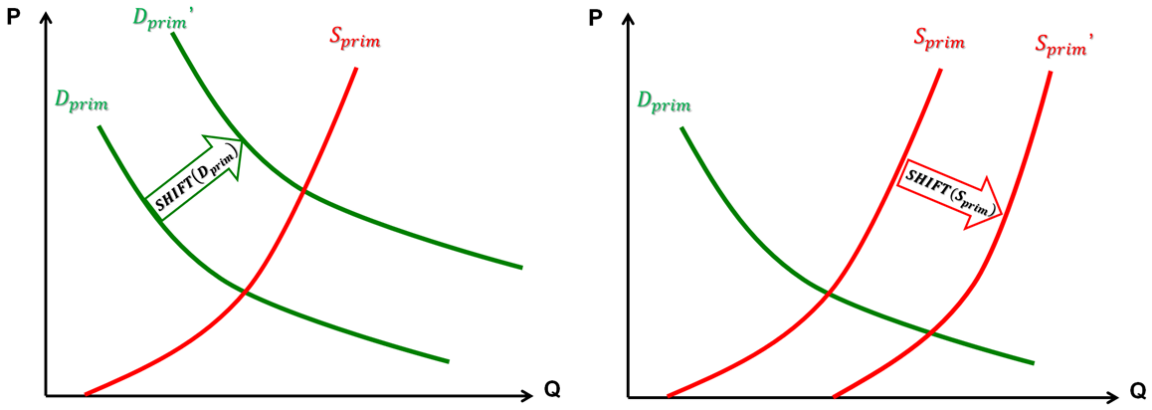

Figure 3.2: Causal pathways in the supply and demand framework illustrated via price-quantity (P-Q) relationships. Panel (a) shows that one instruments for the primary supply equation shifts the primary demand curve from D to D', while panel (b) shows that one instrument for the primary demand equation shifts the primary supply curve from S to S'.

3.4.2 **Case Study**

The lone case study using this methodology explores the question of whether or not aluminum recycling in the U.S. displaces primary production between 1971 and 2013 (Zink et al., 2017). The exogenous shifters are prices of substitutes as well as a series of process inputs and economic factors (Blomberg and Hellmer, 2000; Blomberg and Söderholm, 2009), which are not as strong as the idealized shifters I propose above. This is a ubiquitous issue in the identification of causal effects using structural market models. The authors use 43 annual observations of all variables on the national level. The small number of observations contributed to a high level of uncertainty in the results. In fact, in the initial year following a 5% shock to secondary supply, displacement estimated via Monte Carlo simulations has a 5th to 95th percentile range of approximately [-50%, 100%] (Zink et al., 2017).

3.4.3 **Advantages & Disadvantages**

Structural supply and demand models offer a methodology for estimating displacement in competitive markets based on classical economic theory. The structural equations for supply and demand determine the instruments, which are the unique exogenous shifters used in the 2SLS regressions. Thus, setting up the structural equations implicitly provides a solution to price endogeneity and establishes identification of causal effects.

On the other hand, the causal interpretation of supply and demand models requires that the market in question be competitive, in that no individual agent or small group of agents can determine how that market operates. A model of the form of Equation 3.2 further requires that the effect of price is linear and homogenous. Identifying four unique and exogenous shifters of supply and demand is challenging, and failure to do so introduces bias to the estimation and complicates interpretation of the model. The challenge is amplified in settings where I seek to observe multiple market segments, where shifters are needed for each segment. To overcome these challenges, I developed the following framework for quantifying displacement.

3.5 Novel approach to quantifying displacement: Quasi-experimental

3.5.1 **Framework**

Rather than construct a structural supply and demand model for the two markets, one could approach endogeneity directly through observations of the quantity of primary and secondary material by seeking out natural experiments in observational data. This quasi-experimental design could be achieved through the gathering of public data, or via primary data collection. A quasi-experiment is a situation where endogeneity is addressed by

dividing observations into treatment and control groups based on explanatory characteristics of their values for an outcome variable of interest over time. Observations could be grouped by firms, industries, or geographic regions that may use primary and secondary variants of a material, for example. After some time, an exogenous change to the quantity of secondary material occurs in the treatment group, and the quantity of primary material in the treatment and control groups are compared before and after the exogenous change. Several statistical methods may be applied to a quasi-experiment. Selection of the method depends on the problem at hand and the structure of the data available. Examples include difference-in-differences (DID), regression discontinuity analysis, and propensity score matching (Angrist and Pischke, 2009; Caliendo and Kopeinig, 2005; Imbens and Lemieux, 2007; Lee and Lemieux, 2010). I explore the quasi-experimental approach by applying DID estimation to quantifying displacement for the first time in the literature.

Consider the simplified DID example of Figure 3.3, where there is an exogenous increase in the secondary quantity of a material in a subset of market segments ($TREAT_i = 1$) at time t^*=100. The exogenous increase originates from a source uncorrelated with factors that explain the underlying trend in the material quantity on the market. There is a control group of market segments, which do not see any change in secondary material at t^*=100. In the period after the exogenous change at t^*=100 ($t \geq t^*$), observations of the quantity of primary material in both the treatment and control groups continue to be collected. At time t=300, the difference in primary material in each market segment between t^*=100 and t=300 is measured for both treatment and control groups. If the additional recycling had no effect on primary material, the difference in primary material between t^*=100 and t=300 would be the same in both groups. In Figure 3.3, the treatment group had

a lesser difference in primary material from pre-to post-treatment compared with the control group, thus there is a "difference in the differences", which is reflected by θ. This coefficient is interpreted as the increase in secondary material causing a decrease in primary material given that the identification restrictions outlined in Section 3.5.2 are satisfied. One would determine θ using a regression with form of (3.4):

$$Q_{it}^{prim} = \mu + \delta\{iTREAT_i = 1\} + \rho\{t \geq t^*\} + \theta\{TREAT_i = 1\} * \{t \geq t^*\} + \varepsilon_{it} \quad (3.4)$$

where Q_{it}^{prim} is the observation of primary material in market segment i (treatment or control) in period t (pre- or post-treatment), $\{TREAT_i\}$ takes the value 1 for treated observations and 0 for controls, $\{t \geq t^*\}$ takes the value 1 in the post treatment period and 0 in the pre-treatment period, and ε_{it} is the error term (Angrist and Pischke, 2009). The effect of interest is identified by θ, the coefficient on $\{TREAT_i = 1\} * \{t \geq t^*\}$, which has a value of 1 for observations of the treatment group in the post-treatment period. The change in primary material θ reflected in the regression is converted into displacement by observing the change in secondary material and applying the identity $d = -\frac{\Delta Q_{prim}}{\Delta Q_{sec}} = -\frac{\theta}{\Delta Q_{sec}}$, where ΔQ_{sec} is the increase in recycling that occurs at t^*.

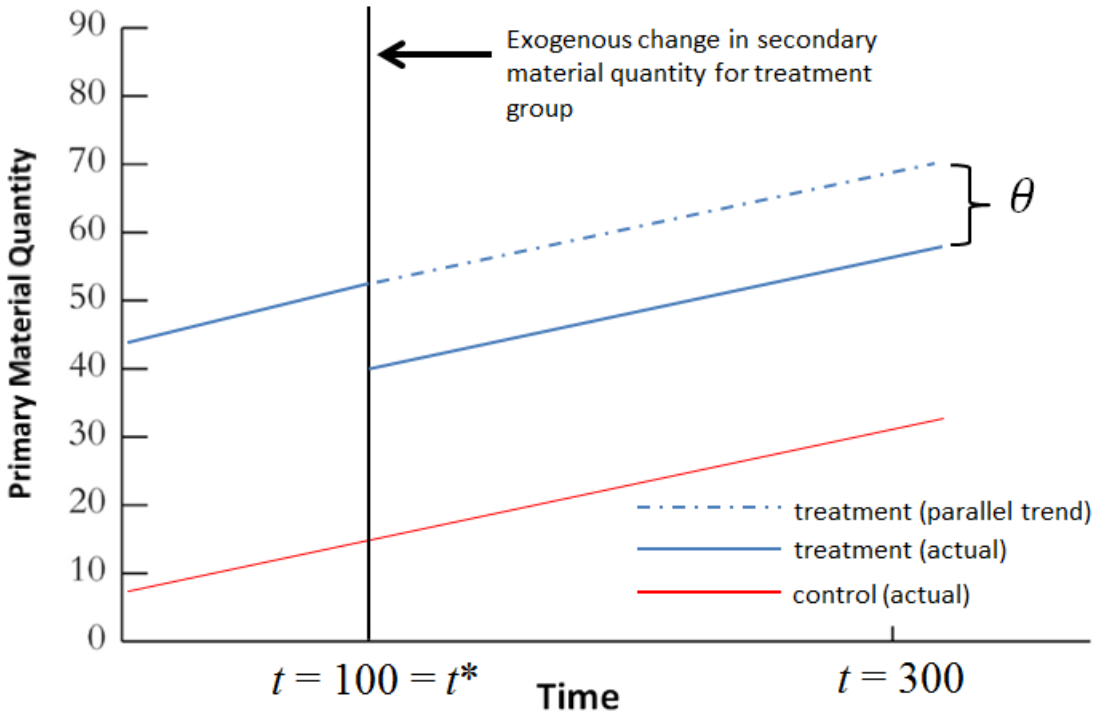

Figure 3.3: Difference-in-differences estimation of displacement due to increases in recycling. The treatment group of market segments experiences a sudden increase in recycling at t=100. The quantity of primary material is measured in each period, and θ gives the DID estimate of the change in the quantity of primary material caused by exogenous shift in recycling activity.*

3.5.2 **Firm-Level Case Study**

Here, I return to the example of automobile manufacturing from the generalized displacement discussion in Section 3.3. Consider the scenario where groups of treatment and control firms operating in similar markets both use primary aluminum. The treatment firms absorb additional secondary aluminum generated from an exogenous, policy-driven shock. The control firms do not pursue use of the additional secondary aluminum provided by the shock. Selection into the treatment group is random conditional on observable

characteristics of the firms. In this hypothetical system, I gather monthly statistics on primary and secondary aluminum used in each firm *i* on a per vehicle basis. At t^*=100, an exogenous, policy-driven shock to the quantity of secondary aluminum ΔQ_{sec} occurs and is absorbed by the treatment group of firms. I continue to measure primary aluminum used per vehicle by the treatment and control firms until t=300.

In this application, use of DID requires that the trends in primary aluminum consumption by the treatment and control firms were parallel prior to t*=100 or that any differences in the trends could be accounted for by observable quantities. For example, the trend in primary aluminum quantity may look different for firms that produce economy class vehicles versus those that produce luxury class vehicles. This is one example of a factor that needs to be included in the DID regression as a control, ensuring that treatment is random conditional on what I observe. With the appropriate controls in place, one could estimate a regression with the form of Equation 3.5, where Q_{it}^{prim} is the quantity of primary aluminum used in firm *i* during month *t.*

$$Q_{it}^{prim} = \mu + \delta\{TREAT_i = 1\} + \rho\{t \geq t^*\} + \theta\{TREAT_i = 1\} * \{t \geq t^*\} + \gamma_1 CLASS_{it} + \cdots + \sum_{k=2}^{K} \gamma_k CONTROL_{it} + \varepsilon_{it} \quad (3.5)$$

The displacement effect is given by $d = -\frac{\Delta Q_{prim}}{\Delta Q_{sec}} = -\frac{\theta}{\Delta Q_{sec}}$.

The first identifying assumption of the DID causal effect is referred to as the parallel trends assumption, and means that I assume the post-treatment trend in per vehicle primary aluminum use would be the same between the treatment and control firms in the absence of treatment (Angrist and Pischke, 2009). The robustness of this assumption can be examined, for example, by comparing the trends in per vehicle primary aluminum use between treatment and control groups for the period prior to t^*=100 and verifying they were actually

parallel. The second necessary condition is that the treatment, or sudden increase in recycling, did not coincide with another exogenous shock affecting primary aluminum use differently in the treatment and control groups. The causal interpretation of the result is threatened if, for example, a policy requiring improved fuel economy emerges at the same time as the exogenous shock to recycled aluminum, and the treatment and control firms respond by decreasing the mass of their vehicle fleets in ways that affect their primary aluminum use differently. Lastly, the causal interpretation requires that the additional secondary aluminum in the treatment group does not interact with the control group. In other words, the additional secondary aluminum cannot be sold by treatment firms to control firms. The trade of secondary aluminum across groups threatens identification because the treatment will have an effect on outcomes in the control group.

I must also consider the estimation of standard errors, which is influenced by assumptions regarding the correlations between values of ε_{it}. Classic standard errors are not sufficient, as they assume the error terms are uncorrelated and of constant variance, something that is highly unlikely in practice. The correct standard error estimator depends on the structure of the data. One general alternative, that adjusts for arbitrary temporal correlation, is to use the Newey-West estimator (Newey and West, 1987; Petersen, 2009). In the case of Equation (3.5), I could also account for the likely scenario that unobserved sources of variance in primary production are clustered by firm, in which case it is more appropriate to use a cluster-robust estimator. These strategies alleviate the risk of constructing standard error estimates that are systematically too small, which would lead to over-rejection of the null hypothesis that $\theta_1 = 0$ (Cameron and Miller, 2015). One must also pay attention to the number of firms and the evenness of the distribution of observations

across clusters, as cluster heterogeneity may present issues in hypothesis testing (Carter et al., 2016; Lee and Steigerwald, 2017).

3.5.3 **Quantitative Example**

Here I present a quantitative example to illustrate how a firm-level case study lends itself to a DID estimation framework, demonstrate the estimation of a DID regression on simulated data, and provide an interpretation of the model coefficients. I illustrate one of the challenges one might face using DID, which is that the mean and variance of the DID estimate will change based on the number of post-treatment periods in the data. In addition, I show how one handles the scenario where the treatment effect is dependent on an observable difference between firms (for example, the class of vehicles produced).

Returning to the example in Section 3.5.2, consider the case where a researcher collects 50 monthly observations on primary aluminum use (in tons) in 100 automotive firms. The 100 firms are divided into two groups, the first group produces economy vehicles and the second group produces luxury vehicles. This setting will allow me to examine models in which the treatment effect differs across different types of firms. In month *t**, a sustained monthly increase in secondary aluminum usage occurs for the firms exposed to an exogenous, policy-driven shock and I refer to these firms as treated.

During the pre-treatment period, $t < t^*$, primary aluminum usage in a firm depends on the class of vehicles produced:

$$Q_{it}^{prim} = \mu + \gamma_1\{CLASS_i = L\} + \varepsilon_{it}, \tag{3.6}$$

where $\{CLASS_i = L\}$ is an indicator variable designating firms that produce luxury class vehicles and ε_{it} is a normally distributed random variable. In this expression, μ is the average quantity of primary aluminum used by firms that produce economy vehicles.

Because, in this example, firms that produce luxury vehicles use more primary aluminum, the coefficient γ_1 is positive.

During the post-treatment period, $t \geq t^*$, primary aluminium usage in a firm also depends on the treatment status of the firm:

$$Q_{it}^{prim} = \mu + \theta\{TREAT_i = 1\} + \gamma_1\{CLASS_i = L\} + \gamma_2\{TREAT_i = 1\} * \{CLASS_i = L\} + \varepsilon_{it}, \quad (3.7)$$

where $\{TREAT_i = 1\}$ is an indicator variable designating firms that are treated. Here θ captures how much the average quantity of primary aluminum used by economy vehicle producers changes when secondary aluminum usage increases due to the policy. The change in the average quantity of primary aluminum usage due to the policy for luxury producers is $\theta + \gamma_2$, so that γ_2 measures how much the policy impact varies between the two types of vehicle producers.

In our simulations, on average half the firms are assigned to be luxury vehicle producers and, within each type of firm, half are randomly assigned treatment. The firms exposed to the policy increase their usage of secondary aluminum by 8 tons per month. Economy vehicle producers have a displacement of 50%, which means that primary aluminum usage falls by 4 tons per month (so $\theta = -4$). Luxury vehicle producers have a displacement of 30%, which means that primary aluminum usage for these firms falls by 2.4 tons per month (so $\gamma_2 = 1.6$).

I focus on the estimators for the treatment effect θ and γ_2 and report the results from 1000 simulations. For each simulation, I generate the data as described above and construct an estimate of the parameters from the difference-in-differences regression

$$Q_{it}^{prim} = \mu + \delta\{TREAT_i = 1\} + \rho\{t \geq t^*\} + \theta\{TREAT_i = 1\} * \{t \geq t^*\} + \gamma_1\{CLASS_i = L\} + \gamma_2\{TREAT_i = 1\} * \{t \geq t^*\} * \{CLASS_i = L\} + \varepsilon_{it} \quad (3.8)$$

where $\{t \geq t^*\}$ is an indicator that the observation occurs in the post-treatment period. Two new coefficients have appeared in (3.8), δ and ρ. These coefficients are included in applied work to account for the possibility that the treatment and control groups differ in the pre-treatment period, which is captured by δ, and for the possibility that the control group differs in the pre- and post-treatment periods, which is captured by ρ. In this setting, $\rho = 0$ because the quantity of primary aluminium usage by control firms does not systematically vary over time. Also, if an equal number of firms of each type are assigned to the treatment group, then the treatment and control groups do not differ in the pre-treatment period and $\delta = 0$. In my simulations, I randomly assign groups to treatment and control with equal probability.

For the first setting $t^* = 25$, ensuring that there are many months in both the pre- and post-treatment periods. For this setting I find highly accurate estimation of θ: the average of the estimates is -4.01, the variance is 0.11, and the minimum and maximum are -5.42 and -2.97 respectively. Thus, approximately 95% of our estimates lie within (-4.6,-3.4). For γ_2 the results are similar: the average of the estimates is 1.61 and 95% of my estimates lie within (1.0, 2.2).

Accurate estimation of the baseline treatment effect θ depends on having a sufficiently large number of observations before and after the treatment. However, analysis often occurs shortly after a policy change, leading to a small number of post-treatment observations. Thus, it is critical to ask: What happens if treatment occurs very late in the sample? To answer, I vary *t** resulting in settings in which there are a decreasing number of observations

in the post-treatment period. Table 3.1 contains the results for estimation of θ, where estimates are notated as $\hat{\theta}$ in accordance with common practice.

t^*	Mean $\hat{\theta}$	Var $\hat{\theta}$	Min $\hat{\theta}$	Max $\hat{\theta}$
25	**-4.01**	**0.11**	**-5.42**	**-2.97**
35	-4.01	0.13	-5.23	-2.88
45	-3.98	0.27	-5.69	-2.14
49	-4.02	0.80	-6.64	-1.57
50	-3.95	1.50	-8.12	0.20

Table 3.1: Features of the distribution of $\hat{\theta}$ when varying the time of the treatment intervention t. This illustrates the importance of having sufficient post-treatment observations when using DID. The base case, where t*=25, is shown in bold.*

From Table 3.1 I see that as the number of observations in the post-treatment period shrinks the variance of the estimator increases (it, of course, remains unbiased across all settings). If only one observation is available post-treatment, the variance increases dramatically. The results for estimation of γ_2 (notated as $\widehat{\gamma_2}$) are contained in Table 3.2. For the settings in which the number of post-treatment observations shrinks, a similar pattern emerges: the estimator remains unbiased but the variance increases as the post-treatment sample is reduced.

t^*	Mean $\widehat{\gamma_2}$	Var $\widehat{\gamma_2}$	Min $\widehat{\gamma_2}$	Max $\widehat{\gamma_2}$
25	**1.61**	**0.10**	**0.49**	**2.58**
35	1.60	0.16	0.41	2.91
45	1.56	0.35	-0.42	3.54

49	1.61	1.03	-1.18	5.00
50	1.63	2.09	-3.85	6.83

Table 3.2: Features of the distribution of $\widehat{\gamma_2}$ when varying the time of the treatment intervention t. This illustrates the importance of having sufficient post-treatment observations in order to adjust the DID results treatment effect for heterogeneity in observable characteristics. The base case, where t*=25, is shown in bold.*

3.5.4 **Advantages & Disadvantages**

DID uses a simpler regression framework with reduced data requirements compared to structural supply and demand models for estimating displacement. It avoids the need for exogenous shifters of supply and demand in two markets, and the aforementioned complications that go with them. However, unlike the supply-demand framework, DID requires careful balancing of treatment and control observations to avoid biased results due to confounding factors. DID treatment interventions are generally easier to defend as plausibly exogenous than the four shifters in the supply-demand framework. This is because the treatment is sharply defined and pre-treatment parallel trends imply quasi-random assignment of treatment.

DID studies also present inherent limitations. The most critical challenge with DID is that the parallel trends assumption is dependent on a counterfactual trend in the treated observations, which cannot be verified, although the testing of pre-treatment trends helps to mitigate this problem. Another key disadvantage of DID is that the parallel trend assumption is dependent on the way in which the parameter is measured (Bertrand et al., 2002; Lechner, 2011). For example, the parallel trends in primary aluminum production from Figure 3 may not hold for elementary transformations of this variable (i.e. log material production).

Underestimation of standard errors due to serial correlation of the error terms is also a known problem leading to misleading conclusions in DID studies (Bertrand et al., 2002).

It is also important to recognize the difference in scope between structural supply and demand models and a firm-level DID approach. Zink and Geyer (2017) compared partial displacement of recycling to the so-called rebound effect of increases in energy efficiency and thus called it 'circular economy rebound'. Energy efficiency rebound literature typically distinguishes between direct and indirect effects. For example, if a household acquires a more energy-efficient car, it could use the fuel cost savings to a) drive more (direct rebound) or b) purchase other goods and services (indirect rebound). In an analogous way, increased use of secondary automotive material could lead to increased total material use in the automotive sector, or increased use in other sectors, such as packaging. A structural supply and demand model would capture direct and indirect effects; while the firm-level DID approach outlined in section 3.5.2 would measure only the direct effect.

3.6 Outlook

I have framed the discussion of displacement in terms of primary and secondary production of a given material, but there are many other related questions of interest. For example, it is possible that aluminum recycling leads to less use of both primary and secondary plastics, as aluminum is used in many packaging applications. Displacement may also be an issue in generalized material substitution, regardless of whether or not the substitute material originates from recycling. Consider the case where primary aluminum is substituted for primary steel in vehicles. Displaced production of primary steel by additional primary aluminum production may not be solely determined by physical parameters in the

product system. Other effects, driven by price disturbances or other social parameters, could influence the production volumes of both materials in significant ways.

Causal inference methods such as DID provide an important addition to the toolbox of industrial ecology. They broaden the scope of what industrial ecology has considered "cause-and-effect" beyond price-driven mechanisms, which is particularly important in the development of CLCA. Approaches that fall outside the domain of classical economic equilibrium modelling allow for analyses of cause-and-effect relationships that are not conditional on perfect information and rational behavior. Perhaps sustainability interventions in product systems, such as increased energy efficiency or recycled content, have shaped perceptions and consumer preferences in a way that creates consequences that are not easily captured via price. Imagine if, for example, marketing a "green" variant of a product has the direct effect of making consumers feel less culpable for environmental damage. As a result, they purchase a larger quantity of the product than they would have without "green" labeling, regardless of price. One could envision a quasi-experimental approach where such products are introduced in a heterogeneous manner across market segments, and testing if there is an increase in total consumption that reduces the purported environmental benefits. A CLCA study of the new variant of the product would need to include this effect. Direct observations can also be coupled with field experiments such as survey studies, in order to directly examine underlying behavioral mechanisms and bridge industrial ecology studies with other disciplines. The DID method is naturally designed to analyze this quasi-experimental approach.

Another case where DID can provide insights into the relationship between recycling and primary material is the increased production of recycled wastewater in drought-prone

areas. Given that water is used, recycled, and used again in localized units with usage tracked at the individual property level by water districts, a quantitative method similar to the one presented in Section 3.5.3 can be readily applied. In fact, I apply the method outlined in this chapter to an empirical data set on wastewater recycling in Chapter 4 of this dissertation.

Understanding the net environmental consequences of changes to product systems requires a deep understanding of the physical *and* social processes that underpin these systems and cause them to evolve over time. This notion is at the core of studies of displacement and of CLCAs in which displacement is a key parameter. Thus, I emphasize the importance of frameworks other than structural models of supply and demand in quantifying the social impacts of changes to product systems. The use of quasi-experimental methods offers an avenue to advance our knowledge of how social processes translate into physical outcomes, a concept that remains in its infancy in LCA and industrial ecology. This undertaking is essential in order to strengthen the relevance of sustainability assessments for decision-making.

3.7 References

Angrist, J., Pischke, J.-S., 2009. Parallel worlds: Fixed effects, differences-in-differences and panel data, in: Mostly Harmless Econometrics: An Empiricist's Companion.

Ashenfelter, O., Card, D., 1985. Using the Longitudinal Structure of Earnings to Estimate the Effect of Training Programs. Rev. Econ. Stat. 67, 648–660. doi:10.2307/1924810

Atherton, J., 2007. Declaration by the metals industry on recycling principles. Int. J. Life Cycle Assess. 12, 59–60. doi:http://dx.doi.org/10.1065/lca2006.11.283

Bertrand, M., Duflo, E., Mullainathan, S., 2002. How Much Should We Trust Differences-in-Differences Estimates?, Nber Working Paper Series. doi:10.1007/s13398-014-0173-7.2

Blomberg, J., Hellmer, S., 2000. Short-run demand and supply elasticities in the West European market for secondary aluminium. Resour. Policy 26, 39–50.

Blomberg, J., Söderholm, P., 2009. The economics of secondary aluminium supply : An econometric analysis based on European data. Resour. Conserv. Recycl. 53, 455–463. doi:10.1016/j.resconrec.2009.03.001

Brander, M., Tipper, R., Hutchison, C., Davis, G., 2009. Consequential and attributional approaches to LCA: a Guide to policy makers with specific reference to greenhouse gas LCA of biofuels. Ecometrica Press 1–14.

Caliendo, M., Kopeinig, S., 2005. Some practical guidance for the implementation of propensity score matching. Inst. Study Labor 1–29.

Cameron, R.C., Miller, D.L., 2015. A Practitioner's Guide to Cluster-Robust Inference. J. Hum. Resour. 50, 317–372. doi:10.3368/jhr.50.2.317

Carter, A. V, Schnepel, K.T., Steigerwald, D.G., 2016. Asymptotic Behavior of a t Test Robust to Cluster Heterogeneity. Rev. Econ. Stat. 1–27. doi:10.1162/rest_a_00639

Container Recycling Institute, 2005. Beverage Container Redemption Rates in Selected Deposit States vs the US Average [WWW Document]. URL http://www.container-recycling.org/index.php/beverage-container-redemption-rates-in-selected-deposit-

states-vs-the-us-average (accessed 1.1.17).

Cucurachi, S., Suh, S., 2017. Cause-effect analysis for sustainable development policy. Environ. Rev. 379, er-2016-0109. doi:10.1139/er-2016-0109

Earles, J.M., Halog, A., 2011. Consequential life cycle assessment: a review. Int. J. Life Cycle Assess. 16, 445–453. doi:10.1007/s11367-011-0275-9

Ekvall, T., 2000. A market-based approach to allocation at open-loop recycling. Resour. Conserv. Recycl. 29, 91–109.

Ekvall, T., Andrae, A., 2006. Attributional and Consequential Environmental Assessment of the Shift to Lead-Free Solders. Int. J. Life Cycle Assess. 11, 344–353.

Ekvall, T., Azapagic, A., Finnveden, G., Rydberg, T., Weidema, B.P., Zamagni, A., 2016. Attributional and consequential LCA in the ILCD handbook. Int. J. Life Cycle Assess. 21, 293–296. doi:10.1007/s11367-015-1026-0

Frischknecht, R., 2010. LCI modelling approaches applied on recycling of materials in view of environmental sustainability , risk perception and eco-efficiency. Int. J. Life Cycle Assess. 15, 666–671. doi:10.1007/s11367-010-0201-6

Geyer, R., 2008. Parametric Assessment of Climate Change Impacts of Automotive Material Substitution. Environ. Sci. Technol. 42, 6973–6979.

Geyer, R., Kuczenski, B., Zink, T., Henderson, A., 2015. Common Misconceptions about Recycling. J. Ind. Ecol. 0, 1–8. doi:10.1111/jiec.12355

Imbens, G., Lemieux, T., 2007. Regression Discontinuity Designs: A Guide to Practice,

NBER Working Series.

Koffler, C., Finkbeiner, M., 2017. Are we still keeping it “real”? Proposing a revised paradigm for recycling credits in attributional life cycle assessment. Int. J. Life Cycle Assess.

Lapola, D.M., Schaldach, R., Alcamo, J., Bondeau, A., Koch, J., Koelking, C., Priess, J.A., 2010. Indirect land-use changes can overcome carbon savings from biofuels in Brazil. Proc. Natl. Acad. Sci. 107, 3388–3393. doi:10.1073/pnas.0907318107

Lechner, M., 2011. The Estimation of Causal Effects by Difference-in-Difference Methods. Found. Trends Econom. 4, 165–224. doi:10.1561/0800000014

Lee, C.H., Steigerwald, D.G., 2017. Inference for Clustered Data (forthcoming). Stata J. 0, 1–23.

Lee, D.S., Lemieux, T., 2010. Regression Discontinuity Designs in Economics. J. Econ. Lit. 48, 281–355. doi:10.1257/jel.48.2.281

Løvik, A.N., Modaresi, R., Mu, D.B., 2014. Long-Term Strategies for Increased Recycling of Automotive Aluminum and Its Alloying Elements. Environ. Sci. Technol. 48, 4257–4265.

Marvuglia, A., Benetto, E., Rege, S., Jury, C., 2013. Modelling approaches for consequential life-cycle assessment (C-LCA) of bioenergy: Critical review and proposed framework for biogas production. Renew. Sustain. Energy Rev. 25, 768–781. doi:10.1016/j.rser.2013.04.031

Mcmillan, C.A., Skerlos, S.J., Keoleian, G.A., 2012. Evaluation of the Metals Industry's Position on Recycling and its Implications for Environmental Emissions. J. Ind. Ecol. 16, 324–333. doi:10.1111/j.1530-9290.2012.00483.x

Modaresi, R., Müller, D.B., 2012. The role of automobiles for the future of aluminum recycling. Environ. Sci. Technol. 46, 8587–8594. doi:10.1021/es300648w

Modaresi, R., Pauliuk, S., Løvik, A.N., Mu, D.B., 2014. Global Carbon Benefits of Material Substitution in Passenger Cars until 2050 and the Impact on the Steel and Aluminum Industries. Environ. Sci. Technol. 48, 10776–10784.

Newey, W.K., West, K.D., 1987. A Simple, Positive Semi-Definite, Heteroskedasticity and Autocorrelation Consistent Covariance Matrix. Econometrica 55, 703–708. doi:10.2307/1913610

Nicholson, A., Olivetti, E., Gregory, J., Field, F., Kirchain, R., 2009. End of Life Allocation Methods: Open Loop Recycling Impacts on Robustness of Material Selection Decisions, IEEE International Symposium on Sustainable Systems and Technology. doi:10.1109/ISSST.2009.5156769

Petersen, M.A., 2009. Estimating standard errors in finance panel data sets: Comparing approaches. Rev. Financ. Stud. 22, 435–480. doi:10.1093/rfs/hhn053

Plevin, R.J., Jones, A.D., Torn, M.S., Group, R., Division, E.S., Berkeley, L., 2010. The greenhouse gas emissions from indirect land use change are uncertain, but may be much greater than previously estimated. Environ. Sci. Technol. 44, 8015–8021. doi:10.1021/es101946t

Rajagopal, D., 2016. A Step Towards a General Framework for Consequential Life Cycle Assessment. J. Ind. Ecol. 0. doi:10.1111/jiec.12433

Searchinger, T., Heimlich, R., Houghton, R.A., Dong, F., Elobeid, A., Fabiosa, J., Tokgoz, S., Hayes, D., Yu, T., 2008. Use of U.S. Croplands for Biofuels Increases Greenhouse Gases Through Emissions from Land-Use Change. Science. 423, 1238–1241.

Sorrell, S., Dimitropoulos, J., Sommerville, M., 2009. Empirical estimates of the direct rebound effect: A review. Energy Policy 37, 1356–1371. doi:10.1016/j.enpol.2008.11.026

State of Hawai'i, 2002. Solid Waste Management Deposit Beverage Container Law.

State of Oregon, 1971. The Beverage Container Act. Oregon State Legislature.

Stock, J.H., 2001. Instrumental Variables in Statistics and Econometrics, 2nd Editio. ed, International Encyclopedia of the Social & Behavioral Sciences. Elsevier. doi:10.1016/B978-0-08-097086-8.42037-4

Vadenbo, C., Hellweg, S., Astrup, T.F., 2017. Let's Be Clear(er) about Substitution: A Reporting Framework to Account for Product Displacement in Life Cycle Assessment. J. Ind. Ecol. 21, 1078–1089. doi:10.1111/jiec.12519

Vázquez-Rowe, I., Marvuglia, A., Rege, S., Benetto, E., 2014. Applying consequential LCA to support energy policy: Land use change effects of bioenergy production. Sci. Total Environ. 472, 78–89. doi:10.1016/j.scitotenv.2013.10.097

Weidema, B., 2001. Avoiding Co-Product Allocation in Life-Cycle Assessment. J. Ind.

Ecol. 4, 11–33.

Weidema, B.P., 2003. Market information in life cycle assessment, Danish Ministry of the Environment. Copenhagen, Denmark.

Weidema, B.P., Ekvall, T., Heijungs, R., 2009. Guidelines for application of deepened and broadened LCA, CALCAS.

Wooldridge, J.M., 2012. Simultanenous Equation Models, in: Introductary Econometrics, A Modern Approach. pp. 554–582.

Yang, Y., 2016. Two sides of the same coin: consequential life cycle assessment based on the attributional framework. J. Clean. Prod. 127, 274–281. doi:10.1016/j.jclepro.2016.03.089

Zamagni, A., Guinée, J., Heijungs, R., Masoni, P., Raggi, A., 2012. Lights and shadows in consequential LCA. Int. J. Life Cycle Assess. 17, 904–918. doi:10.1007/s11367-012-0423-x

Zink, T., Geyer, R., 2018. Recycling and the myth of landfill diversion (forthcoming). J. Ind. Ecol.

Zink, T., Geyer, R., 2017. Circular Economy Rebound. J. Ind. Ecol. 21, 593–602. doi:10.1111/jiec.12545

Zink, T., Geyer, R., Startz, R., 2017. Toward Estimating Displaced Primary Production from Recycling: A Case Study of U.S. Aluminum. J. Ind. Ecol. 0, 1–13. doi:10.1111/jiec.12557

Zink, T., Geyer, R., Startz, R., 2015. A Market-Based Framework for Quantifying Displaced Production from Recycling or Reuse. J. Ind. Ecol. 0, 1–11. doi:10.1111/jiec.12317

4. How much potable water is saved from wastewater recycling? Quasi-experimental evidence from California

4.1 Abstract

Investment in advanced wastewater recycling has increased in drought-prone parts of the world. California has made particularly large investments in wastewater recycling to replace applications that use potable water, but do not require it. In these cases, a conversion of the physical infrastructure on the properties is required, due to regulations that ensure that recycled wastewater does not contaminate potable supplies. This conversion process and discretization of water supplies creates a natural experiment in a large water district in California. Over the period 2001 to 2014 a number of public parks converted from potable to recycled water for landscape purposes in two regions within a water district, while others in those regions remained on potable supply. While the selection of parks for conversion is not random, selection depends on the evolution of a large infrastructure project initiated by the water district in collaboration with the state, with a decision-making process involving many stakeholders, but does not appear to be correlated with the site specific factors that determine water use. In this research, I match converted and unconverted parks based on their location to control for other factors that determine water usage. This enables a quasi-experimental analysis, where we quantify the effect of converting to recycled water on total water use and potable water use. I use two-way fixed effects regression to produce a difference-in-differences estimate of the effect of recycled water on total and potable water usage. I find that total water usage is largely unchanged at parks that are converted to recycled water use, and the finding is robust to a number of sample restrictions. However, I find that potable water usage is reduced significantly when a park is connected to the

recycled water supply. In the study period, I estimate 25 million cubic feet of potable water was saved. The point estimate of displacement, or the ratio of potable water saved to recycled water used, is 93.4%. This analysis provides the first empirical estimate of the water savings claimed by urban water recycling programs, and the first empirical estimate of displacement using quasi-experimental methods. The methodology can be further extended to evaluating the effectiveness of water recycling programs around the world.

4.2 Introduction

The reuse of treated wastewater, or water recycling, is a strategy for the diversification of urban water portfolios in water scarce areas. Increases in water recycling capacity have been a policy driven response to drought in Australia and California. While the use of recycled water in California traces back to the early 1900s, recycled water use has more than doubled since 1990, a time period in which the most extreme droughts in California history have occurred (Kwon and Lall, 2016). Droughts are expected to increase in frequency and intensity as climate change continues, which will stimulate the need for desalinated ocean water and recycled water. How has the increased use of recycled water changed the overall demand for water and, in particular, the demand for potable water? To shed light on this question, I examine data from a California water district that recently introduced treated wastewater into its supply. I find that while potable water demand falls, the overall demand for water does not demonstrably change.

The reuse of wastewater traces back to ancient civilizations in dry areas of the world. Angelakis, Koutsoyiannis, and Tchobanoglous (2005) trace the earliest uses of wastewater for agricultural irrigation to the Minoan civilization, more than a millennium before the Christian era. In modern times, Qatar, Israel, and Kuwait are among the largest users of

recycled water, each of these countries has a long history of water scarcity (Jimenez and Asano, 2008). In semi-arid areas that have been settled in more recent times, such as Australia and California, the use of recycled water is a more recent development. For example, the use of untreated sewer water for agricultural irrigation in California raised public health concerns that resulted in the first regulations related to water reuse in the state in 1918 (Newton et al., 2011). A major proposal for water recycling infrastructure in California came in the form of the Water Recycling Act of 1991, which committed to 1 million acre-feet of annual wastewater recycling by the year 2010 (California State Legislature, 1991). The bill was drafted with the intention to fill a "[…]need for a reliable source of water for uses not related to the supply of potable water to protect investments in agriculture, greenbelts, and recreation and to replenish groundwater basins, and protect and enhance fisheries, wildlife habitat, and riparian areas." In the case of Australia, the idea of recycling urban wastewater for a subsequent use was largely absent from the water supply discourse until the 1990s, when a number of legislative initiatives regarding water management were adopted (Radcliffe, 2015). The "millennium drought" of the mid-2000s prompted the formation of the National Water Commission and a strong commitment to increasing the diversity of water supplies (Apostolidis et al., 2011). Today, advanced water recycling consists of a combination of reverse osmosis and treatment with ultraviolet light, also known as tertiary treatment, in addition to the standard mechanical and biological processing of water that enters a wastewater treatment plant (Australian Academy of Technological Sciences and Engineering, 2004).

It has been highlighted recently that climate change promotes an increase in the harshness and the rate at which droughts occur throughout the world (Dai, 2013; Trenberth

et al., 2014). Moreover, areas of high population are expected to experience a pronounced increase in their exposure to drought (Guneralp et al., 2015). Thus, an increase in water sources that lack dependence on rainfall, such as wastewater recycling, is inevitable especially in urban areas. However, it has been suggested that locales with access to diverse water sources may be less responsive to water conservation initiatives in the face of drought conditions, perhaps due to a perceived lack of scarcity (Baldassare and Katz, 1992; Palazzo et al., 2017). This further reinforces the need for research into methods to precisely quantify the effect of increasing recycled wastewater supplies on potable water usage.

In general, characterizing the environmental benefits that arise from recycling activity is a topic of great interest to the industrial ecology community (Ekvall, 2000; Frischknecht, 2010; Koffler and Finkbeiner, 2018), These benefits are driven by the degree to which recycled materials substitute for their primary equivalents on the material market, a phenomenon referred to as displacement (Geyer et al., 2015; Yang, 2016; Zink and Geyer, 2018). In recent research, authors have shown that paper consumption may increase when users are aware of its recycled content (Catlin and Wang, 2013) and that the complete substitution of recycled aluminum for primary aluminum on the U.S. material market is unlikely (Zink et al., 2017). It has also been shown that resource consumption may increase when recycling is added as a disposal option, in comparison to scenarios where trashing is the only disposal option (Sun and Trudel, 2017). These studies provide evidence that recycling may encourage increases in total resource consumption, a phenomenon known as circular economy rebound (Zink and Geyer, 2017). Another recent paper suggested one can test for the presence of circular economy rebound using quasi-experimental approaches such as difference-in-differences (DID), where data are divided into treatment and control groups

(Palazzo et al., 2019). Data with the resolution required to use DID were not available for the case of aluminum. Water recycling, on the other hand, presents a compelling case study because water is used, recycled, and reused in a localized system with data that are regularly tracked at the level of the individual user by water districts. Furthermore, recycled water is delivered for non-potable applications using a discretized infrastructure in which the usage data of potable and recycled water are metered. Thus, in this research I collect data on water usage of different types over time to conduct the first quasi-experimental estimate of the effect of wastewater recycling on total and potable water usage. I use a two-way fixed effects regression to produce DID estimates of the effect of recycled water conversions on total and potable water usage.

I first discuss the assumptions that qualify the use of the technique and then apply it to a panel of nineteen properties in two regions of the water district. In water districts with active water recycling programs, promotional material states the amount of potable water saved is equivalent to the amount of recycled wastewater supplied to customers (Goleta Water District, 2018; Horticulture Australia Limited, 2011). However, a rigorous statistical estimate of this equivalency is lacking in the literature. In this research, I estimate that an average site that converts to recycled water in one California water district saves an average of 1,224 cubic feet of potable water per day, equivalent to 93.4% of its recycled water usage. I conclude with a discussion of the limitations of my approach, future research directions, and the implications of the findings for water resources management.

4.3 Data & Methods

4.3.1 Data source

To examine the effect of water recycling on total water use, and in turn displacement, I collect a primary data set on site-level water usage from the East Bay Municipal Utility District (EBMUD), a large water district (more than 1 million customers) in California. These data consist of monthly observations of water usage from public recreational properties. For each site, we collect a minimum of 120 monthly observations. Data are collected from a total of 21 sites that are divided into two small regions within EBMUD. A site is considered "treated" once it has been connected to the infrastructure that supplies recycled wastewater. Sites that are never connected to the infrastructure serve as controls. The proximity of treatment and control properties allows us to isolate the effect of conversion to recycled water from the myriad other factors that determine water usage (Arbués et al., 2003; DeOliver, 1999; Gilbertson et al., 2011; Martinez-Espineira, 2002).

Table 4.1 gives a summary of the data set used in the analysis. EBMUD supplied the water usage data without site-specific identifiers. Thus, the exact location and size of all properties is unknown. However, I proceed under the assumption that given their geographic proximity, the treatment and control groups are robust matches in predictors of water usage. The connection to recycled water is staggered over time, with some sites connected later than others. Because of this, there are more observations in the control state than in the treatment state. I account for this staggered adoption in the estimated model.

In addition, I observe the unit price of water of both potable and recycled water, both of which increase over the data collection period. The price of each type of water in a given year is the same across all sites. In all but one year (2010), the price of potable water is

exactly 1.2 times the price of recycled water. In 2010, potable water costs 1.08 times as much as recycled water. The public recreational properties do not pay a tiered water rate based on usage as most residential properties in California do. I note that two potential control sites, one from each region, were excluded due to data anomalies that make them unsuitable controls for the sites that convert from potable to recycled water.

Region	Control Sites	Treated Sites	Mean control observations	Mean treatment observations	Mean pre-treatment monthly water usage for controls (CCUFT/site/month)	Mean pre-treatment monthly water usage for treated (CCUFT/site/month)
R1	5	5	168	129	1390	682
R2	4	5	168	136	272	213

Table 4.1: An overview of the two study regions including the number of control and treatment sites, the mean number of observations for the treatment and control sites, and the mean monthly water usage for treatment and control sites in hundred cubic feet (CCUFT) during the period before any site is connected to recycled water.

Table 4.1 compares average water use in the pre-treatment period for the sites that will eventually be treated and those that serve as corresponding controls. Ideally, the average water use is comparable across the two groups. This is true in Region 2, where the average usage in control sites, 272, is quite similar to the average usage in the sites selected for treatment, 213. Thus in Region 2, the treatment sites appear to be randomly selected. In Region 1, however, the average usage in control sites, 1390, is much larger than the average usage in sites selected for treatment, 682. It could be that in Region 1, larger parks are located closer to the source of recycled water, and so are more likely to be treated. As long as this differential usage pattern does not change over time, then it can be accounted for with

site specific effects and the comparison of treatment and control groups remains valid. In Section 4.3.2.1, I detail why this difference is likely random with respect to selection into recycled water conversion, and thus does not threaten the identification of the effect of recycled water conversion on total and potable water usage.

4.3.2 **Empirical approach**

4.3.2.1 Estimation framework

To estimate the effect on water demand of introducing recycled water I employ the-difference-in-differences (DID) estimator, which Palazzo, Geyer, Startz, and Steigerwald (2019) propose as a method to analyze the effect of recycling on total and primary resource usage. The identification of causal effects depends on several key assumptions. Let Y_{it} measure total water usage at site *i* in period *t*. Each site in each time period is characterized by a pair of potential outcomes $Y_{it}(0)$ and $Y_{it}(1)$. The observed outcome is $Y_{it}(1)$ if the observation is treated and $Y_{it}(0)$ if the observation is not treated. A site is treated once it is connected to the recycled water system.

The first assumption required for the use of DID is that treatment is randomly assigned, or $\{Y_i(0),\ Y_i(1)\} \perp TREAT_i$, where $TREAT_i$ is 1 if a site is treated at any point during the study period and 0 otherwise. The assignment mechanism for the parks that we observe is based on factors that are likely unrelated to their water usage. For example, sites connected to the recycling infrastructure are generally determined based on: distance to the treatment plant, the cost per mile of the system, and the number of sites served. Within EBMUD, main recycled water pipelines are constructed in an alignment that enables recycled water to reach an "anchor" customer such as a golf course or large industrial user. The pipeline going from

the wastewater treatment plant to the anchor customer is configured such that the maximum number of smaller irrigation customers, such as the parks that we collected data on, can be reached at the lowest cost. Thus, although Table 4.1 shows that total usage is higher overall in control parks in Region 1, this imbalance is unlikely to change in response to the introduction of recycled water, because it is a function of the parks' proximity to anchor customers.

A second key assumption, which is sometimes termed the parallel trends assumption, implies that, absent connection to recycled water, water usage would follow the same trend over time in all parks. This assumption would be threatened if, for example, there was another major change that occurred in the treated parks simultaneously with their conversion to recycled water. Because I am unable to run a controlled experiment, my treatment could be correlated with another exogenous effect that is differs in magnitude across treatment and control sites. However, I note that in the sample I have staggered adoption of the treatment. This helps me to mitigate the possibility that another exogenous effect occurs simultaneously. Figure 4.1 examines the robustness of parallel trends in total water usage during the pre-treatment period. The plotted trends are average total water usage across sites in the treatment group (solid line) and control group (dashed lines) during the subset of the study period where all 19 sites are reporting data. I observe a sinusoidal pattern in water usage that peaks in the summer season. The peaks in the control group are lower than that of the treatment group. To focus the comparison on trends rather than levels, treatment and control are plotted on separate axes. In the all-sites reporting period, the pre-treatment trends in average total water usage are approximately parallel in the treatment and control groups.

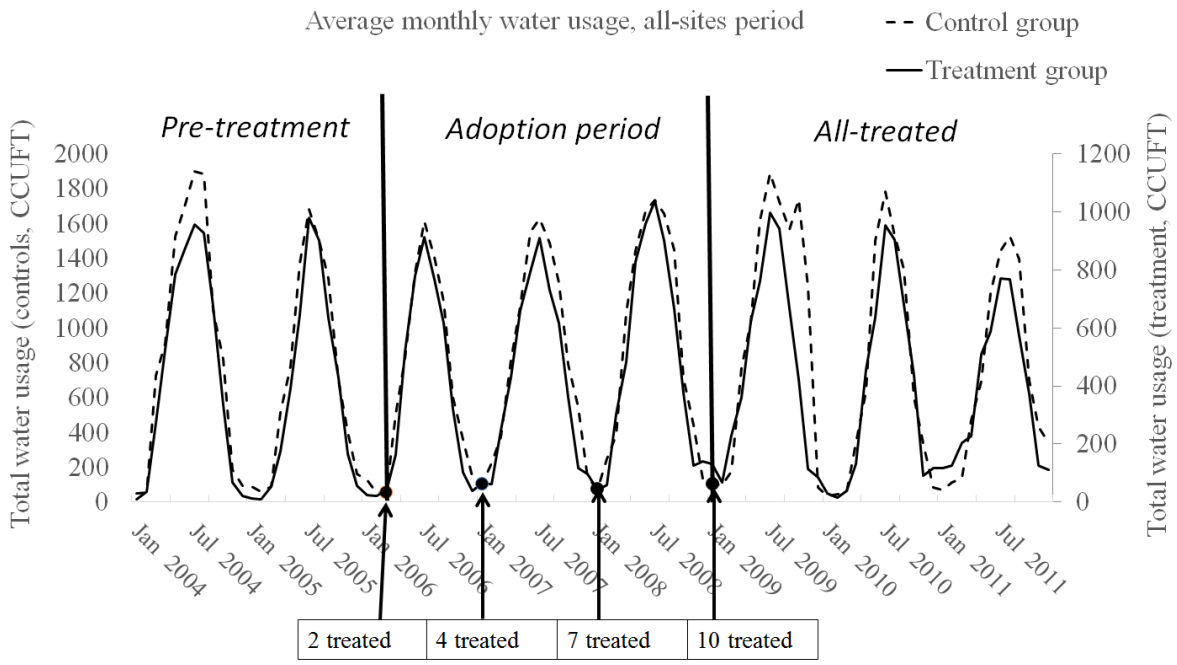

Figure 4.1: Monthly water usage in CCUFT averaged across treated sites (solid line) and control sites (dashed line) during the period where all sites report data. The staggered treatment adoption is indicated with labels the number of treated sites at the beginning of each year where new treated sites are introduced. The all-sites period is broken into three parts, one before any site is treated (per-treatment), a second during the staggered adoption period (adoption period), and a third once all sites are treated (all-treated).

The water usage data collected here lends itself to a DID analysis. First, I seek to understand whether or not the introduction of recycled water had an effect on total water usage in converted sites. This could arise from over irrigation due to the perceived lack of scarcity of recycled water or from the release of pent up demand, for example. A change in total water usage could also originate from qualities of the recycled water itself. For example, recycled water is known to contain higher concentrations of salts that may buildup in soils where it is used (Toor and Lusk, 2011).

To establish the basic regression framework for DID estimation; consider the case where there are two sites, one treated and one control. I observe two months (t=2) of water usage in the two sites (i=2). One of the two properties received the treatment, a conversion to recycled water, in the period t=2. The treated site is assigned the designation $TREAT_i = 1$. To examine whether or not the conversion to recycled water had an effect on total water consumption in the treated site using DID, I estimate (4.1) where Y_{it} is the total water usage in site i during month t:

$$Y_{it} = \mu + \delta\{TREAT_i = 1\} + \rho\{t = 2\} + \theta D_{it} + \varepsilon_{it} \quad (4.1)$$

Here, $\{TREAT_i\}$ takes the value 1 for the treated sites and 0 for the controls, $D_{it} = \{TREAT_i = 1\} * \{t = 2\}$, μ is the intercept, δ captures the difference in levels between the treatment and control properties throughout the study period, ρ captures the effect of being in the post-treatment period of treated unit i, and θ is the DID coefficient. In other words, the estimate $\widehat{\theta}$ captures the change in total water usage that arises from being in the treated state during the post-treatment period. I choose total water usage as the dependent variable because sites often convert completely from potable to recycled water. Thus, using potable water as the dependent variable introduces a large number of zeroes into the dependent variable and inhibits my ability to fit a continuous linear model.

Before moving forward, I take a step back to explore the significance of the elements of (4.1). In essence, the terms $\delta\{TREAT_i = 1\}$ and $\rho\{t = 2\}$ are controls for the quasi-experiment represented by this model. It is likely that mean monthly water usage levels are systematically different in the treatment and control groups throughout the entire study period, regardless of the exposure of the treatment group to recycled water. The coefficient δ captures this difference in means, and including the term in the regression addresses

potential bias in the estimate of the treatment effect. This bias would arise because the previously existing difference in water usage levels between the treatment and control groups would be absorbed into the estimate $\hat{\theta}$. Similarly, ρ captures a change in mean water usage that arises in both the treatment and control groups in the post-treatment period. Including this term in the regression addresses potential bias in the estimate of the treatment effect that arises from time trends that exist across both treatment and control groups. Such time trends are not attributable to the treatment itself. With these controls in place, and the aforementioned identification assumptions met, θ represents an unbiased estimator of the effect of being assigned to treatment, and being in the post-treatment period.

Table 4.2 illustrates the role of the model coefficients from a differences-in-means perspective.

	Pre-treatment mean	Post-treatment mean
Treated	$\mu + \delta$	$\mu + \delta + \rho + \theta$
Control	μ	$\mu + \rho$

Table 4.2: The mean monthly water usage for pre- and post-treatment observations in the treated and control groups when using the difference-in-differences regression model in Equation (4.1)

Let $\bar{Y}$ be the mean monthly water usage in a site throughout the study period. Then, let mean water usage corresponding to the four quadrants of Table 4.2 be labeled using subscripts, such as $\bar{Y}_{pre,treated}$ for pre-treatment observations of a treated site. Table 4.2 gives the four different values of $\bar{Y}$:

$\bar{Y}_{pre,control} = \mu$

$\bar{Y}_{post,control} = \mu + \rho$

$\bar{Y}_{pre,treated} = \mu + \delta$

$\bar{Y}_{post,treated} = \mu + \delta + \rho + \theta$

When $\delta \neq 0$, there is a systematic difference in total water usage levels in the treated and control groups throughout the study period. When $\rho \neq 0$, there is a time trend that exists across both treatment and control groups, which is not attributable to the exposure of the treatment group to the treatment. I note that the terminology difference-in-differences comes from the fact that $\{[\bar{Y}_{post,treated} - \bar{Y}_{pre,treated}] - [\bar{Y}_{post,control} - \bar{Y}_{pre,control}]\} = \{[\mu + \delta + \rho + \theta - \mu - \delta] - [\mu + \rho - \mu]\} = \theta$. The coefficient θ represents the difference between pre-and post-treatment means in the treatment group, minus the difference between pre-and post-treatment means in the control group.

Using the estimate of the effect of recycled water on total water usage, I can also estimate displacement, which is the ratio of the change in primary material usage to the change in secondary material usage (Zink et al., 2015). In this setting, potable water is the primary material and recycled wastewater is the secondary material. Thus, I ask: How much of the recycled water usage comes from reducing, or displacing, potable water usage? To measure displacement effects, let

$$R = \sum_{i=1}^{n} \sum_{t=1}^{T} R_{it}$$

be total recycled water usage and let

$$n_{treat} = \sum_{i=1}^{n} \sum_{t=1}^{T} D_{it}$$

be the number of observations of treated sites. Because θ measures the average monthly

change in total water usage after connection to recycled water, total water usage is changed by $\theta \cdot n_{treat}$ during the study period.

If total water usage is unchanged, then recycled water has replaced potable water 1 for 1 and the displacement ratio is 1. If, instead, total water usage increases, then 1 unit of recycled water replaces less than 1 unit of potable water and the displacement ratio is less than 1. Formally, the displacement ratio is (see appendix for additional details):

$$d = 1 - \frac{\theta \cdot n_{treat}}{R} \tag{4.2}$$

Total potable water savings immediately follow as:

$$\Delta P = R * d = R * \left[1 - \frac{\theta \cdot n_{treat}}{R}\right] = R - \theta \cdot n_{treat} \tag{4.3}$$

In this elementary example, I have only one post-treatment observation of water usage for each site. Thus, I can estimate displacement and total potable water savings in the treated site by applying (4.2) and (4.3):

$\hat{d} = 1 - \frac{\hat{\theta} \cdot n_{treat}}{R} = 1 - \frac{\hat{\theta}}{R_{22}}$, and $\Delta P = R_{22} * d$,

where R_{22} is the recycled water usage observed for the treated site (i=2) in the post-treatment period (t=2), and n_{treat} is equal to one. It is important to note that the numerator in the displacement quantity is an estimate of the average treatment effect for each period t multiplied by the appropriate number of time periods, while the denominator is a summation of the observed recycled water usage. This becomes a critical point, as the actual data set I collected contains multiple treated sites and multiple post-treatment periods. Handling this data set requires some adaptation of the simple DID regression method outlined above, as discussed in the following section.

4.3.2.2 Two-way fixed effects

To examine the effect of recycled water conversions on total and potable water usage in the setting where I have multiple control units, treated units, and time periods, I use the two-way fixed effects regression approach to DID estimation. A two-way fixed effects approach allows for there to be an individual intercept, or dummy variable coefficient, for each site. Two-way fixed effects also allows for an individual intercept, or dummy variable coefficient, for each time period of data collection. This is a more flexible approach than the standard DID example given in section 4.3.2.1, where I estimate a single intercept for treatment sites, a single intercept for control sites, and one indicator variable for the post-treatment period. In two-way fixed effects settings I can control for time-invariant factors in individual sites, such as management structures, by estimating individual site intercepts. In addition, I can control for site-invariant factors that are distinct during each time period, such as the unit prices of potable and recycled water, by estimating individual time period intercepts.

The effect of introducing recycled water on total water usage is estimated using (4.4), where γ is the fixed effect for the excluded site in the base year, α_i is the difference between the fixed effect for site i and the excluded site, β_t is the difference between the fixed effect for period t and the base year, D_{it} remains the indicator for a treated site in the post treatment period, and π is the estimate of the DID treatment effect,

$$Y_{it} = \gamma + \alpha_i + \beta_t + \pi D_{it} + \varepsilon_{it} \quad (4.4)$$

I note that when there are only two sites and two time periods, equation (4.4) collapses into the form of equation (4.1).

Following the example in section 4.3.2.1, total water usage is changed by $\pi \cdot n_{treat}$ due to the introduction of recycled water to the treated sites. A reasonable proxy for the displacement ratio is then

$$d = 1 - \frac{\pi \cdot n_{treat}}{R} \tag{4.5}$$

and total potable water savings are

$$\Delta P = R * d = R * \left[1 - \frac{\pi \cdot n_{treat}}{R}\right] = R - \pi \cdot n_{treat} \tag{4.6}$$

4.3.2.3 Inference

Thus far, I have shown how one obtains an unbiased point estimate for the effect of recycled water on total and potable water usage given the study design and data structure. However, in order to perform proper statistical inference, the calculation of standard errors is a critical undertaking. Classical standard errors assume that there is no correlation between the error terms (the unobserved factors), ε_{it}, in the fixed-effects models. In my data it is likely that there is correlation, specifically among the multiple observations for a park. To see why, the park fixed effect accounts for all components that are site specific and do not vary over time, such as the soil condition and the size of the park. But there are other components that are also specific to the park but that do vary over time, such as the intensity of usage of athletic fields. These factors cause the unobserved components, captured in the error terms, to be correlated over time at the park level. As the specific form of these correlations is unknown, we account for this by allowing for general correlation patterns across the errors for each park. Formally, the error terms are clustered by park and I report cluster-robust standard errors.

The appropriate method of inference with cluster-robust standard errors depends on the number of clusters, not the number of observations, and in particular on the effective number of clusters. The effective number of clusters, defined by Carter, Schnepel, and Steigerwald (2016), accounts for variation across clusters in the observed and unobserved components (for example, if the general correlations in the unobserved components vary across clusters, as they likely do) and adjusts the number of clusters downward to account for this variation. I report this value in Table 4.4 using the code developed by Lee and Steigerwald (2018). Because there are 19 sites in the sample, I have 19 clusters in the data used in estimates (1), (2) and (5) of Tables 4.4 and 4.5. Estimates (3) and (4) are restricted to one particular region. Estimate (3) has 10 clusters, and estimate (4) has 9 clusters. In estimate (1) the reported effective number of clusters is 16.9, nearly equal to 19, indicating little variation in the clusters. However, for the model reported in column (2), there is more variation across the clusters, reflected in an effective number of clusters that falls from 16.9 to 13.

Because the effective number of clusters in our data is small, I follow the recommendation of Lee and Steigerwald (2018), and use the wild cluster bootstrap to compute the critical values for the *t*-statistic. I adopt the procedure outlined by Cameron and Miller (2015) to obtain the bootstrap critical values. In detail, the vector of estimated residuals for each cluster, $\{\widehat{\varepsilon_{it}}\}_i$ is multiplied by either 1 or -1 with equal probability. A bootstrap sample is created by combining the residual vectors with the regressors and estimating the coefficient of interest using OLS. From each OLS estimate, a Wald statistic is calculated. The procedure is repeated 1,000 times and the distribution of Wald statistics determines the upper and lower wild cluster bootstrap critical values.

4.4 Results

4.4.1 Pre and post-treatment total water usage

First, I present total water usage levels during the pre- and post-treatment periods at the treated sites, in Table 4.3. Water usage levels vary widely across the treated sites, as public parks tend to have wide variance in irrigated areas and utilization. Seven sites decrease water usage after treatment, and three increase water usage. However, I note that two of the sites that increase their water usage do so by more than 100% (treated sites 1 and 3 in region 2). The water data provider confirmed that these are valid measurements, but provided no reason as to the sudden increase in water usage. From Table 4.3, it is not possible to provide a robust analysis of the average effect of recycled water conversions on potable water usage in EBMUD. This is because the timing of treatment is staggered across the sites, which means that the counterfactual post-treatment water usage levels established by the control group are different for each site. The staggering in treatment timing, combined with the variance in site-level behavior, calls for regression analysis in which I estimate the average treatment effect of recycled water usage on total and potable water usage.

Region	Treated Site	Pre-treatment mean monthly water usage (CCUFT)	Post-treatment mean monthly water usage (CCUFT)	% Change
R1	T1	328.8	381.6	+16.1%
R1	T2	532.9	474.1	-11.0%
R1	T3	544.5	478.2	-12.2%

R1	T4	300.0	190.6	-36.4%
R1	T5	1558.7	1433.5	-8.0%
R2	T1	157.2	461.8	+194%
R2	T2	159.1	130.8	-17.9%
R2	T3	110.0	211.9	+92.6%
R2	T4	519.3	447.6	-13.8%
R2	T5	86.2	65.1	-24.5%

Table 4.3: Pre and post-treatment mean monthly water usage in treated sites in CCUFT

4.4.2 **Fixed-effects regression**

Using the data described in Section 4.3.1 and the regression specification given by (4.4), I estimate the effect of water recycling conversions on total water usage across ten public recreational properties. In column (1) of Table 4.4, I estimate $\hat{\pi}$ using the entire set of 2,836 observations. The estimated coefficient is small in magnitude relative to average monthly water usage in the sites, and due to the lack of precision I am unable to conclude that the introduction of recycling has an effect on total water usage. I test for cluster heterogeneity using the program developed by Lee and Steigerwald (2018). The effective number of clusters is 16.9, which is considered small enough to advise the use of wild bootstrap critical values for inference, as described in Section 4.3.2.3. The use of wild cluster bootstrap critical values results in a 95% confidence interval of [-61.94, 117.6] for the effect of

recycled water conversions on total monthly water usage across the sites, where all values are in units of hundred cubic feet (CCUFT).

To further examine the overall estimate, which implies no effect of recycling on total water use, I apply several sample restrictions. Perhaps there is an initial reduction in water use, which diminishes over time. In Column (2) I include only the first year of water usage after connecting to recycled water. I again observe a small coefficient with a wide confidence interval regarding the effect of recycled water on total water usage. It may be that water usage is most sensitive to recycling when water demands are highest, namely June through September. I restrict attention to these four months in Column (5) and, again, am unable to conclude that access to recycled water changes total water usage. Columns (3) and (4) restrict the sample to one of the two regions within EBMUD. I impose this restriction to explore if there is a fundamentally different response to recycled water conversions by region. Although the point estimates are quite different, the lack of precision again leaves me unable to conclude that access to recycled water changes total water usage. In Table B.1 of Appendix B, I present the treatment effect as a percentage of pre-treatment water usage by estimating a model where the dependent variable is the log of total water usage, instead of the level. This provides an interpretation of the treatment effect which reflects the fact that treated sites, present and future, vary widely in scale.

	(1)	(2)	(3)	(4)	(5)
$\hat{\pi}$	25.96	-14.10	-12.84	77.99	-16.68
(S.E)	(44.75)	(79.52)	(70.18)	(80.44)	(118.4)
N	2,836	2,275	1,485	1,351	947

Actual Clusters	19	19	10	9	19
Effective Clusters	16.9	13.0	8.17	8.94	16.9
Bootstrap critical values	[-1.96, 2.05]	[-2.01, 2.07]	[-2.47, 1.94]	[-1.83, 2.56]	[-2.09, 2.19]
Bootstrap 95% CI	[-61.94,117.6]	[-173.8,150.5]	[-186.1,123.2]	[-69.03,283.9]	[-264.2,242.7]
Restrictions	None	1-year post	Region 1	Region 2	Peak only

Table 4.4: Two-way fixed effects results with total water usage as the dependent variable, using cluster-robust standard errors and wild bootstrap critical values. Actual clusters, effective clusters, number of observations, critical values, 95% confidence intervals, and sample restrictions are also shown.

4.4.3 **Displacement and total potable water savings**

In Section 4.3.2.2 I introduced the calculation of displacement in treated sites as equation (4.5). Table 4.5 presents displacement findings for each of the sample restrictions. The 95% confidence interval for displacement is calculated using an analogous procedure, where I substitute the upper and lower boundaries shown in Table 4 for $\hat{\pi}$ in equation (4.5) to generate the upper and lower boundaries for displacement. For example, in the full sample (column 1), the point estimate of displacement is calculated as: $\hat{d} = 1 - \frac{\hat{\pi} * n_{treat}}{R} = 1 - \frac{25.96 * 681}{267056} = 93.4\%$. The bootstrap 95% CI immediately follows by substituting the upper and lower boundaries of the 95% CI from Table 4 for $\hat{\pi}$.

	(1)	(2)	(3)	(4)	(5)
$\hat{\pi}$	25.96	-14.10	-12.84	77.99	-16.68
Total recycled water usage (CCUFT)	267,056	48,672	179,119	87,937	166,407
Treated observations	681	120	326	355	232
Displacement	93.4%	103%	102%	68.5%	102%
Bootstrap 95% CI	[70.0%,116%]	[62.9%,143%]	[77.6%,134%]	[-14.6%,128%]	[66.2%,137%]
Restrictions	None	1-year post	Region 1	Region 2	Peak only

Table 4.5: Estimated mean monthly change in total water usage ($\hat{\pi}$), total recycled water usage, total observations of treated sites in post-treatment periods, displacement, and bootstrap 95% confidence intervals for displacement across all sample restrictions.

Displacement, and in turn potable water savings, is present across all sample restrictions. Columns (1), (2), and (5) of Table 4.5 show that the point estimate of monthly displacement hovers around 100% regardless of whether or not I restrict the post-treatment observations to just the first post-treatment year or only the summer months. Columns (3) and (4) suggest that displacement may be higher in region 1 in comparison with region 2.

Using the elements of Table 4.5, namely displacement and total recycled water usage, I estimate the total amount of potable water saved during the study period using equation (4.6) and compare this with California household usage. In 2016, average residential water usage in California was 11.4 cubic feet (85 gallons) per person per day (Legislative Analyst's Office, 2017). This quantity varies by season, and in the peak months of June through

September residential usage was 14.6 cubic feet (109 gallons) per person per day. In the sites in my sample that converted to recycled water, I estimate that a total of 25 million cubic feet of potable water ($267{,}056\ CCUFT * 0.934$) were saved during the study period, or approximately 1,224 cubic feet per site, per day. Thus, my estimate of daily potable water savings at each treated site is enough to cover the daily usage of 107 California residents.

4.5 Discussion

4.5.1 Limitations and future work

I produce the first quasi-experimental estimate of the potable water savings that arise from recycled water conversions, and the first quasi-experimental displacement metric in the industrial ecology literature. In the East Bay Municipal Utility District, conversions from potable to recycled water achieve high levels of potable water savings and displacement. Because these data are collected from only one water district in a relatively small geographical area, future research can examine the relevance of the conclusions on a larger sample of water districts from diverse geographic areas, for example in other parts of California or across Australia, where infrastructure conversions to recycling have become common in recent decades. Such an undertaking would also require collection of observable characteristics that predict water usage such as rainfall, temperature, and local income levels. A more sophisticated approach, such as propensity score matching, may need to be applied in a more geographically diverse sample if the treatment is not assigned randomly conditional on these observables.

4.5.2 **Conclusions**

I am unable to conclude that total water usage increased in treated sites, a finding that is somewhat surprising to both the author of this research and the community affairs representative from EBMUD who supplied these data. The unit cost of recycled wastewater is less than that of potable water, and recycled wastewater is sometimes perceived as an abundant resource relative to potable water, which can lessen the sensitivity of users to drought conditions. However, in EBMUD the recycled water program is part of a greater water conservation unit. Thus, it is possible that the treated units are exposed to additional information about conservation best practices, a possible mechanism that could contribute to this outcome. Nevertheless, it is clear that in EBMUD, conversions to recycled water lead to significant potable water savings resulting in high displacement, and may not stimulate an increase in overall water consumption (i.e. circular economy rebound). The presented research provides statistical evidence to support this for the first time in the literature, and the finding should be encouraging to water districts and management entities that are considering the expansion of non-potable, discretized recycled wastewater infrastructure in an effort to save potable water.

Conversions to recycled wastewater as a water source for irrigation are expected to increase in the face of climate change. This research provides a general methodology that can be readily applied in water districts to rigorously monitor the effectiveness of their recycled water conversion programs. In general, I recommend that quasi-experimental methodologies be adopted when possible to ensure that policies that intend to produce conservation outcomes are meeting these objectives.

4.6 References

Angelakis, A.N., Koutsoyiannis, D., Tchobanoglous, G., 2005. Urban wastewater and stormwater technologies in ancient Greece. Water Res. 39, 210–220. doi:10.1016/j.watres.2004.08.033

Apostolidis, N., Hertle, C., Young, R., 2011. Water recycling in Australia. Water 3, 869–881. doi:10.3390/w3030869

Arbués, F., Garc, Á., Mart, R., 2003. Estimation of residential water demand : a state-of-the-art review. J. Socio. Econ. 32, 81–102. doi:10.1016/S1053-5357(03)00005-2

Australian Academy of Technological Sciences and Engineering, 2004. Water Recycling in Australia.

Baldassare, M., Katz, C., 1992. The Personal Threat of Environmental Problems as Predictor of Environmental Practices. Environ. Behav. 24, 602–616.

California State Legislature, 1991. Water Recycling Act of 1991. Sacramento, California.

Cameron, R.C., Miller, D.L., 2015. A Practitioner's Guide to Cluster-Robust Inference. J. Hum. Resour. 50, 317–372. doi:10.3368/jhr.50.2.317

Carter, A. V, Schnepel, K.T., Steigerwald, D.G., 2016. Asymptotic Behavior of a t Test Robust to Cluster Heterogeneity. Rev. Econ. Stat. 1–27. doi:10.1162/rest_a_00639

Catlin, J.R., Wang, Y., 2013. Recycling Gone Bad: When the Option to Recycling Increases Resource Consumption. J. Consum. Psychol. 23, 122–127. doi:10.5465/amr.2011.0193

Dai, A., 2013. Increasing drought under global warming in observations and models. Nat. Clim. Chang. 3, 52–58. doi:10.1038/nclimate1633

DeOliver, M., 1999. Attitudes and Inaction: A Case Study of the Manifest Demographics of Urban Water Conservation. Environ. Behav. 31, 372–394.

Ekvall, T., 2000. A market-based approach to allocation at open-loop recycling. Resour. Conserv. Recycl. 29, 91–109.

Frischknecht, R., 2010. LCI modelling approaches applied on recycling of materials in view of environmental sustainability , risk perception and eco-efficiency. Int. J. Life Cycle Assess. 15, 666–671. doi:10.1007/s11367-010-0201-6

Geyer, R., Kuczenski, B., Zink, T., Henderson, A., 2015. Common Misconceptions about Recycling. J. Ind. Ecol. 0, 1–8. doi:10.1111/jiec.12355

Gilbertson, M., Hurlimann, A., Dolnicar, S., 2011. Does water context influence behaviour and attitudes to water conservation ? Australas. J. Environ. Manag. 18. doi:10.1080/14486563.2011.566160

Goleta Water District, 2018. Recycled Water Program [WWW Document]. URL http://www.goletawater.com/conservation/recycled-water-program

Guneralp, B., Guneralp, I., Liu, Y., 2015. Changing global patterns of urban exposure to flood and drought hazards. Glob. Environ. Chang. 31, 217–225. doi:10.1016/j.gloenvcha.2015.01.002

Horticulture Australia Limited, 2011. Recycled water treatment plant for Melbourne. ReWater 2–4.

Jimenez, B., Asano, T., 2008. Water Reclamation and Reuse around the World, in: Water Reuse: An International Survey of Current Practice, Issues, and Needs. IWA Publishing, pp. 3–27.

Koffler, C., Finkbeiner, M., 2018. Are we still keeping it “real”? Proposing a revised paradigm for recycling credits in attributional life cycle assessment. Int. J. Life Cycle Assess. 23, 181–190.

Kwon, H.-H., Lall, U., 2016. A coupla-based nonstationary frequency analysis for the 2012-2015 drought in California. Water Resour. Res. 52, 5662–5675. doi:10.1002/2016WR018959

Lee, C.H., Steigerwald, D.G., 2018. Inference for Clustered Data. Stata J. 18, 447–460.

Legislative Analyst's Office, 2017. Residential Water Use Trends and Implications for Conservation Policy [WWW Document]. URL https://lao.ca.gov/Publications/Report/3611 (accessed 10.12.18).

Martinez-Espineira, R., 2002. Residential Water Demand in the Northwest of Spain. Environ. Resour. Econ. 21, 161–187.

Newton, D., Balgobin, D., Badyal, D., Mills, R., Pezzetti, T., Ross, H.M., 2011. Results, challenges, and future approaches to California's municipal wastewater recycling survey, State Water Resources Control Board of California.

Palazzo, J., Geyer, R., Startz, R., Steigerwald, D.G., 2019. Causal Inference for Quantifying Displaced Primary Production from Recycling. J. Clean. Prod. 210, 1076–1084. doi:10.1016/j.jclepro.2018.11.006

Palazzo, J., Liu, O.R., Stillinger, T., Song, R., Wang, Y., Hiroyasu, E.H.T., Zenteno, J., Anderson, S., Tague, C., 2017. Urban responses to restrictive conservation policy during drought. Water Resour. Res. 53, 1–17. doi:10.1002/2016WR020136

Radcliffe, J.C., 2015. Water recycling in Australia – during and after the drought. Environ. Sci. Water Res. Technol. 1, 554–562. doi:10.1039/C5EW00048C

Sun, M., Trudel, R., 2017. The Effect of Recycling Versus Trashing on Consumption: Theory and Experimental Evidence. J. Mark. Res. 54, 293–305. doi:10.1509/jmr.15.0574

Toor, G.S., Lusk, M., 2011. Reclaimed Water Use in the Landscape: Managing Salinity, Sodicity, and Specific Ions in Sites Irrigated with Reclaimed Water.

Trenberth, K.E., Dai, A., Schrier, G. Van Der, Jones, P.D., Barichivich, J., Briffa, K.R., Sheffield, J., 2014. Global warming and changes in drought. Nat. Clim. Chang. 4, 3–8. doi:10.1038/NCLIMATE2067

United States Census Bureau, 2011. Census Bureau Releases 2010 Census Demographic Profiles for Alaska, Arizona, California, Connecticut, Georgia, Idaho, Minnesota, Montana, New Hampshire, New York, Ohio, Puerto Rico and Wisconsin [WWW Document]. URL https://www.census.gov/newsroom/releases/archives/2010_census/cb11-cn137.html (accessed 10.12.18).

Yang, Y., 2016. Two sides of the same coin: consequential life cycle assessment based on the attributional framework. J. Clean. Prod. 127, 274–281. doi:10.1016/j.jclepro.2016.03.089

Zink, T., Geyer, R., 2018. Recycling and the myth of landfill diversion (forthcoming). J. Ind. Ecol.

Zink, T., Geyer, R., 2017. Circular Economy Rebound. J. Ind. Ecol. 21, 593–602. doi:10.1111/jiec.12545

Zink, T., Geyer, R., Startz, R., 2017. Toward Estimating Displaced Primary Production from Recycling: A Case Study of U.S. Aluminum. J. Ind. Ecol. 0, 1–13. doi:10.1111/jiec.12557

Zink, T., Geyer, R., Startz, R., 2015. A Market-Based Framework for Quantifying Displaced Production from Recycling or Reuse. J. Ind. Ecol. 0, 1–11. doi:10.1111/jiec.12317

A. Appendix A: Supporting Information for Chapter 2

A.1. Derivation of formulas from Chapter 2

Here, I provide detailed derivations of all formulas from Chapter 2. I only provide equation numbers when I arrive at a step that corresponds directly with Section 2.3.3 of Chapter 2. The equation numbers then line up exactly with those from Chapter 2. This streamlines the connection between main text and Appendix.

A.1.1 Material production impacts

Every year, the total aluminum additions $TAA(t) = \sum_l TAA_l(t)$ are used to replace $S(t)$ steel, where l denotes the types of aluminum (sheet, extrusions, or castings). The replacement ratio is $TAA(t)/S(t) = k$, which means that the primary mass savings are $S(t) - TAA(t) = S(t) - kS(t) = (1-k)S(t)$.

This, in turn, enables secondary mass savings of $s(1-k)S(t)$.

The total amount of removed steel is thus $S(t) + s(1-k)S(t)$. Expressed as a function of total aluminum additions, total removed steel is $\frac{TAA(t)}{k} + s(1-k)\frac{TAA(t)}{k}$.

If pf_l and sf_l denote the fractions of primary and secondary steel removals that are of steel type l, the total amount of steel type l removed due to total aluminum additions of $TAA(t)$ is calculated as $\frac{TAA(t)}{k}pf_l + s(1-k)\frac{TAA(t)}{k}sf_l = TAA(t)\frac{pf_l - s(1-k)sf_l}{k}$.

If γ_l^a and γ_l^s denote the manufacturing yields of aluminum and steel type l, the additional amount aluminum production and shipments is $\sum_l \frac{TAA_l(t)}{\gamma_l^a}$ and the annual reduction in steel production is $\sum_l \frac{1}{\gamma_l^s}\left[-\sum_m TAA_m\,(t)\left(\frac{pf_l + (1-k)\cdot s \cdot sf_l}{k}\right)\right]$, where m denotes the type of aluminum.

If $I_l^a(t)$ and $I_l^s(t)$ denote the amount of environmental impact per marginal unit of aluminum and steel production, the environmental impact of additional aluminum production is

$$\boldsymbol{I}^1(t) = \sum_l \frac{TAA_l(t)}{\gamma_l^a} I_l^a(t) > 0, \tag{2.1}$$

and the environmental impact reduction from reduction in steel production is

$$\boldsymbol{I}^2(t) = \sum_l \frac{1}{\gamma_l^s} \left[-\sum_m TAA_m(t) \left(\frac{pf_l + (1-k)\cdot s \cdot sf_l}{k} \right) \right] I_l^s(t) < 0. \tag{2.2}$$

For each material type l, $I_l^a(t)$ and $I_l^s(t)$ account for the amount of secondary content $sc_l^x(t)$ that is in the aluminum additions and in the steel removals:

$$I_l^x(t) = sc_l^x(t) \cdot I_{ingot}^{sx}(t) + \left(1 - sc_l^x(t)\right) \cdot I_{ingot}^{px}(t) + I_l^{fx},\ x = a, s \tag{2.3}$$

$I_{ingot}^{sx}(t)$, $I_{ingot}^{px}(t)$, and I_l^{fx} are the environmental impact per marginal unit of secondary ingot production, primary ingot production, and ingot forming (rolling, extruding, casting). The first two are cradle-to-gate processes; the third is a gate-to-gate process.

A.1.2 Use phase impacts

$AAA_i(T)$ denotes the average amount of aluminum added per vehicle type i produced in year T. The considered vehicle types are gasoline, diesel, standard hybrid, plug-in hybrid, and pure electric. $AAA_i(T)$ is different for each vehicle type, since each vehicle type has different vehicle class distributions, and vehicle composition data shows that the use of aluminum varies across vehicle classes. E.g. electric power trains are more prevalent in the smaller vehicle classes, while larger vehicle classes use more aluminum. All this information is used in spreadsheet "Fleet composition" to calculate the data array $AAA_i(T)$. Note that $TAA(T) = \sum_i AAA_i(T) \cdot N_i(T)$, with $N_i(T)$ being the number of vehicles of type i produced in year T.

Using $AAA_i(T)$, the total mass reduction (in kg) of vehicle type i is calculated as

$\left[\frac{AAA_i(T)}{k} - AAA_i(T)\right] + s\left[\frac{AAA_i(T)}{k} - AAA_i(T)\right] = \frac{(1+s)(1-k)}{k} AAA_i(T)$.

ΔF_i and ΔE_i denote the relative fuel and electricity savings (in MJ/kg saved and km driven) for vehicle type i. If VM denotes the lifetime vehicle driving distance and VL the vehicle life in years, then VM/VL is the average distance driven per year (in km/year).

If es_i denotes the share of driving energy coming from electricity, the absolute annual fuel and electricity savings (in MJ) for each vehicle type i are calculated as

$[es_i \cdot \Delta E_i + (1 - es_i)\Delta F_i] \frac{(1+s)(1-k)}{k} AAA_i(T) \frac{VM}{VL}$.

If $I^e(T)$ and $I^f(T)$ denote the average environmental impact per MJ of electricity and fuel inputs to vehicles produced in year T, the annual environmental impact reductions per vehicle type i due to the electricity and fuel savings are calculated as:

$$[es_i \cdot \Delta E_i \cdot I^e(T) + (1 - es_i)\Delta F_i \cdot I^f(T)] \frac{(1+s)(1-k)}{k} AAA_i(T) \frac{VM}{VL}.$$

The equation above needs to be multiplied with the total number of mass-reduced vehicles of type i that are in use during any given year t. This number is calculated as the product between $N_i(T)$, the number of vehicles of type i produced in year T, and $FIU(t-T)$, the fraction of vehicles still in use after time $(t-T)$. Vehicle lifetime distribution is modeled as a lognormal function. FIU is 1 minus the cumulative lognormal function. The total amount of impact reduction during year t for all mass-reduced vehicles in use during that year is calculated as $\boldsymbol{I}^3(t) =$

$\sum_{T,i}\left[[es_i \Delta E_i I^e(T) + (1 - es_i)\Delta F_i I^f(T)](1+s)\frac{k-1}{k} AAA_i(T) \frac{VM}{VL} N_i(T) FIU(t-T)\right]$.

This simplifies to

$$\boldsymbol{I}^3(t) = \sum_{T,i}\left[IR_i^u \cdot (1+s)\frac{k-1}{k} AAA_i(T)\frac{VM}{VL} N_i(T) FIU(t-T)\right] < 0 \quad (2.4)$$

when I denote the environmental impact reduction per kg mass savings and km driven as:

$$IR_i^u = es_i \cdot \Delta E_i \cdot I^e(T) + (1-es_i)\Delta F_i \cdot I^f(T) \quad (2.5)$$

A.1.3 Material recycling impacts during production of vehicles

Replacing steel with aluminum causes changes in the scrap flows during vehicle production: 1) A reduction in steel scrap input, $SIn_l^s(t) < 0$, due to reduced steel production, and a likely increase in aluminum scrap input, $SIn_l^a(t) > 0$, due to increased aluminum production. 2) A reduction in prompt steel scrap generation, $ProS_l^s(t) < 0$, due to less steel use, and an increase in aluminum prompt scrap generation, $ProS_l^a(t) > 0$, due to more aluminum use. The external scrap market can respond to the net change in scrap flow to or from vehicle production through changes in external scrap consumption and changes in external scrap supply/collection. External scrap market response depends on many factors and is not well understood. It is thus modeled parametrically through scrap market response parameter $\propto$. $\propto = 1$ models a completely unresponsive (inelastic) external scrap supply. $\propto = 0$ models a completely unresponsive (inelastic) external scrap demand.

One assumption in solving the scrap market model shown in Figure A.1 is that the scrap market clears every year. In the case of steel, the annual scrap flow balance is complicated by the fact that primary production is a scrap consumer. A change in external primary steel production due to a change in external secondary steel production (shown by the green arrows in Figure A.1) causes a change in external scrap consumption (shown as the blue arrow from external primary production).

In the case of steel, the annual scrap flow balance is

$$ProS + (\alpha - 1)(ProS - SIn) + s_p \beta Y(ProS - SIn) = SIn + s_r Y(ProS - SIn), \quad (2.6)$$

with s_p and s_r being the scrap inputs into recycled and primary production (in kg/kg), and parameter $\beta \in [0; 1]$ quantifying the effect that a change in external secondary production has on external primary production. It follows that the unknown Y is

$Y = \frac{\alpha}{s_r - s_p \beta}$.

In the case of aluminum, the annual scrap flow balance is simply

$ProS + (\alpha - 1)(ProS - SIn) = SIn + \alpha(ProS - SIn)$,

Which follows from the equations above by setting $s_p = 0$.

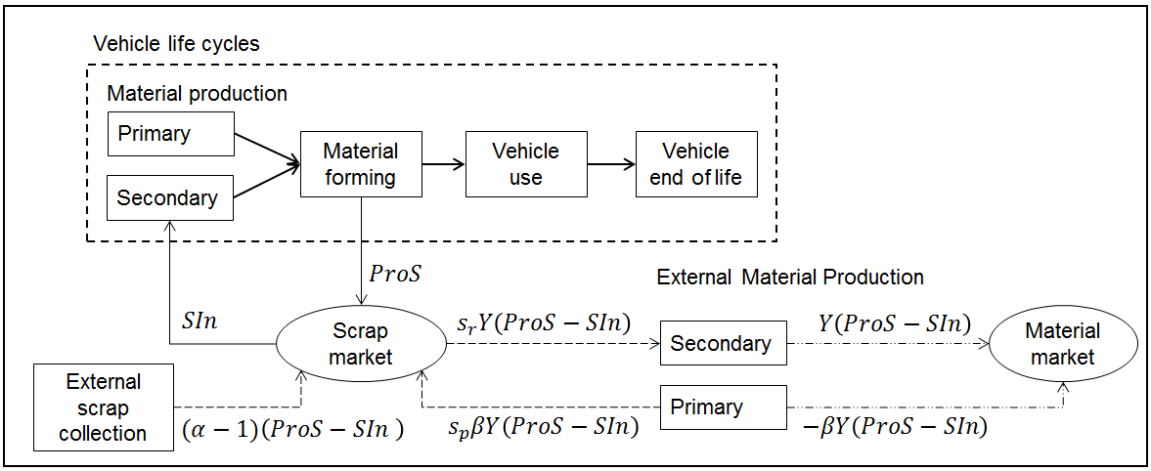

Figure A.1: External scrap flow balance during vehicle production

As can be seen in Figure A.1, external secondary production changes by $Y(ProS - SIn)$ and, in response, external primary production changes by $-\beta Y(ProS - SIn)$.

For aluminum, the resulting changes in environmental impact are

$(ProS^a - SIn^a)\ \frac{\alpha^a}{s_r^a} \cdot I_{ingot}^{sa}(t)$ and $-(ProS^a - SIn^a)\ \beta^a \cdot \frac{\alpha^a}{s_r^a} \cdot I_{ingot}^{pa}(t)$,

with $I_{ingot}^{sa}(t)$ and $I_{ingot}^{pa}(t)$ being the environmental impact of secondary and primary aluminum production (per kg of ingot).

For steel, the resulting changes in environmental impact are

$(ProS^s - SIn^s)\ \frac{\alpha^s}{s_r^s - \beta^s \cdot s_p^s} \cdot I_{ingot}^{ss}(t)$ and $-(ProS^s - SIn^s)\ \beta^s \cdot \frac{\alpha^s}{s_r^s - \beta^s \cdot s_p^s} \cdot I_{ingot}^{ps}(t)$,

with $I_{ingot}^{ss}(t)$ and $I_{ingot}^{ps}(t)$ being the environmental impact of secondary and primary steel production (per kg of ingot).

The resulting general equation for material recycling impacts during vehicle production is

$$\boldsymbol{I}^{4,5}(t) = \alpha^x \cdot \frac{(\sum_l ProS_l^x(t) - SIn_l^x(t))}{s_r^x - \beta^x \cdot s_p^x} \left(I_{ingot}^{sx}(t) - \beta^x \cdot I_{ingot}^{px}(t) \right), x = a, s \quad (2.7)$$

A.1.4 Material recycling impacts during end-of-life

Replacing steel with aluminum causes changes in the scrap flows during vehicle end of life: A reduction in end-of-life (eol) steel scrap generation, $ProS_l^s(t) < 0$, due to less steel use, and an increase in aluminum eol scrap generation, $ProS_l^a(t) > 0$, due to more aluminum use. The response of the external scrap market is modeled in the same way as during vehicle production. Resulting scrap market model and scrap flow balance are shown in Figure A.2.

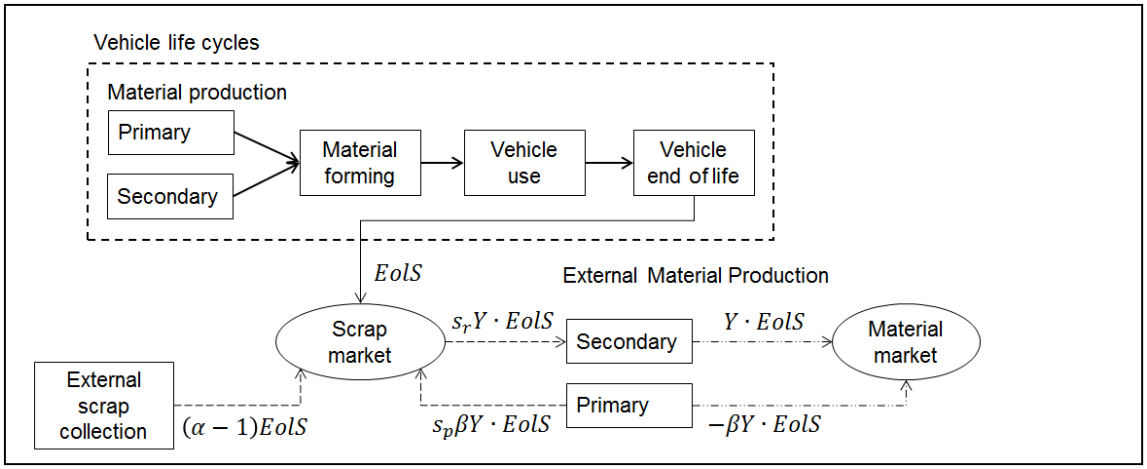

Figure A.2: External scrap flow balance during vehicle end of life

As can be seen in Figure A.2, external secondary production changes by $Y \cdot EolS$ and, in response, external primary production changes by $-\beta Y \cdot EolS$.

Analogous to (2.6), the scrap flow balance at end-of-life is:

$$EolS + (\alpha - 1)EolS + s_p\beta YEolS = s_r YEolS$$

$$\Rightarrow Y = \frac{\alpha}{s_r - s_p\beta} \quad (2.8)$$

For aluminum, the resulting changes in environmental impact are

$EolS^a \ \frac{\alpha^a}{s_r^a} \cdot I_{ingot}^{sa}(t)$ and $-EolS^a \ \beta^a \cdot \frac{\alpha^a}{s_r^a} \cdot I_{ingot}^{pa}(t)$.

For steel, the resulting changes in environmental impact are

$EolS^s \ \frac{\alpha^s}{s_r^s - \beta^s \cdot s_p^s} \cdot I_{ingot}^{ss}(t)$ and $-EolS^s \ \beta^s \cdot \frac{\alpha^s}{s_r^s - \beta^s \cdot s_p^s} \cdot I_{ingot}^{ps}(t)$.

The resulting general equation for material recycling impacts during vehicle production is

$$\boldsymbol{I}^{6,7}(t) = \alpha^x \cdot \frac{EolS^x(t)}{s_r^x - \beta^x \cdot s_p^x}\left(I_{ingot}^{sx} - \beta^x \cdot I_{ingot}^{px}(t)\right), x = a, s \quad (2.9)$$

A.2. Documentation of Spreadsheet Formulas

Here, I document the formulas used to compile the spreadsheet model, which is also provided as Supporting Information for this chapter. It is important to note that I restart the numbering, and begin with Equation A.1. This is to separate these equations from those that map directly onto the main text, from Section A.1. The spreadsheet model can be found on the website that hosts the published version of this chapter: https://www.sciencedirect.com/science/article/pii/S0195925518301343#s0130

A.2.1 Fleet composition

For each year of the modelling period (2012-2050), the CLCA spreadsheet used to computer the results in Chapter 2 calculates the power train composition of the light duty vehicles assumed to be produced in North America during that year. It also calculates, for each production year *T* and power train type *i*, the average amount of body and closure parts made from aluminum, $AC_i(T)$.

The resulting output table contains 5 power train types *i*, which are Gasoline ICV, Diesel ICV, Standard HEV, Plug-in HEV, and BEV. For each power train type *i* and production year *T* is lists

- $AC_i(T)$: Average amount of body and closure parts made from aluminum (in kg per vehicle).
- $TAA_i(T)$: Total amount of aluminum added to body and closure parts (in kg). This is the average amount multiplied by the total number of vehicles of that power train type produced during that year, $TAA_i(T) = AC_i(T) \cdot N_i(T)$.
- $PT_i(T)$: Share of the power train type *i* as % of the total number of vehicles produced during production year *T*. This is the number of vehicles of that power train type divided by the total number of vehicle produced during year *T*.

A significant amount of input data are required to calculate the outputs described above. Below is a comprehensive list:

- Total amount of aluminum body and closure parts added to light duty vehicles produced each year (in kg), $TAA(T)$. This data is also broken down into sheet, extrusions, and castings for other modelling purposes, $TAA_l(T)$ with $\sum_l TAA_l(T) = TAA(T)$.
- Total number of light duty vehicles assumed to be produced each year, $N(T)$ in #.
- For each year, the share of annually produced vehicles that are ICVs, $PT_{ICV}(T)$.
- For each year, the share of annually produced ICVs that are Gasoline ICVs.
- For each year, the share of annually produced vehicles that are HEVs, $PT_{HEV}(T)$.
- For each year, the share of annually produced HEVs that are Standard HEVs.

- The share of each vehicle class as % of the total number of vehicles produced in 2015, VC_{all}^{j} with j being the vehicle class.
- For each vehicle class j, the average amount of aluminum in vehicles produced in 2015 (in lbs).
- The vehicle class composition of HEVs produced in 2014, VC_{HEV}^{j}. Assumed to be constant over the modelling period and the same for Standard and Plug-in HEVs.
- The vehicle class composition of BEVs produced in 2014, VC_{BEV}^{j}. Assumed to be constant over the modelling period.

8 different vehicle classes are considered. They are A/B, C, D, E, MPV, SUV, VAN, PUP.

Calculating the average amount of body and closure aluminum per vehicle for each power train type is complicated by the fact that each power train type has a different composition of vehicle classes and vehicle classes differ in the amount of aluminum they contain.

The first step is to calculate $AC^{all}(T)$, the body and closure aluminum added to each average vehicle in production year *T*. This is done by dividing the total amount of body and closure aluminum added in year *T* by the total number of vehicles produced in year *T*. The results are in cells T55:T93. The next step is to express the amount of aluminum per 2015 vehicle for each vehicle class (in lbs/vehicle) relative to the amount of aluminum per 2015 vehicle across all vehicle classes (in lbs/vehicle), which was 398 pounds. The results are in cells L53:S53 and denote the amount of aluminum per vehicle class as percent of average amount of aluminum across all vehicles. Multiplying the added body and closure aluminum per vehicle and production year, $AC^{all}(T)$, with those ratios yields the added body and closure aluminum per vehicle and production year for each vehicle class, $AC^{j}(T)$. This data

is stored in cells L55:S93. One more intermediate step needed to calculate the added body and closure aluminum per vehicle for each power train type and production year is to calculate the vehicle class composition for ICVs:

$$PT_{ICV}(T) \cdot VC_{ICV}^{j} + PT_{HEV}(T) \cdot VC_{HEV}^{j} + PT_{BEV}(T) \cdot VC_{BEV}^{j} = VC_{all}^{j} \quad \text{(A.1)}$$

$$\Rightarrow VC_{ICV}^{j}(T) = \frac{VC_{all}^{j} - PT_{HEV}(T) \cdot VC_{HEV}^{j} - PT_{BEV}(T) \cdot VC_{BEV}^{j}}{PT_{ICV}(T)} \quad \text{(A.2)}$$

with *j* being the vehicle class.

Since $PT_i(T)$ varies with each production year this calculation is repeated for each vehicle class *j* and each production year *T*. The results are stored in cells L110:S148. Finally, the added body and closure aluminum per vehicle for each power train and production year, $AC_i(T)$, can be calculated:

$$AC_i(T) = \sum_j AC^j(T) \cdot VC_i^j(T) \quad \text{(A.3)}$$

Note that the calculated values are the same for Gasoline and Diesel ICVs, i.e. $AC_{ICV-G}(T) = AC_{ICV-D}(T) = AC_{ICV}(T)$, and for Standard and Plug-in Hybrids, i.e. $AC_{HEV-S}(T) = AC_{HEV-P}(T) = AC_{HEV}(T)$, since the vehicle class shares VC_i^j are assumed to be identical for the two ICV types and the two HEV types. The total amount of added body and closure aluminum as a function of power train and production year, $TAA_i(T)$ is calculated as follows:

$$TAA_i(T) = AC_i(T) \cdot N_i(T) = AC_i(T) \cdot PT_i(T) \cdot N(T) \quad \text{(A.4)}$$

Variable	Description	Location of data
$AC_i(T)$	Average amount of body and closure parts made from aluminum for powertrain type i and production year T (in kg/car)	B5:B43, E5:E43, H5:H43, K5:K43, N5:N43
$TAA_i(T)$	Total amount of body and closure parts made from	C5:C43, F5:F43, I5:I43,

	aluminum for powertrain type i and production year T (in kg)	L5:L43, O5:O43
$PT_i(T)$	Share of the power train type as % of the total number of vehicle produced during production year *T*	D5:D43, G5:G43, J5:J43, M5:M43, P5:P43

Table A.1: Output data from the spreadsheet 'Fleet composition'

A.2.2 Vehicle Use

For each calendar year *t* of the modelling period (2012-2050), this spreadsheet calculates the total amount of GHG savings (in million kgCO2eq) that result from driving the mass-reduced vehicle fleet modeled on the spreadsheet 'Fleet composition'. These total GHG savings per calendar year are reported in cells AO232:AO269. The total GHG savings in each calendar year *t* are a function of the age composition of the fleet during year *t*, i.e. how many vehicles of each production year *T* were in use. Each production year is characterized by the total number of vehicle produced, $N(T)$, and the total amount of aluminum closures and body parts, $TAA(T)$, added to those vehicles. For each calendar year *t*, the total use phase GHG reductions are thus calculated as the sum of use phase GHG reductions from the vehicles of each production year *T*. The table of use phase GHG savings for each year of driving *t* and each year of vehicle production *T* is given in cells B232:AN269.

Use phase savings are calculated separately for each power train type, but the calculation process is identical. The starting point is the added amount of aluminum body and closure parts per vehicle, $AC_i(T)$, which is given in kg per vehicle. The first step is to calculate the resulting mass reductions per vehicle, $\Delta M_i(T)$, which are given in kg per vehicle and are calculated as

$$\Delta M_i(T) = AC_i(T) \cdot (1+s)\frac{(k-1)}{k} \quad \text{(A.5)}$$

With k being the material replacement coefficient of aluminum relative to steel (in kg aluminum/kg steel) and s being the secondary mass savings (in kg secondary mass savings/kg primary mass savings). The next step is to calculate the life time fuel and electricity savings per car, FS_i (in liters per car) and ES_i (in MJ per car), according to the following equations:

$$FS_i(T) = (1 - EL) \cdot \Delta M_i(T) \cdot \Delta F_i(T) \cdot VM \cdot 0.0001$$

$$ES_i(T) = EL \cdot \Delta M_i(t) \cdot \Delta E_i(T) \cdot VM \cdot 0.0001 \quad \text{(A.6)}$$

with *EL* being the share of life time driving powered by plug electricity (in %), $\Delta F_i(T)$ the fuel savings per mass savings (in liters per 100km driven and 100kg mass reduction), $\Delta E_i(T)$ the electricity savings per mass savings (in MJ per 100km driven and 100kg mass reduction), and *VM* the assumed vehicle life (in km). Life time fuel and electricity savings per vehicle are converted into lifetime GHG emissions savings per vehicle, $GHGS_i(T)$, according to this equation:

$$GHGS_i(T) = FS_i(T) \cdot GHG_f + ES_i(T) \cdot GHG_e \quad \text{(A.7)}$$

with GHG_f and GHG_e being the GHG intensities of the fuel and the electricity, in kg CO_2eq per liter and kg CO_2eq per MJ respectively. The final step in calculating the life time use phase GHG savings per power train type and production year is to multiply the life time use phase savings per car with the total number of vehicles of the given power train *i* being produced in each given production year *T*, i.e. $GHGS_i(T) \cdot N_i(T)$.

The calculations above require various additional input parameters, such as the material replacement coefficient *k*, the secondary mass savings coefficient *s*, the plug electricity share *EL*, the life time vehicle driving *VM*, the GHG intensities of fuel and electricity GHG_f and GHG_e, and finally the fuel and electricity savings per mass savings $\Delta F_i(T)$ and $\Delta E_i(T)$. The

last two parameters can be modeled as time dependent but are currently assumed to be constant over time, i.e. $\Delta F_i(T) = \Delta F_i$ and $\Delta E_i(T) = \Delta E_i$. For each power train type the energy savings per mass savings are calculated from a set of input parameters. Energy savings per mass savings are significantly higher in the case that the power train of the vehicle is resized, i.e. optimized to the new, reduced vehicle mass. However, this is not always feasible or cost-effective. Also, fuel consumption models show that energy savings per mass savings vary across power train types and vehicle classes. For this reason, they are calculated as follows for each power train type *i*:

$$\Delta F_i = RE \cdot Avg\left(\Delta F_{i,re}^{j}\right) + (1 - RE) \cdot Avg\left(\Delta F_{i,no-re}^{j}\right)$$

$$\Delta E_i = RE \cdot Avg\left(\Delta E_{i,re}^{j}\right) + (1 - RE) \cdot Avg\left(\Delta E_{i,no-re}^{j}\right) \quad \text{(A.8)}$$

where *RE* is the fraction of power train resizing benefit that mass-reduced vehicles can realize on average, superscript *j* denotes the vehicle class, and subscripts *re* and *no-re* stand for resizing and no-resizing, respectively. The average is calculated over the input values for the different vehicle classes (the yellow cells on the spreadsheet in columns J to V). Different numbers of vehicle classes may be used to characterize different power trains.

$GHGS(T)$ are the lifetime GHG use phase savings from all vehicles produced in year *T* and calculated as follows:

$$GHGS(T) = \sum_i GHGS_i(T) \cdot N_i(T) \quad \text{(A.9)}$$

These values need to be converted into the GHG use phase savings that occur during each calendar year of the modeling period. The first step is to convert the lifetime savings into annual savings according to the following equation:

$$AS(T,t) = \begin{cases} FIU(t) \cdot \frac{GHGS(T)}{VL} & for\ T < t \\ 0 & for\ T \geq t \end{cases} \quad \text{(A.10)}$$

where *VL* is the mean lifetime of each vehicle (assumed to be constant across time and all vehicles), and *FIU(t)* is the fraction of vehicles still in use after *t* years of driving. *FIU(t)* is defined as $FIU(t) = 1 - lognormal(VL, SD)$, with *VL* as the mean and an additional parameter *SD*, the standard deviation. The total GHG use phase savings in each calendar year is now calculated as the sum of all annual savings across all production years:

$$GHGS(t) = \sum_T AS(T, t) \quad \text{(A.11)}$$

In the model, vehicles are being produced every year of the modeling period (2012-2050). This means that not all vehicles will reach the end of their lives and as a result the use phase savings accruing during the modeling period are smaller than the sum of the lifetime savings of all cars produced during the modeling period, i.e. the following inequality holds:

$$\sum_t GHGS(t) < \sum_T GHGS(T) \quad \text{(A.12)}$$

Variable	Description	Location of data
$GHGS(t)$	Total GHG use phase savings per calendar year t (in million kg CO2eq)	AO232:AO269

Table A.2: Output data from spreadsheet 'Vehicle use"

A.2.3 Material production

The aim of this spreadsheet is to calculate all changes in GHG emissions from material production, both for the added aluminum and the removed steel. The spreadsheet calculates and tallies all direct emission changes, i.e. it reflects to what extent the added aluminum and removed steel come from primary or secondary production. In other words, the results on this spreadsheet reflect the recycled content of the added and removed material. The implications of changes in scrap input and output are calculated on two separate, dedicated spreadsheets.

The starting point for calculating the changes in production GHGs from the added aluminum are the total amount of aluminum body and closure parts added to light duty vehicles produced each year (in million kg), broken down into sheet, extrusions, and castings. The three time series are denoted by $TAA_l(t)$, with subscript *l* standing for sheet, extrusions, and castings. The first calculation step is to convert the aluminum contained in the vehicles as body and closure parts into shipped primary and secondary aluminum, denoted by $SM_l^{pa}(t)$ and $SM_l^{sa}(t)$, where superscript *pa* stands for primary aluminum and *sa* for secondary aluminum. The calculations are as follows:

$$SM_l^{pa}(t) = \left(1 - sc_l^a(t)\right) \cdot \frac{TAA_l(t)}{\gamma_l^a}$$

$$SM_l^{sa}(t) = sc_l^a(t) \cdot \frac{TAA_l(t)}{\gamma_l^a} \quad \text{(A.13)}$$

where $sc_l^a(t)$ is the secondary (recycled) content of aluminum type *l* in production year *t*, and γ_l^a is the manufacturing yield of aluminum type *l*. The results of these calculations are also in million kg and stored in cells B6:G44. The next step is to calculate the resulting production GHG emissions for each aluminum type by multiplying the shipped material quantities with the GHG intensities of aluminum production:

$$GHGP_l^{pa}(t) = SM_l^{pa}(t) \cdot \left(GHG_{ingot}^{pa}(t) + GHG_l^a\right)$$

$$GHGP_l^{sa}(t) = SM_l^{sa}(t) \cdot \left(GHG_{ingot}^{sa} + GHG_l^a\right) \quad \text{(A.14)}$$

where GHG_{ingot}^{pa} and GHG_{ingot}^{sa} are the GHG intensities of primary and secondary aluminum ingot production and GHG_l^a the GHG intensities of aluminum ingot rolling, extruding, and casting. The final step is to sum over all aluminum types *l* in order to calculate the GHG emissions that result from increases in aluminum production and forming in any given production year:

$$GHGP^{a}(t) = \sum_{l}\left(GHGP_{l}^{pa}(t) + GHGP_{l}^{sa}(t)\right) \quad \text{(A.15)}$$

The changes in GHG emissions due to increased aluminum production $GHGP^{a}(t)$ are stored in cells S6:S44. Calculating the changes in production GHGs from the removed steel has the same computational structure, once the total amount of removed steel has been determined. The latter is complicated somewhat by the fact that it needs to account for both primary and secondary mass savings and the different steel types *l*, which are flat, long, and cast. The total amount of steel type *l* removed from all vehicles produced in year *t* is calculated as follows:

$$TSR_{l}(t) = -\frac{TAA(t)}{k} \cdot pf_{l} - \frac{TAA(t)}{k}(1-k) \cdot s \cdot sf_{l} \quad \text{(A.16)}$$

where $TAA(t)$ is the total amount of aluminum body and closure parts added to the vehicles produced in year *t*, *k* is the material replacement coefficient of aluminum relative to steel (in kg aluminum/kg steel), *s* is the secondary mass savings coefficient (in kg secondary mass savings/kg primary mass savings), and pf_{l} and sf_{l} are the fractions of primary and secondary mass savings that are of steel type *l*. Note that $TAA(t) = \sum_{l} TAA_{l}(t)$ and is one of the central data inputs into the model. The subsequent calculation steps are the same as for the added aluminum. First, the amount of no longer shipped primary and secondary steel, $SM_{l}^{ps}(t)$ and $SM_{l}^{ss}(t)$, is calculated:

$$SM_{l}^{ps}(t) = \left(1 - sc_{l}^{s}(t)\right) \cdot \frac{TSR_{l}(t)}{\gamma_{l}^{s}}$$

$$SM_{l}^{ss}(t) = sc_{l}^{s}(t) \cdot \frac{TSR_{l}(t)}{\gamma_{l}^{s}} \quad \text{(A.17)}$$

where $sc_{l}^{s}(t)$ is the electric arc furnace (EAF) content of steel type *l* in production year *t*, and γ_{l}^{s} is the manufacturing yield of steel type *l*. The next step is to calculate the avoided

production GHG emissions for each steel type by multiplying the no longer shipped material quantities with the GHG intensities of steel production:

$$GHGP_l^{ps}(t) = SM_l^{ps}(t) \cdot \left(GHG_{ingot}^{ps} + GHG_l^s\right)$$

$$GHGP_l^{ss}(t) = SM_l^{ss}(t) \cdot \left(GHG_{ingot}^{ss} + GHG_l^s\right) \quad \text{(A.18)}$$

where GHG_{ingot}^{ps} and GHG_{ingot}^{ss} are the GHG intensities of primary and secondary steel ingot production and GHG_l^s the GHG intensities of steel ingot rolling and casting. The final step is to add over all steel types *l* in order to calculate the GHG emissions that result from reductions in steel production and forming in any given production year:

$$GHGP^s(t) = \sum_l \left(GHGP_l^{ps}(t) + GHGP_l^{ss}(t)\right) \quad \text{(A.19)}$$

The changes in GHG emissions due to reduced steel production $GHGP^s(t)$ are stored in cells S52:S90.

There are three different ways in which recycled content is modeled for aluminum. The first models recycling as an open loop, which means that scrap inputs and outputs are independent from each other and modeled exogenously. In this case the recycled content of aluminum sheet, extrusions, and castings is given through time-dependent input values, which means that recycled content could be different every year. In the default setting the values are assumed to be constant over time and are set to zero for the recycled content of sheet and extrusions, and 0.85 for the recycled content of castings. This open loop methodology is the only way available to model the EAF fraction for flat, long, and cast steel. In the default setting the EAF fractions are assumed to be constant over time and are set to 5% for flat, 85% for long, and 100% for cast steel. As with all input variables, the values can be changed by the model user. The other two approaches available for aluminum model recycling as a closed loop, i.e. the scrap inputs into production of aluminum body and

closure parts come from scrap generated within the modeled North American light duty vehicle life cycles. In option one of the closed-loop model, only production scrap is used in a closed loop, i.e. for aluminum body and closure production; the scrap at vehicle end-of-life is still recycled externally, i.e. in an open loop. The calculations for shipped primary and secondary aluminum are now as follows:

$$SM_l^{sa}(t) = \frac{ProS_l^a(t)}{s_r^a}$$

$$SM_l^{pa}(t) = \frac{TAA_l(t)}{\gamma_l^a} - SM_l^{sa}(t) \quad \text{(A.20)}$$

where $ProS_l^a(t)$ is the amount of prompt scrap of aluminum type *l* generated and collected during calendar/production year *t*, and s_r^a is the amount of scrap used to produce one kg of recycled (secondary) aluminum ingot. In option two of the closed-loop model, production and end-of-life scrap is used in a closed loop, i.e. for aluminum body and closure production. The calculations for shipped primary and secondary aluminum change to the following:

$$SM_l^{sa}(t) = \frac{ProS_l^a(t) + EolS_l^a(t)}{s_r^a}$$

$$SM_l^{pa}(t) = \frac{TAA_l(t)}{\gamma_l^a} - SM_l^{sa}(t) \quad \text{(A.21)}$$

where $EolS_l^a$ is the amount of end-of-life (eol) scrap of aluminum type *l* generated and collected during calendar/production year *t*.

Variable	Description	Location of data
$GHGP^a(t)$	GHG emission changes from increases in aluminum production and forming in calendar year t (in million kg CO2eq)	S6:S44
$GHGP^s(t)$	GHG emission changes from reductions in steel	S52:S90

	production and forming in calendar year t (in million kg CO2eq)	

Table A.3: Output data from spreadsheet 'Material production'

A.2.4 Scrap at production

Changing the material composition of North American light duty vehicles produced between 2012 and 2050 changes the quantities and types of scrap that are generated during vehicle production. The aim of this spreadsheet is to calculate the GHG implications of changes in the use and generation of scrap during material production and forming. In rows 2 to 45 this is done for aluminum, and in rows 48 to 90 it is done for steel.

For aluminum, the starting point is the total amount of aluminum body and closure parts in light duty vehicles produced each year (in million kg), broken down into sheet, extrusions, and castings, i.e. $TAA_l(t)$, with subscript l standing for sheet, extrusions, and castings. These values are turned into amounts of generated and collected production scrap as follows:

$$ProS_l^a(t) = c_{pro}^a \cdot \frac{(1-\gamma_l^a)}{\gamma_l^a} \cdot TAA_l(t) \quad \text{(A.22)}$$

where c_{pro}^a is the production scrap collection rate for aluminum and γ_l^a is the forming yield of aluminum type *l*.

The next step depends on which recycling model is chosen for aluminum production scrap. If closed-loop recycling is selected, the values for collected production scrap, $ProS_l^a(t)$, are forwarded to the 'Material production' spreadsheet and used to calculate the recycled content of the aluminum body and closure parts in North American light vehicle production. If open-loop recycling is selected, the first step is to calculate the scrap input into vehicle production according to this equation:

$$SIn_l^a(t) = \left(s_p^a \cdot \left(1 - sc_l^a(t)\right) + s_r^a \cdot sc_l^a(t)\right) \cdot \frac{TAA_l(t)}{\gamma_l^a} \quad \text{(A.23)}$$

where s_p^a the scrap input into primary aluminum production (in kg/kg), s_r^a the scrap input into secondary (recycled) aluminum production (in kg/kg), and $sc_l^a(t)$ is the exogenously given recycled (secondary) content of aluminum type *l* used in body and closure parts in production year *t*. The second step is to calculate the net change in external secondary aluminum production caused by the net scrap flow into or out of vehicle production according to the following equation:

$$\alpha_a \cdot \frac{ProS_l^a(t) - SIn_l^a(t)}{s_r^a - \beta_a \cdot s_p^a} \quad \text{(A.24)}$$

where α_a models the response of the aluminum scrap market to a change in automotive aluminum scrap generation and use, and β_a models the response of external primary aluminum production to a change in external secondary aluminum production. The penultimate step of the open-loop recycling model is to calculate the GHG implications of the net change in external secondary aluminum production:

$$GHGProS_l^a(t) = \alpha_a \cdot \frac{ProS_l^a(t) - SIn_l^a(t)}{s_r^a - \beta_a \cdot s_p^a}\left(GHG_{ingot}^{sa} - \beta_a \cdot GHG_{ingot}^{pa}(t)\right) \quad \text{(A.25)}$$

In the final step, the total external GHG implications due to changes in aluminum scrap use and generation during material production and forming are calculated by summing over aluminum sheet, extrusions, and castings:

$$GHGProS^a(t) = \sum_l GHGProS_l^a(t) \quad \text{(A.26)}$$

For steel, the calculations are identical to the open-loop recycling calculations for aluminum. Here, the starting point is the total steel removed from the vehicles, $TSR_l(t)$, which has been calculated in the 'Material production' spreadsheet. These values are

converted into amounts of production scrap no longer generated and collected, $ProS_l^s(t)$, and amounts of steel scrap no longer used into vehicle production, $SIn_l^s(t)$:

$$ProS_l^s(t) = c_{pro}^s \cdot \frac{(1-\gamma_l^s)}{\gamma_l^s} \cdot TSR_l(t)$$

$$SIn_l^s(t) = \left(s_p^s \cdot (1 - sc_l^s) + s_r^s \cdot sc_l^s\right) \cdot \frac{TSR_l(t)}{\gamma_l^s} \quad \text{(A.27)}$$

where c_{pro}^s is the collection rate for steel production scrap, γ_l^s is the forming yield of steel type *l*, sc_l^s is the secondary content of steel type *l*, s_p^s is the scrap input into primary steel production (in kg/kg), and s_r^s is the scrap input into secondary steel production (in kg/kg). The net change in external secondary steel production is now calculated as follows:

$$\alpha_s \cdot \frac{ProS_l^s(t) - SIn_l^s(t)}{s_r^s - \beta_s \cdot s_p^s} \quad \text{(A.28)}$$

where α_s models the response of the steel scrap market to a change in automotive steel scrap generation and use, and β_s models the response of external primary steel production to a change in external secondary steel production. As in the case of aluminum production scrap, the last two steps are to calculate and aggregate the GHG implications of the net change in external secondary steel production:

$$GHGProS_l^s(t) = \alpha_s \cdot \frac{ProS_l^s(t) - SIn_l^s(t)}{s_r^s - \beta_s \cdot s_p^s}\left(GHG_{ingot}^{ss} - \beta_s \cdot GHG_{ingot}^{ps}(t)\right)$$

$$GHGProS^s(t) = \sum_l GHGProS_l^s(t) \quad \text{(A.29)}$$

Variable	Description	Location of data
$GHGProS^a(t)$	GHG changes due to changes in external use of aluminum production scrap in calendar year t (in million kg CO2eq)	S6:S44
$GHGProS^s(t)$	GHG changes due to changes in external use of steel production scrap in calendar year t (in million kg	S51:S89

	CO2eq)	

Table A.4: Output data from spreadsheet 'Scrap at production'

A.2.5 Scrap at end-of-life

Changing the material composition of the vehicles produced between 2012 and 2050 means that the quantities of end-of-life aluminum and steel scrap change when these vehicles reach the end of their lives. The aim of this spreadsheet is to calculate the GHG implications of these changes in automotive end-of-life scrap generation, collection, and recycling.

The main data input into this spreadsheet is the total amount of aluminum body and closure parts added to the vehicles produced in year *T*, $TAA(T) = \sum_l TAA_l(t)$, and the total amount of steel removed from all vehicles produced in year *T*, $TSR(T) = \sum_l TSR_l(t)$. The first step is to calculate the changes in end-of-life scrap generated and collected in calendar year *t*, taking into account the lifetime distribution of the vehicles. For aluminum and steel the calculations are identical and as follows:

$$EolS^a(t) = c_{eol}^a \cdot ssr_{eol}^a \cdot \sum_{T=2012}^{t-1} TAA(T) \cdot \big(FIU(T-t-1) - FIU(T-t)\big)$$

$$EolS^s(t) = c_{eol}^s \cdot ssr_{eol}^s \cdot \sum_{T=2012}^{t-1} TSR(T) \cdot \big(FIU(T-t-1) - FIU(T-t)\big) \qquad \text{(A.30)}$$

where c_{eol}^a and c_{eol}^s are the end-of-life collection rates for aluminum and steel scrap, ssr_{eol}^a and ssr_{eol}^s are the shredder separation rates for end-of-life aluminum and steel scrap. $FIU(T-t)$ is the fraction of vehicles still in use after $T-t$ years of driving, and $FIU(T-t-1)$ is the fraction of vehicles still in use after $T-t-1$ years of driving (see also Section A.2.2). Therefore, $\big(FIU(T-t-1) - FIU(T-t)\big)$ is the fraction of vehicles that reach end of life during calendar year $T-t$.

If closed-loop recycling is selected for the end-of-life aluminum scrap, $EolS^a(t)$ is broken out into sheet, extrusions, and castings, $EolS_l^a(t)$, forwarded to the 'Material production' spreadsheet, and used to calculate the recycled content of the aluminum body and closure parts in North American light vehicle production (see Section A.2.3).

If open-loop recycling is selected for end-of-life aluminum scrap, $EolS^a(t)$ is recycled externally and has the following GHG implications:

$$GHGEolS^a(t) = \alpha_a \cdot \frac{EolS^a(t)}{s_r^a - \beta_a \cdot s_p^a}\left(GHG_{ingot}^{sa} - \beta_a \cdot GHG_{ingot}^{pa}(t)\right) \quad \text{(A.31)}$$

where α_a models the response of the aluminum scrap market to a change in automotive aluminum scrap generation and use, and β_a models the response of external primary aluminum production to a change in external secondary aluminum production. The open-loop model used to calculate the GHG consequences of changes in end-of-life scrap flows is the same as the one used for changes in prompt scrap flows. Other parameters used in the calculation above are the GHG intensities of primary and secondary aluminum ingot production (in $kgCO_2eq/kg$), GHG_{ingot}^{pa} and GHG_{ingot}^{sa}, and the scrap input into primary and secondary (recycled) aluminum production (in kg/kg), s_p^a and s_r^a.

The changes in end-of-life steel scrap are always modeled in an open loop. The GHG implications of reducing the amount of end end-of-life steel scrap are calculated as follows:

$$GHGEolS^s(t) = \alpha_s \cdot \frac{EolS^s(t)}{s_r^s - \beta_s \cdot s_p^s}\left(GHG_{ingot}^{ss} - \beta_s \cdot GHG_{ingot}^{ps}(t)\right) \quad \text{(A.32)}$$

where α_s models the response of the steel scrap market to a change in automotive steel scrap generation and use, and β_s models the response of external primary steel production to a change in external secondary steel production. Other parameters used in the calculation above are the GHG intensities of primary and secondary steel ingot production (in

kgCO_2eq/kg), GHG_{ingot}^{ps} and GHG_{ingot}^{ss}, and the scrap input into primary and secondary (recycled) steel production (in kg/kg), s_p^a and s_r^a.

Variable	Description	Location of data
$GHGEolS^a(t)$	GHG changes due to changes in external use of end-of-life aluminum scrap in calendar year t (in million kg CO2eq)	Q5:Q43
$GHGEolS^s(t)$	GHG changes due to changes in external use of end-of-life steel scrap in calendar year t (in million kg CO2eq)	N5:N43

Table A.5: Output data from spreadsheet 'Scrap at end-of-life'

A.3 Baseline Input Data

The following are the input data used to generate the baseline result, which serves as an initial estimate of the incremental inventory for the system, and a point of departure for the sensitivity analyses. The subsections refer to the particular spreadsheets in the model to which the data were input.

A.3.1 Results & data input

Parameter	**Value**	**Source**
Material replacement coefficient (aluminum to mild steel)	0.55	Kim and Wallington, 2013
Material replacement coefficient (HSS to mild steel)	0.7	Kim and Wallington, 2013
Fraction of aluminum replacing mild steel	0.5	Ducker, 2015
Flat steel fraction of total replaced steel	0.9	Geyer, 2013
Secondary mass savings coefficient	0.5	Kim and Wallington, 2013
Flat share of secondary mass savings	0.4	Geyer, 2013

Long share of secondary mass savings	0.3	Geyer, 2013
Year-over-year decarbonization of material production processes & electricity production for BEVs	0.5%	n/a
Year-over-year carbon intensification of gasoline & diesel production	0.5%	n/a

Table A.6: General input data

Note: Final material replacement coefficient is derived from the values for aluminum to mild steel and HSS to mild steel along with the fraction of aluminum replacing mild steel, where the remaining aluminum replaces HSS per Chapp and Shah, 2007, Ducker Worldwide, 2015, Morgans, 2012, and Pafumi, 2006.

$$k_{final} = fraction_{mild\ replaced} * k_{al\ to\ mild} + \left(1 - fraction_{mild\ replaced}\right) * \frac{k_{al\ to\ mild}}{k_{HSS\ to\ mild}}$$

$$= 0.5 * 0.55 + (1 - 0.5) * \frac{0.55}{0.7} = 0.275 + 0.3928 = \mathbf{0.6678}$$

Parameter	**Value**	**Source**
Scrap input to primary production	0	IAI, 2013
Scrap input to secondary production	1.048	TAA, 2013
Prompt scrap collection rate	0.99	Geyer, 2013
EOL scrap collection rate	0.97	Kelly and Apelian, 2016
Shredder separation rate	0.9	Geyer, 2013
Alpha	1	n/a
Beta	1	n/a

Table A.7: Aluminum recycling parameters

Parameter	**Value**	**Source**
Scrap input to primary production	0.209	AISI, 2016
Scrap input to secondary production	1.05	WSA, 2010
Prompt scrap collection rate	0.99	Geyer, 2013

EOL scrap collection rate	0.97	Steel Recycling Institute, 2017
Shredder separation rate	0.98	Geyer, 2013
Alpha	1	n/a
Beta	1	n/a

Table A.8: Steel recycling parameters

Process	**GHG intensity**	**Source**
Primary ingot (North America) (cradle-to-gate)	8.937	TAA, 2013
Secondary ingot (cradle-to-gate)	0.508	Thinkstep, 2015, PE, EU27
Rolled aluminum (ingot-to-gate, aluminum rolling)	0.589	Thinkstep, 2015, PE, EU27
Extruded aluminum (ingot-to-gate, aluminum extrusion)	0.689	Thinkstep, 2015, PE, EU27
Cast aluminum (ingot-to-gate, aluminum casting)	0.590	Thinkstep, 2015, PE, DE

Table A.9: GHG intensities of aluminum production and forming (in $kgCO_2eq/kg$ output)

Process	**GHG intensity**	**Source**
BF/BOF slab *Note: Time series entry optional*	2.02	Hasanbeigi et al., 2016
EAF slab (slab-to-gate)	0.399	WSA, 2010
Flat steel (slab-to-gate)	0.485	WSA, 2010
Long steel (gate-to-gate, steel rolling)	0.290	WSA, 2010
Cast steel (gate-to-gate, steel casting)	0.135	WSA, 2010

Table A.10: GHG intensities of steel production and forming (in $kgCO_2eq/kg$ output)

Parameter	Value	Unit	Source
NCV of gasoline	32.27	MJ/liter	Thinkstep, 2015, PE, EU27
GHG intensity of gasoline production (cradle-to-gate, at gas station))	15.50	gCO2eq/MJ	Thinkstep, 2015, PE, EU27
GHG intensity of gasoline combustion (gate-to-gate, combustion in light duty vehicle)	72	gCO2eq/MJ	Thinkstep, 2015, PE, GLO
NCV of diesel	36.00	MJ/liter	Thinkstep, 2015, PE, EU27
GHG intensity of diesel production (cradle-to-gate, at gas station))	7.74	gCO2eq/MJ	Thinkstep, 2015, PE, EU27
GHG intensity of diesel combustion (gate-to-gate, combustion in light duty vehicle)	75	gCO2eq/MJ	Thinkstep, 2015, PE, GLO
GHG intensity of electricity production (cradle-to-gate, U.S. average, at consumer)	0.150	kgCO2eq/MJ	ANL, 2015
Fraction of powertrains resized	50	%	n/a
Share of plug electricity as energy source	50	%	Geyer, 2013
Vehicle lifetime driving	245,000	km	NHTSA, 2006
Mean vehicle lifetime	13	years	NHTSA, 2006
Standard deviation of vehicle lifetime	3	years	NHTSA, 2006

Table A.11: Vehicle use phase parameters

Material	Yield	Source
Aluminum, Sheet	0.62	Milford et al., 2011
Aluminum, Extrusion	0.8	Geyer, 2013
Aluminum, Castings	0.8	Geyer, 2013
Steel, Flat	0.6	Milford et al., 2011
Steel, Long	0.8	Geyer, 2013

Steel, Castings	0.8	Geyer, 2013

Table A.12: Forming yields

Note: Aluminum sheet and flat steel yields are calculated from Milford et al., 2011 SI tables 3 and 4 as $yield = Slitting\_yield * Blanking\_yield * Stamping\_yield$.

Year	**Imported Al kgCO2/kg[4,5]**	**% Imported[3]**
2012	16.50[1]	0.25
2013	16.27	0.29
2014	16.05	0.32
2015	15.83	0.36[2]
2016	15.61	0.40
2017	15.39	0.43
2018	15.17	0.47
2019	14.96	0.50
2020	14.76	0.54
2021	14.55	0.58
2022	14.35	0.61
2023	14.15	0.65
2024	13.95	0.68
2025	13.76	0.72
2026	13.69	0.72

Table A.13: A sample of the imported primary aluminum ingot production share and GHGs.

Notes:

1. Initial imported GHG intensity (16.5 kgCO2/kg) is a global average from International Aluminum Institute, 2014.

2. 2015 Aluminum import share (36%) is derived from The Aluminum Association, 2015.
3. Growth rate of aluminum imports (3.6% per year until 2025) is derived from Accenture LLC, 2015.
4. Downward trend in imported aluminum GHGs is derived from a downward projection in electricity consumption for aluminum production in China from Hao et al., 2015 and applied to the global average.
5. In addition, a year-over-year decarbonization factor of 0.5% is applied in the baseline scenario which continues through the modelling period

A.3.2 Fleet Composition

Year	**# of Vehicles**
2012	16,181,282
2013	16,200,000
2014	16,752,614
2015	17,500,000
2016	17,323,946
2017	17,609,612
2018	17,900,000
2019	18,180,944
2020	18,200,000
2021	18,752,277
2022	19,000,000
2023	19,323,609
2024	19,609,275
2025-2050	20,000,000

Table A.14: Light duty vehicle production forecast (Ducker, 2015, p.55)

The resulting cumulative light duty vehicle production between 2012 and 2015 is therefore 752,533,558, i.e. just over 750 million cars.

Year	ICV Share	Gasoline Share of ICV	Hybrid Share	Standard Share of Hybrid
2012	0.982	0.932	0.018	0.500
2013	0.976	0.931	0.024	0.500
2014	0.972	0.935	0.026	0.500
2015	0.965	0.936	0.034	0.500
2016	0.952	0.932	0.046	0.500
2017	0.947	0.931	0.050	0.500
2018	0.938	0.932	0.057	0.500
2019	0.924	0.931	0.070	0.500
2020	0.913	0.934	0.081	0.500
2021	0.909	0.932	0.084	0.500
2022	0.900	0.931	0.092	0.500
2023	0.892	0.932	0.100	0.500
2024	0.883	0.931	0.108	0.500
2025	0.874	0.934	0.110	0.500
2026-2050	0.870	0.934	0.110	0.500

Table A.15: Powertrain type inputs (Ducker, 2015, p. 21 & 22)

Year	Sheet (million kg)	Extrusions (million kg)	Castings (million kg)
2012	81.9	0.0	0.0
2013	100.3	7.3	0.0
2014	200.5	12.7	1.8
2015	420.9	20.0	18.2
2016	592.2	32.8	23.7
2017	681.6	38.2	27.3

2018	738.1	41.9	29.1
2019	878.4	56.4	29.1
2020	1,078.8	69.2	45.5
2021	1,228.2	80.1	45.5
2022	1,303.0	81.9	65.5
2023	1,419.7	87.4	74.6
2024	1,640.1	111.0	78.3
2025	1,707.6	112.9	85.6
2026	1,755	114	91
2027	1,778	115	93
2028-2050	1,790	115	95

Table A.16: Projected amount of aluminum body & closure parts in North American light vehicle production (Ducker, 2014, p.20)

Class	**lbs of aluminum**	**NA LDV fleet share**	**HEV share**	**BEV share**
Source	**Ducker 2014 p. 9**		**ANL 2014**	
A/B	251.60	0.03	0.09	0.18
C	273.90	0.17	0.35	0.51
D	363.30	0.21	0.42	0.31
E	546.90	0.03	0.11	0.00
MPV	396.50	0.04	0.00	0.00
SUV	410.30	0.33	0.02	0.01
VAN	273.20	0.02	0.00	0.00
PUP	548.90	0.17	0.00	0.00

Table A.17: Vehicle class data (ANL, 2015; Ducker, 2014, p.9)

A.3.3 Vehicle Use

		No powertrain resizing (MJ/100km100kg)			Powertrain Resizing (MJ/100km100kg)		
PT type	**Fuel**	**Compact**	**Midsize**	**SUV**	**Compact**	**Midsize**	**SUV**
ICEV-G	Gasoline	4.992	4.635	4.775	7.202	8.728	9.766
ICEV-D	Diesel	4.340	4.470	4.311	6.958	7.272	7.112
HEV-S	Gasoline	2.994	3.329	2.927	4.998	6.324	6.409
HEV-P	Gasoline	4.290	4.437	n/a	5.973	6.299	n/a
HEV-P	Electricity	1.395	1.439	n/a	1.942	2.048	n/a
BEV	Electricity	1.393	1.446	n/a	1.965	2.079	n/a

Table A.18: Fuel and electricity savings per mass savings with and without powertrain resizing

		Baseline vehicle mass (kg)			Baseline fuel economy (MJ/100km)		
PT type	**Fuel**	**Compact**	**Midsize**	**SUV**	**Compact**	**Midsize**	**SUV**
ICEV-G	Gasoline	1260	1640	2195	148.61	198.24	285.11
ICEV-D	Diesel	1350	1740	2320	141.86	169.14	231.23
HEV-S	Gasoline	1335	1752	2345	121.20	163.39	247.92
HEV-P	Gasoline	1188	1431	n/a	111.82	136.29	n/a
HEV-P	Electricity			n/a	36.36	44.32	n/a
BEV	Electricity	1097	1334	n/a	34.78	42.83	n/a

Table A.19: Baseline vehicle mass used in power train models and resulting baseline fuel economy (Geyer and Malen, 2017; Malen and Geyer, 2017)

Note: Time series entry optional

Other parameters used in the power train models:

Frontal area (m^2): ICEV-G, ICEV-D, HEV-S: Compact: 2.16, Midsize: 2.24 SUV: 2.78; HEV-P, BEV: Compact: 2.03, Midsize: 2.26

Tire rolling radius (m): ICEV-G&D, HEV-S: Compact: 0.308, Midsize: 0.317, SUV: 0.356; HEV-P, BEV: Compact: 0.285, Midsize: 0.300

Drag coefficient: ICEV-G, ICEV-D, HEV-S: Compact: 0.31, Midsize: 0.27, SUV: 0.36; HEV-P, BEV: Compact: 0.25, Midsize: 0.25

Tire rolling resistance coefficient: 0.07

A.3.4 Monte Carlo simulation

The following is the table of parameter value ranges entered into the Monte Carlo simulation shown in Figure 2.5:

Parameter	**Unit**	**Minimum**	**Maximum**
Material Replacement Coefficient	kg aluminum/kg steel	0.55	0.75
Initial GHG intensity of Imported Primary Aluminum Production	kg CO2eq/kg	6.70	21.70
Secondary Mass Savings	kg secondary/kg primary mass savings	0	1
Fraction of Powertrains Resized	%	0	100
Aluminum Beta	unitless	0	1
Aluminum Alpha	unitless	0	1
Vehicle Lifetime Distance Driven	km	200,000	300,000
Aluminum Sheet Yield	%	52	72
Year-over-year decarbonization of material production processes and electricity production for BEVs	%/year	0	2
Initial GHG intensity of Primary Steel Production	kg CO2eq/kg	1.27	2.80
Growth Rate of Imported Primary Aluminum Production	%/year	0.00	6.00
Flat Steel Yield	%	50	70

Initial GHG intensity of North American Primary Aluminum Production	kg CO2eq/kg	6.70	8.94
Initial GHG intensity of Secondary Aluminum Production	kg CO2eq/kg	0.254	1.016
Initial GHG intensity of Secondary Steel Production	kg CO2eq/kg	0.199	0.798
Initial GHG intensity of Electricity Production for BEVs	kg CO2eq/MJ	0.075	0.15
Initial GHG intensity of Gasoline Production	kg CO2eq/MJ	15.50	23.25
Initial GHG intensity of Diesel Production	kg CO2eq/MJ	7.74	11.61
Steel Alpha	unitless	0	1
Steel Beta	unitless	0	1
Year-over-year carbon intensification of gasoline and diesel production	%/year	0	2

Table A.20: The initial Monte Carlo simulation, with contributions to variance shown in Figure 2.5 of Chapter 2.

Note: I determined the approximate threshold of 2050 cumulative GHG emissions for which GHG payback is never achieved by lowering the parameter value for aluminum beta until it triggers an upward slope at the end of the modelling period (GHG payback = "Never"). With all else fixed at baseline values, the threshold of aluminum beta that triggers GHG payback = "Never" is 0.352. Cumulative 2050 GHG emissions in that scenario are equal to 207 million tonnes CO_2eq. Thus, I say that Monte Carlo trials with cumulative GHG emissions greater than 207 million tonnes CO2eq are trials where GHG payback is never achieved.

This is an approximation, because when other parameter values are changed in order to trigger GHG payback = "Never", the value of cumulative GHG emissions in 2050 may be slightly different.

A.4 Additional Sensitivity Analyses

In Section 2.4.1 (Figure 2.3), I show the results of inputting all of the baseline parameters as outlined in Section A.3. Key parameters corresponding to each life cycle stage are then varied to generate a number of sensitivity analyses. In the production phase, it is shown that the results are highly sensitive to the material replacement coefficient *k* and secondary mass savings *s*. I also show the effect of the GHG intensities of primary aluminum and steel production. In the use phase, I explore the effects of increasing the share of the fleet that with powertrain resizing, as well as showing the effect of accelerating the adoption of hybrid and electric vehicle in accordance with the IEA BLUE map projections (IEA, 2010). Finally, for the case of recycling it is shown that the model is highly sensitive to the displacement of primary production resulting from the recycling of aluminum in the end-of-life stage, and that the displacement rate of steel has a much less pronounced effect. The contributions of the various life cycle calculations to the cumulative baseline GHG curve are shown. The remainder of this section explores additional sensitivity analyses of interest from each life cycle stage, as well as selected interactions between parameters.

A.4.1 Primary Production

Figure A.3 shows the sensitivity of the result to the growth in the material replacement coefficient, the secondary mass savings factor, the production yields of both steel and aluminum sheet, the growth rate of the imported share of primary aluminum, the GHG intensity of imported primary aluminum, the GHG intensity of primary steel production, and

the starting year of modelling additional aluminum production.

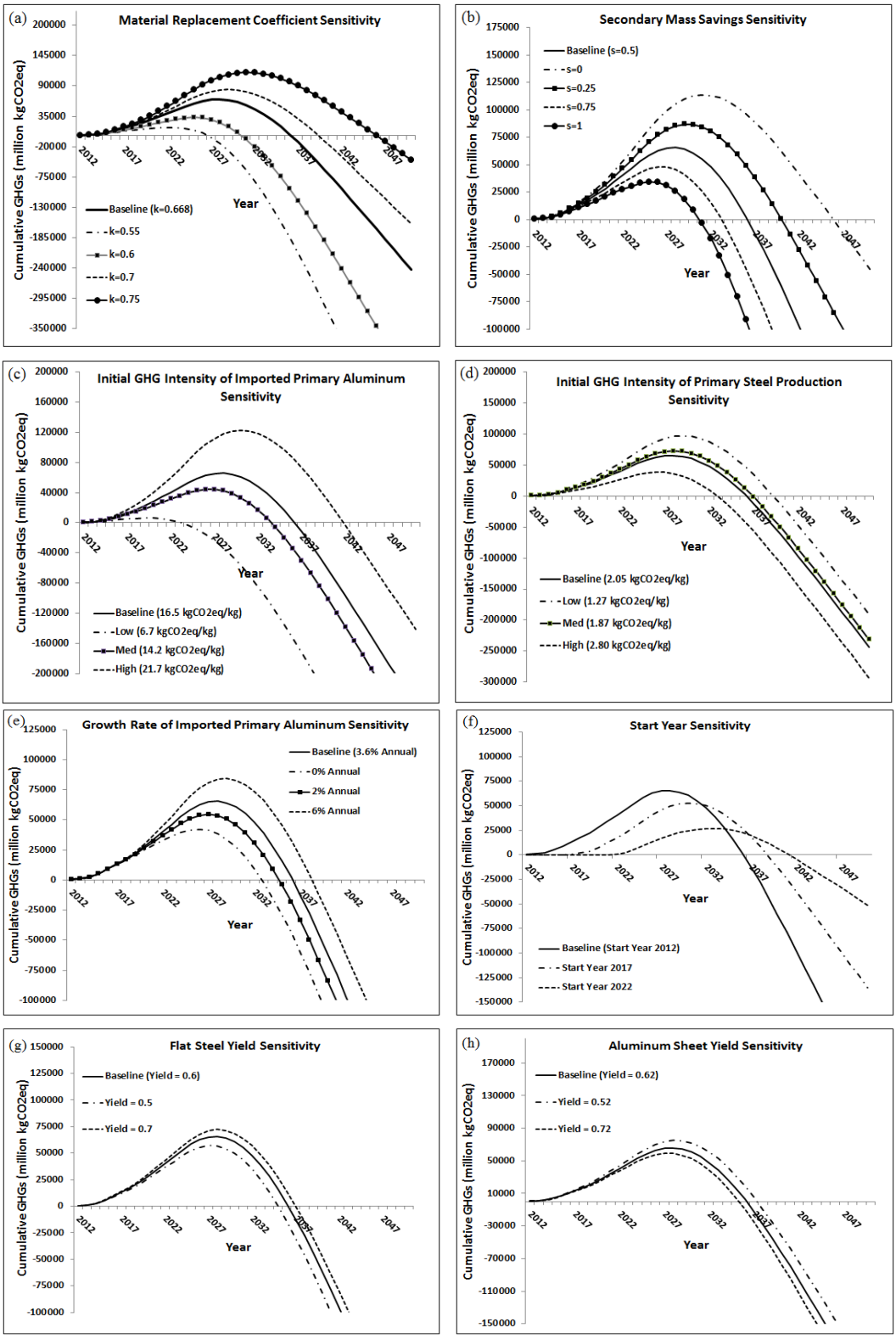

Figure A.3: (a) Sensitivity of cumulative GHG curve to the material replacement coefficient, (b) Sensitivity of cumulative GHG results to secondary mass savings factor,(c) Sensitivity of the cumulative GHG curve to the initial GHG intensity of imported primary aluminum production, (d) Sensitivity of the cumulative GHG curve to the GHG intensity of primary steel production, (e) Sensitivity of cumulative GHG curve to the growth rate of the imported share of primary aluminum ingot, (f) Sensitivity of cumulative GHG curve to the starting year of additional aluminum production modelling, (g) Sensitivity of cumulative GHG curve to flat steel forming yield, (h) Sensitivity of cumulative GHG curve to aluminum sheet forming yield.

The first insight provided by Figure A.3 is that the results are most sensitive to the material replacement coefficient, and the effect is clearly non-linear. Equation A.16 illustrates how the quantity of steel removed depends non-linearly on the material replacement coefficient. This model is based on a fixed industry projection of aluminum content. Therefore, lowering the material replacement coefficient increases the amount of steel removed from vehicles because of the increasing aluminum content. In turn, the amount of fuel savings in the use phase is increased as the material replacement coefficient decreases. The illustrated values of the material replacement coefficient fall within the range observed by the meta-analysis of automotive material substitution referenced in this paper (Kim and Wallington, 2013).

In addition, the cumulative GHG curve is sensitive to the growth rate of imported primary aluminum production. Figure A.3 (e) covers the range from 0% growth to a theoretical maximum of 6%, which would drive the imported share of additional production

to 100% during the steady state. The response of the cumulative GHG curve to the production yield of flat steel is smaller compared to all other tested parameters.

It is also useful to observe the change in GHG payback when varying the start date of modelled additional aluminum production. In order to test this, I created two scenarios where additional aluminum production begins in 2017 and 2022, rather than the beginning of the Ducker forecast in 2012. In the 2017 case, the Ducker figures from 2016 are used as the counterfactual to which all other years are compared. In the 2022 case, the Ducker figures from 2021 are used as the counterfactual. This means, for example, that in the "Start Date 2017" scenario, the additional aluminum inputs for 2017 are (681.6-592.2=89.4) for sheet, (38.2-32.7=5.5) for extrusions, and (27.3-23.7=3.6) for castings. These calculated time series for the 2017 and 2022 scenarios are shown on the "Fleet Composition" tab in cells B134:D172 and B178:D216, respectively.

Modifying the start year has a two-fold effect on GHG payback. First, the peak of the curve is lower when the starting year is later, a trivial consequence of the fact that the cumulative amount of additional aluminum becomes smaller. Secondly, there is a slight effect on GHG payback time. The baseline case, with additional aluminum beginning in 2012, has a payback year of 2039 and a payback time of (2039-2012) = 27 years. When starting in 2017, the payback year is 2042 and the payback time is (2042-2017) = 25 years. Finally, when beginning in 2022, the payback year is 2044 and the payback time is (2048-2022) = 22 years.

In Figure A.4, I explore the possibility that the aluminum content of vehicles continues to increase after 2028, the end of the industry projection used to form the baseline curve. To explore the sensitivity of the model to the steady state assumption, I (a) extrapolate the trend

in sheet aluminum production from the Ducker data to 2050 using linear regression, and (b) accelerate the trend so that in 2050 aluminum makes up 100% of the body and closure material. Then, I perform the Monte Carlo analysis using the accelerated aluminum content in order to verify whether or not the overall results of the study change.

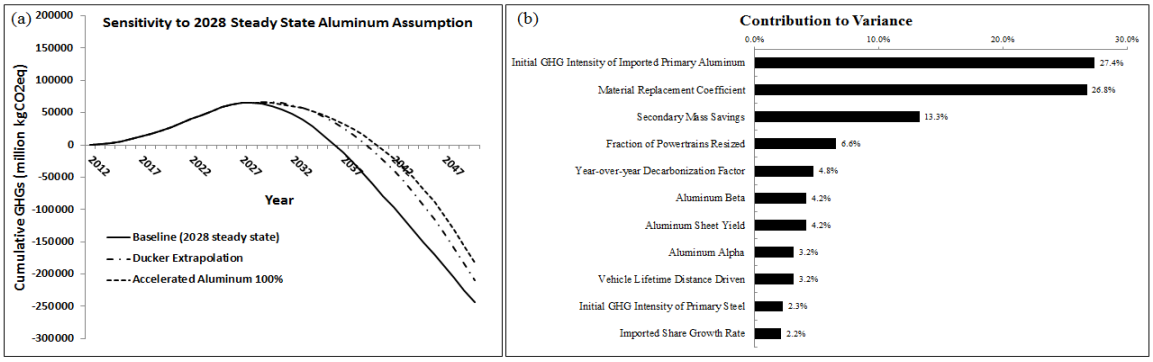

Figure A.4: (a) Sensitivity of cumulative GHG curve to alternative additional aluminum production curves that do not level off to a steady state in 2028. "Ducker extrapolation" is a continuation of a linear trend that produced the baseline case, and "Accelerated aluminum" brings the aluminum content of body and closures to 100% by 2050. (b) The Monte Carlo simulation from the main text (Figure 5) using the accelerated aluminum content and showing that the top ten contributions to variance are not significantly affected.

Figure A.4 (a) shows that continuing to increase aluminum production beyond 2028 changes the shape of the cumulative GHG curve. It broadens the curve so that the peak in net GHGs occurs later, and GHG payback is delayed as a result. However, the core features of the cumulative GHG curve and the conclusions of the analysis are not changed, even when aluminum production is accelerated such that it makes up 100% of the body and closure composition by 2050. The most noticeable change is that the contribution to variance from year-over-year decarbonization of material production processes increases when more aluminum is produced.

As shown in Figure A.4 (b), the Monte Carlo simulation returns the same top 11 parameters (>1% contribution) in terms of contribution to variance in the model when accelerated aluminum production is considered. The magnitudes of the contributions to variance for the 11 parameters are also quite similar to what is shown in Figure 2.5 of Chapter 2. Since accelerating aluminum content to 100% by 2050 is the most extreme scenario, and the curve still reaches its peak before the end of the modelling period, I also conclude that extending the modelling period beyond 2050 will not have a significant effect on the overall conclusions of the study.

A.4.2 Use

In Section 2.4, I show that increasing the efficiency of the fleet actually extends the GHG payback time, which challenges the intuition that increasing use phase efficiency is beneficial. This is due to the fact that the fuel savings per mass savings is decreased in hybrid and electric vehicles relative to their gasoline and diesel-powered counterparts, as shown in Table A.18. I also show the interaction of the two fleet compositions with baseline powertrain resizing shares (50%) and an increase to 100% resizing. This is reflected in Figure A.5 (a). Additional use phase effects of interest are covered in Figure A.5 (b), (c), (d), (e), and (f). These include the effects of changing the mean lifetime of the fleet, changing the distance driven over a fixed mean lifetime, varying the fuel savings per mass savings (Fuel Reduction Value), and changing the GHG intensity of gasoline, diesel, and electricity production.

Figure A.5 (b) highlights another counterintuitive result related to the use phase. Conventional wisdom says that lengthening the lifetime of products is a benefit to their environmental profile. However, in this case, longer lifetimes actually delay the GHG

payback of the system. Shorter lifetimes achieve payback faster for two reasons. First of all, the end-of-life aluminum scrap becomes available sooner. The scenarios are relative to the baseline, where all aluminum scrap is recycled and displaces primary production on a 1-to-1 basis, therefore large assumed GHG benefits are captured sooner when the lifetime is shorter. Additionally, the changes in the mean lifetime still assume a fixed distance driven of 245,000 km. This means that the fuel savings for the total distance travelled is captured in a shorter period when a shorter mean lifetime is assumed.

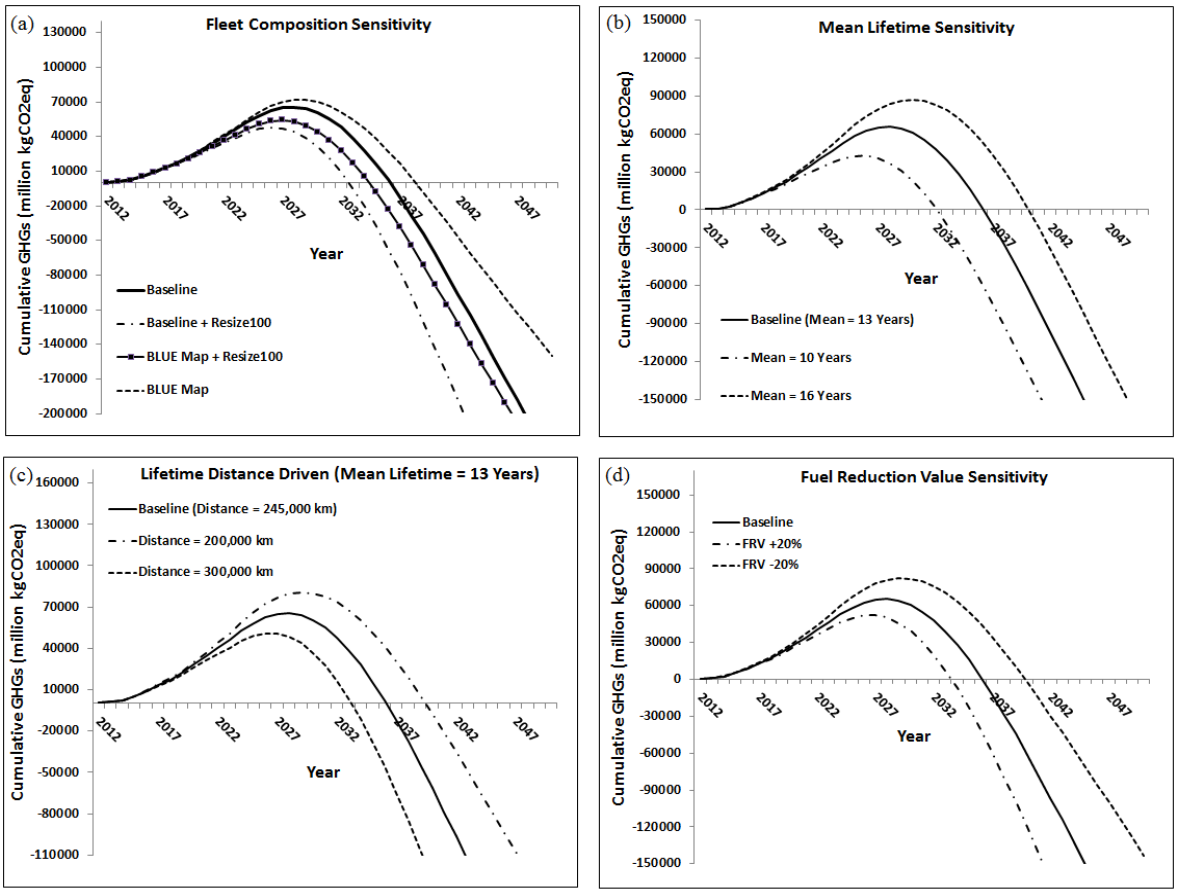

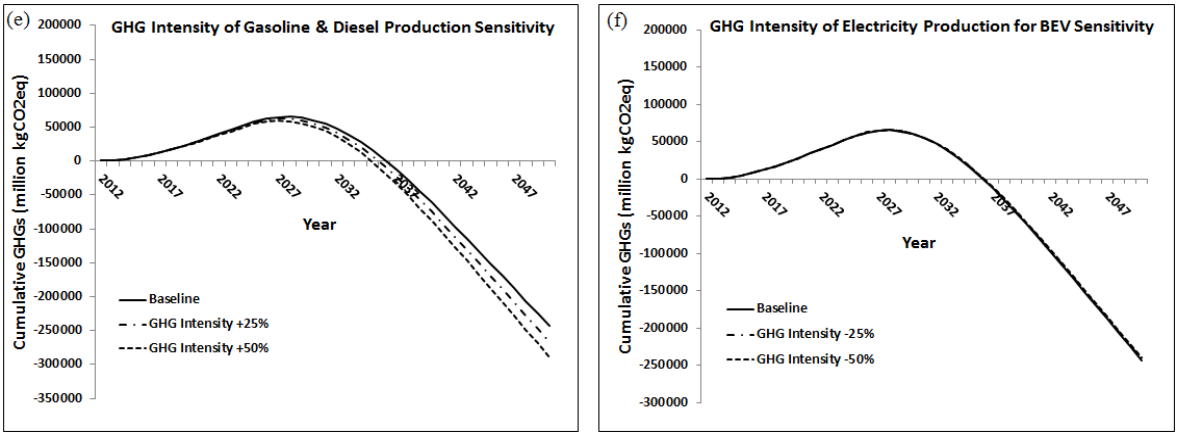

Figure A.5: (a) Scenarios interacting the efficiency of the fleet (Baseline & IEA BLUE Map) and the share of powertrain resizing in the fleet, 50% (Baseline) & 100% (Resize100). (b) Shifting of the cumulative GHG curve in response to changes in the mean lifetime of vehicles in the fleet. (c) Shifting of the cumulative GHG curve in response to changes in the distance driven over a fixed mean lifetime. (d) Sensitivity of GHG payback to changes in the fuel savings per mass savings (Fuel Reduction Value).(e) Sensitivity of the cumulative GHG curve to the GHG intensity of gasoline & diesel production. (f) Sensitivity of the cumulative GHG curve to the GHG intensity of electricity production for BEVs.

When the distance travelled over a fixed lifetime is increased, as shown in Figure A.5 (c), GHG payback is accelerated. This is due to increased accumulation of use-phase energy savings across the fleet. Keeping the mean lifetime fixed at 13 years and changing the lifetime distance travelled to 300,000 km shortens payback to 2036, while changing it to 200,000 km delays payback to 2043.

Changing the fuel reduction values with and without powertrain resizing (Table A.18) shifts the cumulative GHG curve in an intuitive way. Increasing fuel and electricity savings per mass savings by 20% shortens GHG payback from 2039 to 2036. Decreasing the fuel reduction values by 20% extends GHG payback to 2043.

Finally, possible shapes of the lifetime distribution curve are compared in Figure A.6. I acknowledge that the Weibull distribution has been used to model vehicle lifetimes in some studies (Sakai et al., 2014; Yano et al., 2014). However, log-normal has been used for this model because the parameters governing the shape and position of the curve are input directly as mean and standard deviation, which is not possible when using the Weibull. In addition, Figure A.2 (d) and prior literature both suggest that the results of using log-normal and Weibull for lifetime distribution modeling yield similar outcomes (Davis et al., 2007).

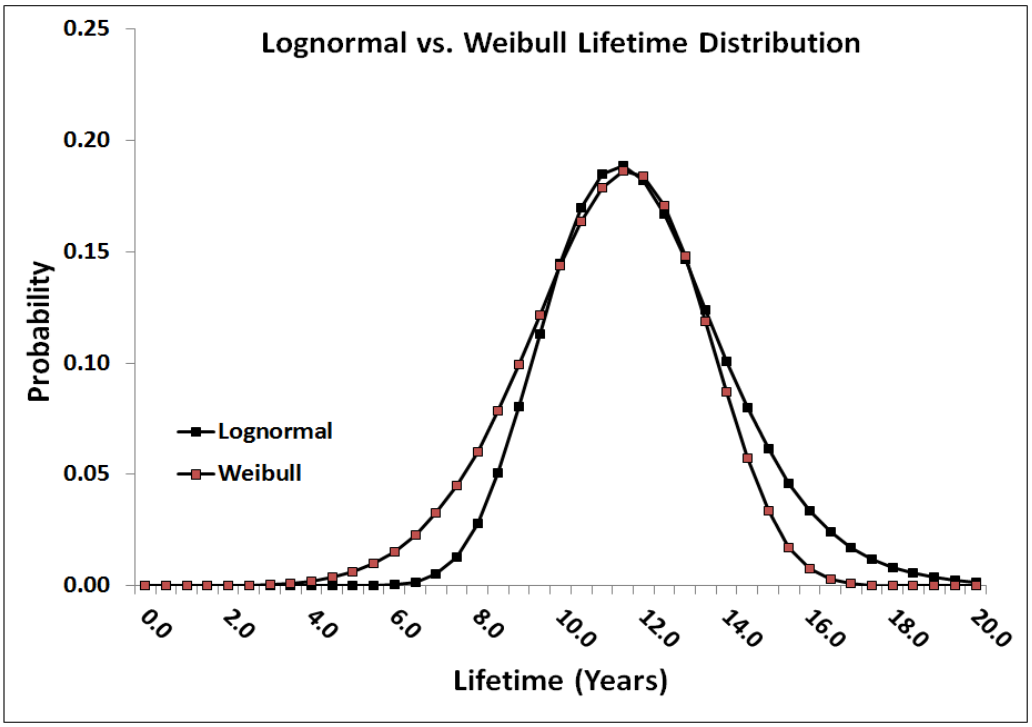

Figure A.6: Comparison of lognormal and Weibull lifetime distributions

A.4.3 Recycling

The implications of reducing the displacement of primary production due to recycling of aluminum as characterized by the parameter β_a are explored in the main text. However, I have not yet explored the sensitivity of the model to the scrap market parameters corresponding to the response of scrap collection to increases and decreases in aluminum

and steel scrap generation, α_a and α_s. In addition, the parameter corresponding to reduced displacement from reduced secondary steel production, β_s, may also have an impact. The response of the cumulative GHG curve to these parameters is largely governed by the difference between primary and secondary production, as shown in equations A.31 and A.32. Therefore, I expect that the responses to changes in the aluminum scrap market responses are stronger than those for steel. This is reflected in Figure A.7.

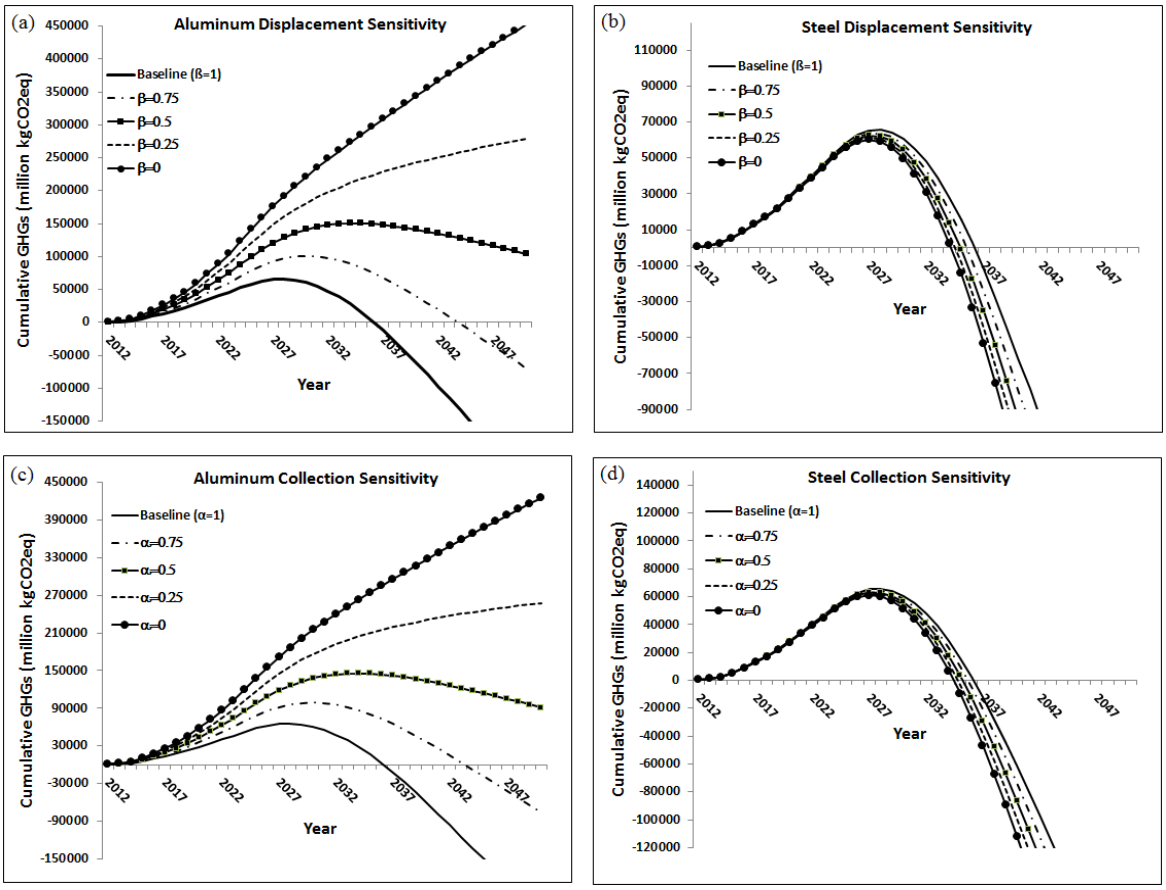

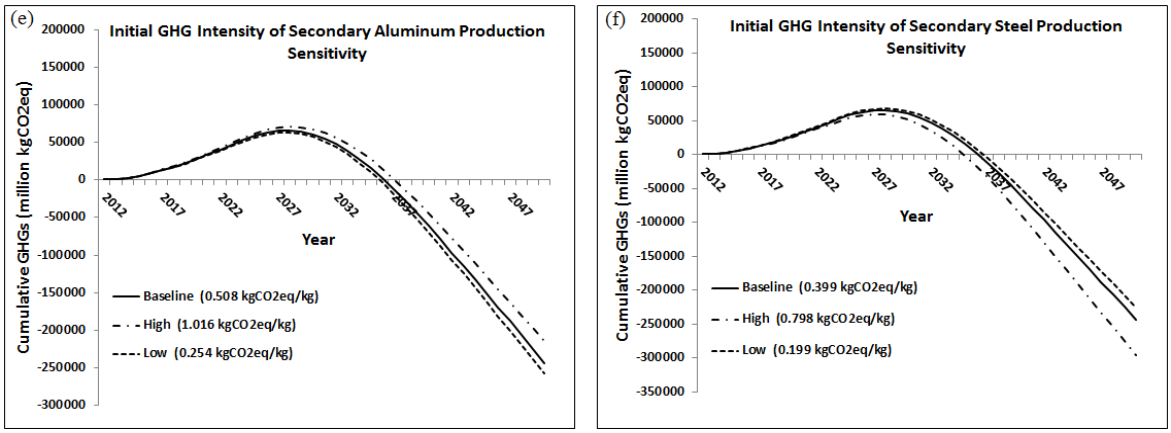

Figure A.7: Sensitivity of the cumulative GHG curve to (a) aluminum displacement β_a, (b) steel displacement β_s, (c) aluminum collection α_a, and (d) steel collection α_s. The sensitivity of cumulative GHG emissions to the GHG intensity of secondary aluminum and steel production are shown in (e) and (f), respectively.

There are a few noteworthy features of the responses shown above. First of all, the responses to variation in aluminum collection and displacement parameters relative to the baseline values are extremely similar. This implies that it is equally important that additional aluminum scrap generation both leads to additional scrap collection, and that the additional secondary production in turn displaces primary production. Secondly, the expectation that the cumulative GHG curve is dramatically more responsive to aluminum recycling parameters in comparison to steel is confirmed. Finally, I note that lowering the scrap collection effect and displacement of steel production actually improves the GHG performance of the system over time relative to the baseline. This is because full collection and displacement implies that equivalent amounts of primary steel must be produced to compensate for the reduction in secondary steel on the market. In the event that collection and displacement are less than 100%, less primary steel production is required to compensate. This is the opposite of the case of aluminum, where I am modelling an *increase* of secondary material on the market, and lower displacement is interpreted as greater net

primary production relative to the baseline. Lastly, I note that the model shows limited sensitivity to the GHG intensities of secondary aluminum and steel production.

A.3.4 Interactions

Here, interactions between key parameters are explored. It has been shown that the model is highly responsive to the displacement of primary aluminum production from recycling, and to the material replacement coefficient. Figure A.8 (a) explores whether or not reducing the material replacement coefficient can help mitigate the problems caused by partial displacement. I have also shown that the use phase is sensitive to the share of the fleet that resizes its powertrains. Figure A.8 (b) shows the possibilities resulting from both varying the material replacement coefficient and increasing or decreasing powertrain resizing.

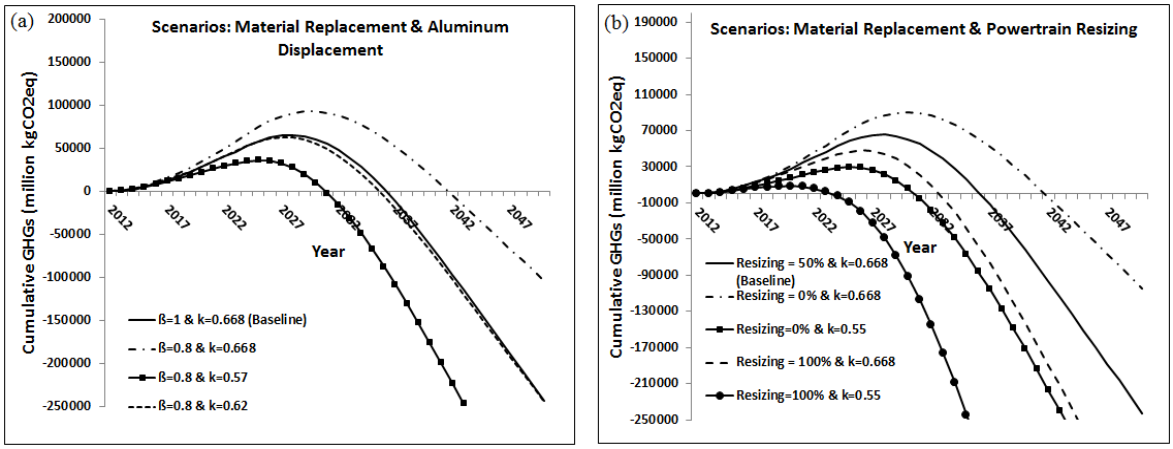

Figure A.8: (a) Interaction of the material replacement coefficient with partial aluminum displacement from recycling. (b) Interaction of the material replacement coefficient with the share of the fleet that resizes its powertrains.

Figure A.8 (a) offers some suggestion of how a partial displacement scenario involving aluminum might be mitigated under large-scale material substitution. The baseline curve and the first scenario are familiar from other figures. While holding all else constant, lowering

β_a to 0.8 leads delays GHG payback significantly. However, lowering the material replacement coefficient, as I do in the other two interaction scenarios, restores the GHG payback effect. In fact, for $\beta_a = 0.8$ and $k = 0.57$, cumulative GHGs are lower than the baseline for all years.

Figure A.8 (b) explores the use of two opportunities to reduce GHG payback time simultaneously. When the share of powertrain resizing is 0%, GHG payback is delayed in comparison with the baseline case. However, the delay in GHG payback can be counteracted by reducing the material replacement coefficient. This scenario produces lower cumulative GHGs compared to the baseline. If the material replacement coefficient is fixed at the baseline value, increasing the share of resized powertrains to 100% provides a vast improvement in cumulative GHGs. Finally, by increasing the share of resized powertrains to 100% and decreasing the material replacement coefficient simultaneously, the fastest GHG payback time of all presented interaction scenarios.

Another sensitivity analysis applies to the annual year-over-year decarbonization and carbon intensification factors. The decarbonization factor is applied to aluminum and steel production processes, as well as electricity production for BEVs. This factor is a proxy for the gradual decarbonization of the electricity grid, which contributes a significant proportion of GHG emissions to these production processes. The baseline estimate for this variable is a year-over-year 0.5% decarbonization, and in Figure A.9 (a) I show how the results change when varying year-over-year decarbonization from 0% to 2%. In the case of gasoline and diesel production, evidence suggests that the carbon intensity of their production may actually intensify over time due to the extraction of less conventional sources (Brandt and Farrell, 2007). For these production processes, I apply a carbon intensification of 0.5% year-

over-year as a baseline. Figure A.9 (b) shows how the results change when varying the carbon intensification of gasoline and diesel production from 0% to 2%.

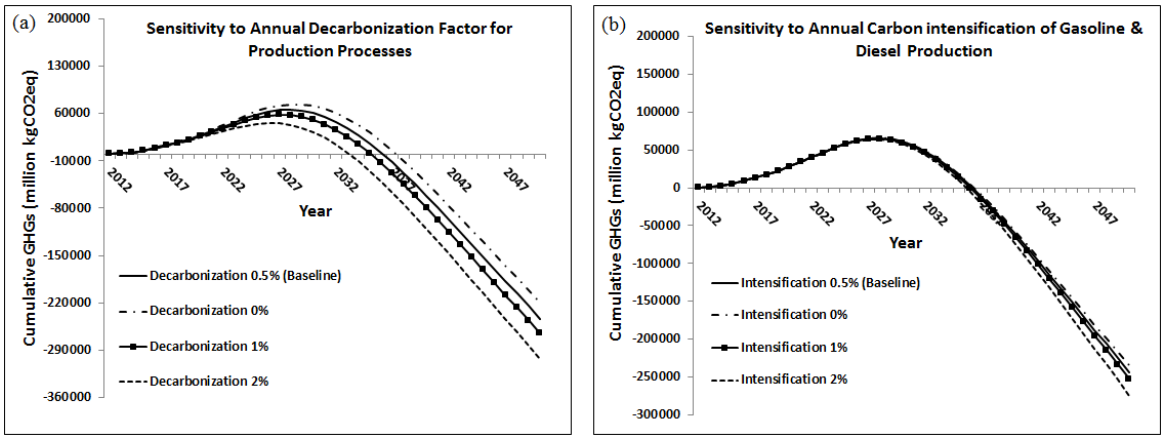

Figure A.9: (a) Sensitivity of the cumulative GHG curve to variation in the year-over-year decarbonization factor for production processes. (b) Sensitivity of the cumulative GHG curve to variation in the year-over-year carbon intensification factor for gasoline and diesel production.

Figure A.9 shows that the model is more sensitive to year-over-year decarbonization of production processes than it is to the year-over-year carbon intensification of gasoline and diesel production. The sensitivity of the model to decarbonization is primarily driven by its effect on primary aluminum production. I note that while it is not possible to estimate what a decarbonization curve projected this far into the future would look like, it is important to consider the effect of this possibility on the model.

Finally, I consider the possibility that there is a narrowed range of GHG intensities of initial imported primary aluminum production. The case I present in Chapter 2 uses a broad range based on literature related to the GHG intensity of aluminum production from all over the world. If the range is bounded by more moderate values from the literature, the results may change because the input distributions to the Monte Carlo simulation are different.

However, if I find a similar result in terms of contributions to variance, it shows that my analysis is reflective of the model structure itself. To illustrate the response of our Monte Carlo analysis to a narrowed range of GHG intensity of primary aluminum production, I run an alternative simulation using a range of 8.937 kg CO_2eq/kg (The Aluminum Association, 2013) to 16.5 kg CO_2eq/kg (Hao et al., 2015). I find that the initial GHG intensity of imported primary aluminum production drops from the 2nd to the 4th highest contributor to the variance. However, the top five and top eleven parameters (with >1% contribution) remain unchanged.

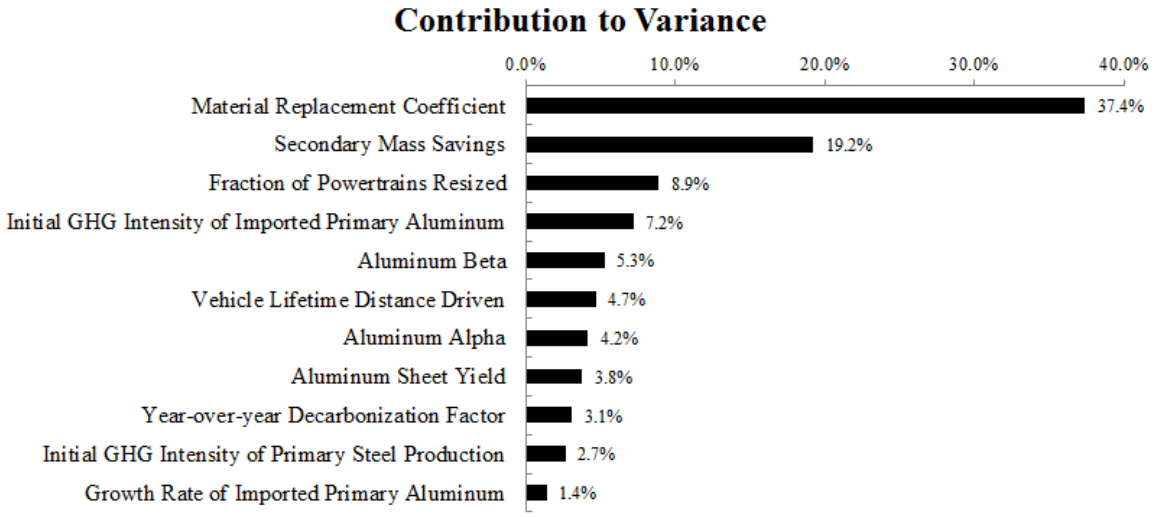

Figure A.10: Contributions to variance from an alternative Monte Carlo simulation where the range of GHG intensities for initial imported primary aluminum production is narrowed compared with the case from the main text.

A.5 References

Accenture LLC, 2015. Executive Summary : North American Primary Aluminum Smelter Study.

American Iron and Steel Institute, 2016. Data Provided by American Iron and Steel Institute (AISI).

ANL, 2015. Light Duty Electric Drive Vehicles Monthly Sales Updates [WWW Document]. Argonne Natl. Lab. URL http://www.anl.gov/energy-systems/project/light-duty-electric-drive-vehicles-monthly-sales-updates (accessed 10.8.15).

Argonne National Laboratory, 2015. GREET 2015.

Brandt, A.R., Farrell, A.E., 2007. Scraping the bottom of the barrel: Greenhouse gas emission consequences of a transition to low-quality and synthetic petroleum resources. Clim. Change 84, 241–263. doi:10.1007/s10584-007-9275-y

Chapp, J., Shah, V.C., 2007. Steel Use in Chrysler Sebring Sedan/ Convertible and Dodge Avenger [WWW Document]. URL http://www.autosteel.org/~/media/Files/Autosteel/Great Designs in Steel/GDIS 2007/05 - AHSS Technology in the 2007 Daimler Chrysler Sebring.pdf (accessed 7.11.17).

Davis, J., Geyer, R., Ley, J., He, J., Clift, R., Kwan, A., Sansom, M., Jackson, T., 2007. Time-dependent material flow analysis of iron and steel in the UK. Part 2. Scrap generation and recycling. Resour. Conserv. Recycl. 51, 118–140. doi:10.1016/j.resconrec.2006.08.007

Ducker Worldwide, 2015. AISI Materials Content Analysis: Final Report.

Ducker Worldwide, 2014. 2015 North American Light Vehicle Aluminum Content Study [WWW Document]. URL http://www.autonews.com/assets/PDF/CA95065611.PDF

Geyer, R., 2013. User Guide for Version 4 of the WorldAutoSteel Energy and GHG Model, on behalf of the World Steel Association. Brussels, Belgium.

Geyer, R., Malen, D., 2018. Parsimonious powertrain modeling for environmental vehicle assessments: Part 2 - Electric and hybrid electric vehicles. In preparation.

Hao, H., Geng, Y., Hang, W., 2015. GHG emissions from primary aluminum production in China : Regional disparity and policy implications. Appl. Energy. doi:10.1016/j.apenergy.2015.05.056

Hasanbeigi, A., Arens, M., Cardenas, J.C.R., Price, L., Triolo, R., 2016. Comparison of carbon dioxide emissions intensity of steel production in China, Germany, Mexico, and the United States. Resour. Conserv. Recycl. 113, 127–139. doi:10.1016/j.resconrec.2016.06.008

IEA, 2010. Energy Technology Perspectives: Scenarios & Strategies to 2050. International Energy Agency.

International Aluminum Institute, 2014. 2014 Environmental Metrics Report - Year 2010 Data - Final. London, United Kingdom.

Kelly, S., Apelian, D., 2016. Automotive aluminum recycling at end of life: a grave-to-gate analysis. Worcester, MA.

Kim, H.C., Wallington, T.J., 2013. Life-Cycle Energy and Greenhouse Gas Emission Benefits of Lightweighting in Automobiles : Review and Harmonization. Environ. Sci. Technol. 47, 6089–6097.

Malen, D., Geyer, R., 2018. Parsimonious powertrain modeling for environmental vehicle assessments: Part 1 - Internal combustion vehicles. In preparation.

Milford, R.L., Allwood, J.M., Cullen, J.M., 2011. Assessing the potential of yield improvements, through process scrap reduction, for energy and CO2 abatement in the steel and aluminium sectors. Resour. Conserv. Recycl. 55, 1185–1195. doi:10.1016/j.resconrec.2011.05.021

Morgans, S., 2012. Advanced High- High - Strength Steel Technologies in the 2013 Ford

Fusion [WWW Document]. URL http://www.autosteel.org/~/media/Files/Autosteel/Great Designs in Steel/GDIS 2012/Advanced High-Strength Steel Technologies in the 2013 Ford Fusion.pdf (accessed 7.11.17).

National Highway Traffic Safety Administration, 2006. Vehicle Survivability and Travel Mileage Schedules, Vehicle Survivability and Travel Mileage Schedules. doi:DOT HS 809 952

Pafumi, M., 2006. Advanced High Strength Steel Technology in the 2006 Honda Civic [WWW Document]. URL http://www.autosteel.org/~/media/Files/Autosteel/Great Designs in Steel/GDIS 2007/07 - Advanced High Strength Steel Technology in the 2006 Honda Civic.pdf (accessed 7.11.17).

Sakai, S. ichi, Yoshida, H., Hiratsuka, J., Vandecasteele, C., Kohlmeyer, R., Rotter, V.S., Passarini, F., Santini, A., Peeler, M., Li, J., Oh, G.J., Chi, N.K., Bastian, L., Moore, S., Kajiwara, N., Takigami, H., Itai, T., Takahashi, S., Tanabe, S., Tomoda, K., Hirakawa, T., Hirai, Y., Asari, M., Yano, J., 2014. An international comparative study of end-of-life vehicle (ELV) recycling systems. J. Mater. Cycles Waste Manag. 16, 1–20. doi:10.1007/s10163-013-0173-2

Steel Recycling Institute, 2017. Steel: Driving Auto Recycling Success [WWW Document]. URL http://www.recycle-steel.org/steel-markets/automotive.aspx (accessed 5.18.17).

The Aluminum Association, 2015. Industry Statistics - Facts at a Glance - 2015.

The Aluminum Association, 2013. The Environmental Footprint of Semi-Finished Aluminum Products in North America. Arlington, VA.

Thinkstep, 2015. GaBi Professional Database.

World Steel Association, 2010. Data Provided by World Steel Association (WSA).

Yano, J., Hirai, Y., Okamoto, K., Sakai, S. ichi, 2014. Dynamic flow analysis of current and future end-of-life vehicles generation and lead content in automobile shredder residue. J. Mater. Cycles Waste Manag. 16, 52–61. doi:10.1007/s10163-013-0166-1

B. Appendix B: Supporting Information for Chapter 4

B.1. Estimating the treatment effect in percentage changes

As discussed in Section 4.4.2, sites exposed to recycled water can vary widely in scale. Thus, it is sensible to estimate the effect of recycled water on total water usage as a percentage change. Here, I estimate the two-way fixed effects regression given by (4.5) using the log of total water usage as the dependent variable. To be explicit, the model is:

$$ln(Y_{it}) = \gamma + \alpha_i + \beta_t + \pi D_{it} + \varepsilon_{it} \quad \text{(B.1)}$$

In this case, the coefficient π has the interpretation of a percentage change. The sign of the coefficients and the width of the confidence intervals are consistent with those found in Table 4.4, as expected.

	(1)	(2)	(3)	(4)	(5)
$\hat{\pi}$ *(%)*	9.65	-0.24	-1.21	21.0	-5.10
(S.E)	(16.0)	(28.8)	(14.6)	(28.7)	(16.8)
N	2,707	2,175	1,458	1,249	946
Actual Clusters	19	19	10	9	19
Effective Clusters	16.9	13.0	8.17	8.94	16.9
Bootstrap critical values	[-2.02, 2.25]	[-2.21, 2.40]	[-2.52, 2.03]	[-2.33, 2.34]	[-1.97, 2.27]
Bootstrap 95% CI (%)	[-22.6,45.6]	[-63.9,68.9]	[-38.0,28.5]	[-46.0,88.2]	[-38.2,33.1]
Restrictions	None	1-year post	Region 1	Region 2	Peak only

Table B.1: Two-way fixed effects results with log total water usage as the dependent variable, using cluster-robust standard errors and wild bootstrap critical values. Actual clusters, effective clusters, number of observations, critical values, 95% confidence intervals, and sample restrictions are also shown.

B.2. Additional details on the displacement ratio

The displacement ratio is defined by Zink, et. al (2015) as $d = -\frac{\Delta Q_{prim}}{\Delta Q_{sec}}$, where ΔQ_{prim} is the change in the quantity of primary material in response to a change in the quantity of secondary material ΔQ_{sec}. The negative sign dictates that when ΔQ_{prim} is negative (i.e. the quantity of primary material decreases), displacement is positive. In this research, the secondary material is recycled wastewater and the primary material is potable water. Here, I add another layer of sophistication to the definition since I also estimate a counterfactual for potable water usage after the change in the quantity of recycled water.

Returning to the example of Section 4.3.2.1, consider the case where there are two time periods (t=1 is pre-treatment, t=2 is post-treatment) and two sites (i=1 is the control site, and i=2 is the treated site). Let $Y_{it} = P_{it} + R_{it}$, where Y_{it} is total water usage in site i in period t, and P_{it} and R_{it} are potable and recycled water usage. I assume that site 1 is a suitable control for site 2, i.e. the identification conditions for DID discussed in Section 2.2.1 are met. In addition, site 2 has no access to recycled water in the pre-treatment period, and converts a portion of its supplies to recycled water in the post treatment period, while site 1 uses potable water in both periods (i.e. $R_{11,}R_{12,}R_{21,} = 0$, and $R_{22} \neq 0$). I use the change in water usage in site 1, the control site, as a counterfactual for what would have happened in site 2 in the absence of a conversion to recycled water. Now, I can define a quasi-experimental version of the displacement ratio that allows recycled water to also displace

counterfactual potable water as: $d = -\frac{[P_{22}-P_{21}]-[P_{12}-P_{11}]}{R_{22}}$. The numerator is a difference-in-differences estimate of the change in potable water usage in the treated site. The denominator is the only non-zero quantity of recycled water usage in the system.

Using the identity $Y_{it} = P_{it} + R_{it}$, displacement can also be expressed as: $d = -\frac{[(Y_{22}-R_{22})-(Y_{21}-R_{21})]-[(Y_{12}-R_{12})-(Y_{11}-R_{11})]}{R_{22}} = -\frac{[(Y_{22}-R_{22})-(Y_{21}-0)]-[(Y_{12}-0)-(Y_{11}-0)]}{R_{22}} = -\frac{[Y_{22}-Y_{21}]-[Y_{12}-Y_{11}]-R_{22}]}{R_{22}} = 1 - \frac{[Y_{22}-Y_{21}]-[Y_{12}-Y_{11}]}{R_{22}}$. Now, consider the estimation of the DID regression given by (4.1). The expression $[Y_{22}-Y_{21}] - [Y_{12} - Y_{11}]$ is represented by θ, and the displacement ratio is $d = 1 - \frac{\theta}{R_{22}}$.

In the two-way fixed effects setting, I generalize this to the case of multiple treated units, multiple time periods, and staggered treatment adoption. In equation (4.4), π replaces θ as a DID estimate of the treatment effect. Assuming that $\pi \cdot n_{treat}$ is a suitable proxy for the change in total water usage after accounting for counterfactual trends, the equivalent quasi-experimental displacement expression is $1 - \frac{\pi \cdot n_{treat}}{R}$ as discussed in Section 4.3.2.2.

In order to provide more clarity, I provide several examples of pre- and post-treatment water usage for treatment and control sites in the setting with two time periods and two sites, and show how these translate into displacement ratios. In each example, I give potable and recycled water usage pre- and post-treatment for the treated site, and potable water use in the pre- and post-treatment periods for the control site (in CCUFT). From this information I calculate θ, and in turn displacement, for each example. Then, I show that calculating displacement from the potable water usage gives the same result. Note that the pre-treatment column corresponds to *t*=1, and the post-treatment column to *t*=2, such that P_1 in the pre-treatment column is the potable water usage in site 1 during period 1, or P_{11}.

Example 1:

	Pre-treatment (t=1)	Post-treatment (t=2)	Displacement calculation
$P_{i=1}$	100	110	$\theta = 0$
$P_{i=2}$	100	0	$d = 1 - \frac{\theta}{R_{22}} = 1 - \frac{0}{110} = 100\%$
$R_{i=2}$	0	110	$d = -\frac{[P_{22} - P_{21}] - [P_{12} - P_{11}]}{R_{22}} = -\frac{-110}{110} = 100\%$

Table B.2: Pre and post-treatment water usage values for treatment (i=2) and control (i=1) and the displacement calculation for Example 1.

In this first example, total water usage in the control site and the treated site are the same in both the pre- and post-treatment period. Thus, even though total water usage increased by 10 CCUFT, $\theta = 0$ because the increase was the same in both sites. Displacement is 100%, because the 110 CCUFT of recycled water displaced both the 100 CCUFT from the pre-treatment period and the 10 CCUFT increase in potable water usage that we infer from the behavior of the counterfactual (control site). Thus, I infer that the introduction of recycled water had no effect on total water usage, and displaced potable water on a 1-to-1 basis.

Example 2:

	Pre-treatment (t=1)	Post-treatment (t=2)	Displacement calculation
$P_{i=1}$	100	100	$\theta = 50$
$P_{i=2}$	100	50	$d = 1 - \frac{\theta}{R_{22}} = 1 - \frac{50}{100} = 50.0\%$
$R_{i=2}$	0	100	$d = -\frac{[P_{22} - P_{21}] - [P_{12} - P_{11}]}{R_{22}} = -\frac{-50}{100} = 50.0\%$

Table B.3: Pre and post-treatment water usage values for treatment (i=2) and control (i=1) and the displacement calculation for Example 2.

In the second example, total water usage in the control site stays the same in both periods, while the treated site increases its total water usage by 50 CCUFT after introducing recycled water. In this case, $\theta = 50$. The 100 CCUFT of recycled water displaced 50 CCUFT of potable water usage, and no counterfactual potable water. The other 50 CCUFT of recycled water grew overall water usage at the site. Displacement is then 50%, and the calculation is equivalent when using difference-in-differences in total or potable water as shown above.

Example 3:

	Pre-treatment (t=1)	Post-treatment (t=2)	Displacement calculation
$P_{i=1}$	200	250	$\theta = 50$
$P_{i=2}$	200	70	$d = 1 - \frac{\theta}{R_{22}} = 1 - \frac{50}{230} = 78.3\%$
$R_{i=2}$	0	230	$d = -\frac{[P_{22} - P_{21}] - [P_{12} - P_{11}]}{R_{22}} = -\frac{-180}{230} = 78.3\%$

Table B.4: Pre and post-treatment water usage values for treatment (i=2) and control (i=1) and the displacement calculation for Example 3.

In example 3, I show how displacement is calculated when total water usage increases in both treatment and control groups, but the magnitude of the increase is different. The difference between the change in total water usage in the treated site and the change in total water usage in the control site is 50 CCUFT. Usage in the control site increases from 200 to 250, but in the treated site it increases from 200 to 300 CCUFT. Thus, in this case $\theta = 50$ once again. The treated site introduced 230 CCUFT of recycled water into its supply. This displaced the 130 CCUFT reduction in potable water usage from pre- to post-treatment, and another 50 CCUFT of counterfactual potable water usage inferred from the increase in potable water usage in the control site. The remaining 50 CCUFT of recycled water grew

overall water usage. Thus, 78.3% of the recycled water displaced potable water as shown in the two displacement calculations.

Example 4:

	Pre-treatment (t=1)	Post-treatment (t=2)	Displacement calculation
$P_{i=1}$	100	90	$\theta = 110$
$P_{i=2}$	100	50	$d = 1 - \frac{\theta}{R_{22}} = 1 - \frac{110}{150} = 26.7\%$
$R_{i=2}$	0	150	$d = -\frac{[P_{22} - P_{21}] - [P_{12} - P_{11}]}{R_{22}} = -\frac{-40}{150} = 26.7\%$

Table B.5: Pre and post-treatment water usage values for treatment (i=2) and control (i=1) and the displacement calculation for Example 4.

Finally, I have an example where total water usage decreases in the control site. In this example, the difference-in-differences value of θ is 110, as total water usage increases from 100 to 200 CCUFT in the treatment site, and decreases from 100 to 90 CCUFT in the control site. To first order, 150 CCUFT of recycled water displaces 50 CCUFT of potable water. However, I adjust displacement for the decrease in water usage in the control site, just as I did when the control sites increased water usage in previous examples. Since water usage decreased by 10 CCUFT in the control site, the 150 CCUFT of recycled water only displaced 40 CCUFT (50-10) of potable water after adjusting for the counterfactual. Then, for 150 CCUFT of recycled water, only 40 CCUFT displaced potable water and the displacement ratio is 26.7%.